

University of Leoben

Characterization of Cretaceous Reservoirs  
in the North Arabic Gulf Area



I declare in lieu of oath that I did this thesis by myself and that all the work contained therein is my own, except where stated

Andrea Payer  
November 2006

# ACKNOWLEDGEMENTS

Above all I would like to thank em.O.Univ.-Prof. Dipl.-Ing. Dr.mont. Zoltán Heinemann for giving me the opportunity to work on this thesis.

My sincerest gratitude is due to Marc Blaizot, Georges Zaborowski and Jean Chastang from the department Projets Nouveaux at Total for assigning me to this project.

I am deeply grateful to Jean Chastang in his function as my supervisor for his invaluable guidance and help during the six months of my placement with Total. Furthermore I want to thank him for his efforts to integrate me into the team and for all his tips concerning the life in Paris.

I thank the team of Projets Nouveaux in Paris for making me feel like a part of the group and for all the great discussions during lunchtime.

I want to thank Pierre Masse and the whole team of ISS/STRU in Pau for letting me participate in their meetings and for sharing their findings and knowledge about Middle Eastern structural geology with me.

I am indebted to Béatrice Glachant for sharing her knowledge and insight about the Ahwaz field with me and for always patiently answering my many questions.

I want to thank Alberto Braghioli for providing me with input data for my simulations of the Dorood field.

Thanks go to Michel Verdier for providing me with simulation data of the Mishrif field.

Special thanks go to Husnein Ahmed for always answering my questions concerning Reservoir Engineering topics, for the literature he provided me and for the useful discussions about Ahwaz.

I am much obliged to Christophe Nogaret for his invaluable, kind and always especially rapid support and troubleshooting concerning Eclipse.

I want to thank Didier Janezic for his kind help with the installation of various software on my computer which helped me to perform my work more efficiently.

Special thanks go to Jean – Claude Heidmann and François Weissgerber for discussions and coffee breaks apart from work topics. The same goes to Muriel Pelagatti and Dominique Lorgeril, who always provided their kind assistance and support concerning administrative topics.

I want to thank Martin Moser for his help with Microsoft Office peculiarities and for his support during the time of my thesis.

Last but not least I am grateful to my parents for enabling me to carry out my studies and this thesis, and for their love and support during the entire time.

# ABSTRACT

Despite a long operating period of oil fields, there often exists a considerable amount of uncertainty about certain reservoir parameters still in the late life of the field. The knowledge of these parameters is crucial to an optimized and successful future field development.

Four reservoirs are investigated in this study in order to identify these parameters and to evaluate their impact on oil production. Future decisions on reservoir management and field development can be deduced from the results for these reservoirs or for reservoirs considered as an analogue.

The investigated oil fields are the Ahwaz and the Dorood field, both located in Iran, the Majnoon field in Iraq and the Raudhatain field in Kuwait. The studied reservoirs are quite different in terms of reservoir properties, development options and encountered problems. Therefore, a considerable part of the problems encountered are linked to the particularities of the studied reservoir.

Nevertheless, there are some predominant parameters influencing the production behaviour in all or at least three among the four reservoirs:

Due to reservoir heterogeneity and/or compartmentalization and significant permeability anisotropy, horizontal wells do not benefit as much as expected. Drilling highly deviated wells that penetrate several reservoir layers should be considered as a preferred option.

Reservoir permeability, relative permeability, permeability anisotropy and reservoir vertical transmissibility between layers are crucial parameters. They drive most of the oil production rate and cumulative production. In order to mitigate development risks, it is strongly advisable to perform appropriate core and log measurements with suitable reservoir coverage to not only reduce the range of uncertainties but also to optimize the position of future producers in locations with favourable reservoir properties.

In case of weak aquifer support, it is recommended to implement pressure support in order to maintain both the reservoir offtake and to avoid that reservoir pressure drops below the bubble point and thus reduces well productivity.

# TABLE OF CONTENTS

<b>1. INTRODUCTION.....</b>	<b>1</b>
<b>2. AHWAZ .....</b>	<b>3</b>
2.1. SEDIMENTOLOGY.....	4
2.2. RESERVOIR GEOLOGY .....	7
2.3. UNCERTAINTIES.....	9
2.3.1. <i>Fracture / Drain Network.....</i>	9
2.3.2. <i>Matrix Permeability.....</i>	10
2.3.3. <i>Degree of Compartmentalization.....</i>	11
2.3.4. <i>Aquifer Strength.....</i>	14
2.3.5. <i>Formation Compressibility.....</i>	15
2.3.6. <i>Horizontal Wells.....</i>	15
2.4. RESERVOIR MODEL .....	16
2.5. RESULTS AND DISCUSSION .....	20
2.5.1. <i>Results West.....</i>	20
2.5.2. <i>Results Center.....</i>	23
2.5.3. <i>Results East.....</i>	25
2.5.4. <i>General conclusions on Ahwaz results.....</i>	28
<b>3. DOROOD.....</b>	<b>29</b>
3.1. SEDIMENTOLOGY.....	30
3.2. RESERVOIR GEOLOGY .....	33
3.3. UNCERTAINTIES.....	35
3.3.1. <i>Fault Transmissibility .....</i>	36
3.3.2. <i>Layer Transmissibility .....</i>	36
3.3.3. <i>Extension of high k streaks.....</i>	38
3.3.4. <i>Rock type distribution .....</i>	39
3.3.5. <i>Different relative permeability curves.....</i>	40
3.3.6. <i>Impact of horizontal wells.....</i>	40
3.3.7. <i>Impact of water injection .....</i>	41
3.4. RESERVOIR MODEL .....	42
3.5. RESULTS AND DISCUSSION .....	44
3.5.1. <i>Results South.....</i>	44
3.5.2. <i>Results Center.....</i>	47
3.5.3. <i>Results North.....</i>	50
3.5.4. <i>General conclusions on Dorood results:.....</i>	53

<b>4. MAJNOON / MISHRIF .....</b>	<b>54</b>
4.1. SEDIMENTOLOGY.....	55
4.2. RESERVOIR GEOLOGY .....	57
4.3. UNCERTAINTIES .....	60
4.3.1. <i>Horizontal wells</i> .....	60
4.3.2. <i>Artificial Lift methods</i> .....	61
4.3.3. <i>Permeability anisotropy</i> .....	61
4.3.4. <i>Relative permeability curves</i> .....	62
4.3.5. <i>Permeability field</i> .....	63
4.4. RESERVOIR MODEL .....	64
4.5. RESULTS AND DISCUSSION .....	67
4.5.1. <i>Reservoir parameters</i> .....	67
4.5.2. <i>Artificial lift with vertical wells</i> .....	70
4.5.3. <i>Artificial lift with horizontal wells</i> .....	73
4.5.4. <i>General conclusions on Mishrif results:</i> .....	76
<b>5. RAUDHATAIN / UPPER BURGAN .....</b>	<b>77</b>
5.1. SEDIMENTOLOGY.....	78
5.2. RESERVOIR GEOLOGY .....	80
5.3. UNCERTAINTIES .....	83
5.3.1 <i>Aquifer Presence</i> .....	83
5.3.2 <i>Fault Transmissibility</i> .....	83
5.3.3 <i>Layer Transmissibility</i> .....	84
5.3.4 <i>Relative permeabilities</i> .....	84
5.3.5 <i>Permeability Anisotropy</i> .....	85
5.3.6 <i>Impact of horizontal wells</i> .....	85
5.4. RESERVOIR MODEL .....	86
5.5. RESULTS AND DISCUSSION .....	89
5.5.1 <i>General conclusions on Burgan results:</i> .....	92
<b>6. CONCLUSIONS AND RECOMMENDATIONS.....</b>	<b>93</b>
<b>7. BIBLIOGRAPHY.....</b>	<b>96</b>

## LIST OF FIGURES

Fig. 2.1:	Location of Ahwaz .....	3
Fig. 2.2:	Ahwaz geometry .....	4
Fig. 2.3:	Rock typing .....	5
Fig. 2.4:	Ahwaz reservoir zonation .....	7
Fig. 2.5:	Transmissibility barriers in x - direction .....	12
Fig. 2.6:	Transmissibility barriers in y - direction .....	12
Fig. 2.7:	Transmissibility barriers in z - direction .....	12
Fig. 2.8:	Transmissibility barriers in x - direction .....	13
Fig. 2.9:	Transmissibility barriers in y - direction .....	13
Fig. 2.10:	Transmissibility barriers in z - direction .....	13
Fig. 2.11:	Transmissibility barriers in y - direction .....	14
Fig. 2.12:	Transmissibility barriers in z - direction .....	14
Fig. 2.13:	Ahwaz sector models side and total view.....	17
Fig. 2.14:	Cumulative oil production - base case and sensitivities – sector west.....	20
Fig. 2.15:	Water cut - base case and sensitivities – sector west.....	21
Fig. 2.16:	Pressure depletion - base case and sensitivities – sector west.....	21
Fig. 2.17:	Cumulative oil production - basecase and sensitivities –center sector.....	23
Fig. 2.18:	Water cut - base case and sensitivities –center sector .....	24
Fig. 2.19:	Pressure depletion - base case and sensitivities –center sector .....	24
Fig. 2.20:	Cumulative oil production - base case and sensitivities – sector east .....	26
Fig. 2.21:	Water cut - base case and sensitivities – sector east .....	26
Fig. 2.22:	Pressure depletion - base case and sensitivities – sector east .....	27
Fig. 3.1:	Location and geometry of Dorood.....	29
Fig. 3.2:	$\Phi/k$ – relationship in Upper Yamama .....	31
Fig. 3.3:	$\Phi/k$ – relationship in Lower Yamama .....	31
Fig. 3.4:	$\Phi/k$ – relationship in Manifa .....	31
Fig. 3.5:	Dorood reservoir zonation .....	33
Fig. 3.6:	Fault mapping into sector model.....	36
Fig. 3.7:	distribution of tight layers, southern sector .....	37
Fig. 3.8:	distribution of tight layers, center sector, left basecase, right sensitivity.....	38
Fig. 3.9:	Yamama/Manifa barrier, northern sector, left base case, right sensitivity.....	38
Fig. 3.10:	high k streaks, southern sector, left base case, right sensitivity .....	39
Fig. 3.11:	Basecase and sensitivity relative - k curves for each saturation region.....	40
Fig. 3.12:	Dorood sector models side and total view.....	42
Fig. 3.13:	Cumulative oil production, basecase and sensitivities – sector south .....	45
Fig. 3.14:	Water cut, basecase and sensitivities – sector south .....	45

Fig. 3.15: Pressure depletion, basecase and sensitivities – sector south .....	46
Fig. 3.16: Cumulative oil production, basecase and sensitivities, center sector .....	47
Fig. 3.17: Water cut, basecase and sensitivities, center sector .....	48
Fig. 3.18: Pressure depletion, basecase and sensitivities – center sector .....	49
Fig. 3.19: Cumulative oil production, basecase and sensitivities, sector north.....	50
Fig. 3.20: Water cut, basecase and sensitivities, sector model north.....	51
Fig. 3.21: Pressure depletion, basecase and sensitivities, sector north.....	52
Fig. 4.1: Location of Majnoon .....	54
Fig. 4.2: Top Mishrif .....	54
Fig. 4.3: Majnoon field zonation.....	56
Fig. 4.4: Mishrif rock types .....	58
Fig. 4.5: Zonation of the Mishrif reservoir .....	59
Fig. 4.6: Original and sensitivity relative – k curves for every region.....	63
Fig. 4.7: Mishrif sector model side view .....	64
Fig. 4.8: Mishrif sector model length and side view.....	64
Fig. 4.9: Transmissibility barriers in Mishrif.....	66
Fig. 4.10: Cumulative oil production, basecase and sensitivities – reservoir case .....	68
Fig. 4.11: Water cut, basecase and sensitivities – reservoir case.....	69
Fig. 4.12: Depletion, basecase and sensitivities – reservoir case.....	69
Fig. 4.13: Cum. oil prod., basecase and sensitivities – artificial lift, vertical wells.....	71
Fig. 4.14: Water cut, basecase and sensitivities – artificial lift, vertical wells.....	72
Fig. 4.15: Depletion, basecase and sensitivities – artificial lift, vertical wells.....	72
Fig. 4.16: Cum. oil prod., basecase and sensitivities, artificial lift, horizontal wells.....	73
Fig. 4.17: Water cut, basecase and sensitivities, artificial lift, horizontal wells .....	74
Fig. 4.18: Depletion, basecase and sensitivities, artificial lift, horizontal wells.....	75
Fig. 5.1: Raudhatain field location .....	77
Fig. 5.2: Top Burgan reservoir.....	77
Fig. 5.3: Raudhatain reservoir zonation .....	79
Fig. 5.4: Upper Burgan Zonation .....	81
Fig. 5.5: Burgan faults.....	83
Fig. 5.6: Intransmissible barriers, from left to right: layer 2/3, layer 4/5, layer 5/6.....	84
Fig. 5.7: Relative permeability curves .....	84
Fig. 5.9: Upper Burgan model side view .....	86
Fig. 5.10: Cumulative oil production match.....	88
Fig. 5.11: Pressure depletion match.....	88
Fig. 5.12: Water cut match.....	88
Fig. 5.13: Cumulative oil production, basecase and sensitivities .....	89
Fig. 5.14: Water cut in the basecase and sensitivities.....	90
Fig. 5.15: Pressure depletion, basecase and sensitivities .....	91



## LIST OF TABLES

Table 2.1:	Formation lithology per layer .....	6
Table 2.2:	Average reservoir properties field wide.....	7
Table 2.3:	Oil Field Fluid Parameters.....	9
Table 2.4:	Ahwaz hypothetical aquifer properties .....	15
Table 2.5:	Wells and completions .....	17
Table 2.6:	Reservoir model properties – western part .....	17
Table 2.7:	Reservoir model properties – center part.....	18
Table 2.8:	Reservoir model properties – eastern part.....	18
Table 2.9:	Sensitivity analysis input data west .....	20
Table 2.10:	Result overview Ahwaz, western sector.....	22
Table 2.11:	Sensitivity analysis input data center.....	23
Table 2.12:	Result overview Ahwaz, center sector .....	25
Table 2.13:	Sensitivity analysis input data east .....	25
Table 2.14:	Result overview Ahwaz, eastern sector .....	27
Table 3.1:	Formation layering .....	32
Table 3.2:	Average reservoir properties fieldwide.....	34
Table 3.3:	Dorood aquifer properties.....	35
Table 3.4:	Oil Field Fluid Parameters.....	35
Table 3.5:	rock type distribution, left base case, right sensitivity .....	39
Table 3.6:	Dorood sector models dimensions .....	42
Table 3.7:	Wells and completions .....	43
Table 3.8:	Reservoir Model petrophysical properties .....	43
Table 3.9:	Sensitivity analysis input data south .....	44
Table 3.10:	Result overview, Dorood sensitivity study, southern sector.....	46
Table 3.11:	Sensitivity analysis input data center.....	47
Table 3.12:	Result overview, Dorood sensitivity study, center sector.....	49
Table 3.13:	Sensitivity analysis input data north.....	50
Table 3.14:	Result overview, Dorood sensitivity study, northern sector.....	52
Table 4.1:	Majnoon reservoir properties.....	57
Table 4.2:	Mishrif average reservoir properties .....	59
Table 4.3:	Average oil field fluid parameters Mishrif .....	60
Table 4.4:	Sector model dimensions.....	65
Table 4.5:	Sector model properties - from Eclipse PRT file.....	65
Table 4.6:	Wells and completions .....	66
Table 4.7:	Sensitivity analysis input data, reservoir parameters.....	67
Table 4.8:	Result overview Majnoon sensitivity study, reservoir properties .....	70
Table 4.9:	Sensitivity analysis input data, artificial lift, vertical wells .....	70
Table 4.10:	Sensitivity analysis input data, artificial lift, horizontal wells .....	73

Table 4.11: Result overview Mishrif sensitivity study, artificial lift .....	75
Table 5.1: Raudhatain reservoir properties .....	78
Table 5.2: Upper Burgan average zonal properties .....	82
Table 5.3: Upper Burgan reservoir fluid and oilfield properties.....	82
Table 5.4: Upper Burgan hypothetical aquifer parameters.....	83
Table 5.5: Upper Burgan model dimensions .....	86
Table 5.6: Upper Burgan wells and completions .....	87
Table 5.7: Upper Burgan reservoir model properties .....	87
Table 5.8: Sensitivity analysis input data.....	89
Table 5.9: Result overview of Burgan sensitivity study .....	92

## ABBREVIATIONS

$\Phi$	porosity
°API	degree API
°C	degree Celsius
Bbl	barrel
bwpd	barrel water per day
cP	Centipoise
cp.	compare
EOR	Enhanced oil recovery
ft	feet
FVF	formation volume factor
Gbbl	billion ( $10^9$ ) bbl
GOR	Gas Oil ratio
k	permeability
$k_h$	horizontal permeability
km	kilometer
km <sup>2</sup>	square kilometer
$k_r$	relative permeability
$k_v$	vertical permeability
m	meter
Mbbl	million ( $10^6$ ) bbl
mD	milli - Darcy
MMBbl	million ( $10^6$ ) barrel
MULTZ	transmissibility in z direction
OOIP	Original oil in place
OWC	Oil Water contact
PermX	permeability in x direction
PermZ	permeability in z direction
PLT	Production logging tool
Psi	pounds per square inch
PVT	pressure, volume, temperature
RB	reservoir barrel
RF	recovery factor
RFT/MDT	repeated formation test / modular formation dynamics test
SCAL	Special core analysis
SCF	standard cubic feet
SG	specific gravity
Sm <sup>3</sup>	standard cubic meter
Sor,w	residual oil saturation to water
STB	stock tank barrel
THP	tubing head pressure
TVDss	true vertical depth sub sea
WI	water injector

## CONVERSION FACTORS

		$\frac{141,5}{SG} - 131,5$	=	°API
acre	×	$4,05 \cdot 10^3$	=	square meter
bar	×	14,5037738	=	pound per square inch
barrel	×	0,1589873	=	cubic meter
centipoise	×	0,0010	=	Pascal - Second
cubic meter	×	6,2898108	=	barrel
feet	×	0,3048	=	meter
meter	×	3,281	=	feet
mile	×	1609	=	meter
milli Darcy	×	$0,9869 \cdot 10^{-9}$	=	meter squared
pound per square inch	×	$6,894757 \cdot 10^3$	=	Pascal
Specific Gravity	×	999,996315	=	kilogram / cubic meter
standard cubic feet	×	$2,831685 \cdot 10^{-2}$	=	cubic meter

# 1. INTRODUCTION

This thesis has been established as part of an ample interdisciplinary study initiated by the department "Projets Nouveaux", New Business, of the French petroleum company Total. The study has the objective of consolidating geoscience knowledge in the Middle Eastern area and of developing a regional analogue data base for recovery factors and recovery mechanisms.

The focus of this study is cretaceous reservoirs in the north Arabic gulf area.

Selected fields and reservoirs with adequate static and dynamic data have been picked as study anchoring points. The examined reservoirs are the Bangestan reservoir in the Ahwaz field in Iran, the Yamama and Manifa reservoirs in the Dorood field in Iran, the Mishrif reservoir in the Majnoon field in Iraq and the Burgan reservoir in the Raudhatain field in Kuwait.

These reservoirs could be considered as analogues of other reservoirs located within the study perimeter or outside, and results provided through this study could be exploited in case of development.

There was and, despite the very long operating period of the fields, exists still a considerable amount of uncertainty about certain reservoir parameters. This thesis has the objective of, for each of the 4 reservoirs studied, highlighting these parameters and evaluating their impact on production in order to support future decisions on reservoir management and field development for this reservoir or another one considered as an analog.

This dynamic part of the study was conducted on the basis of preceding sections of the project which provided characterizations of the depositional processes, description of facies, structural environments and records of the Petroleum system.

For each reservoir the main indeterminate dynamic parameters have been compiled on the grounds of in-house literature, mainly historic studies on the respective fields. Based on these data, reservoir simulation sector models were built with the software Eclipse. An elementary history match was performed for cumulative production, water cut and reservoir pressure to validate the simulation models.

For two of the fields, reservoir simulation models were already available, albeit "full field" models, not suited for repeated evaluation simulations because of their required computation time. These full field models were fractionized into sectors and simplified in order to achieve reasonable simulation times.

Subsequently the main dynamic reservoir parameters influencing the production behaviour were identified based on indications in the literature together with the geological and petrophysical understanding gained about the fields.

For each of the reservoirs a sensitivity analysis was performed to establish the impact of these parameters and to constitute a range of recovery factors. These are the results that will be useful for the constitution of the regional analogue database.

Furthermore some recommendations for the future development of the fields could be deduced, especially regarding the focus of possible measurements and data acquisition.

Nevertheless, these results and recommendations have to be considered from a global perspective, since the simplicity of the models does not allow for a detailed description of the field events.

Each chapter starts with a detailed description of the sedimentological and geological setting of the field. This should help to outline the origin of most of the uncertain parameters. Subsequently the identified uncertainties are listed and described. The following chapter explains the process and properties of the reservoir model and the constraints that were applied for production. Finally a presentation and interpretation of the results is given.

## 2. AHWAZ

The Ahwaz oilfield is located onshore Iran at the northern end of the Persian Gulf next to the town Ahwaz. In geological terms the field is located in the Zagros basin. It was discovered in 1958 and put on production in 1971.

The field geometry is a sinuous northwest/southeast elongated anticline; about 44 miles long and 4,7 miles wide. The structurally closed area is about 50 miles long and 4,5 miles wide. The dips on the north-eastern flank vary from 15-28°; on the south western flank they average about 16°.

Ahwaz is producing out of the Bangestan formation, an Upper Cretaceous fractured limestone. Two reservoirs are present in Bangestan, Ilam and Sarvak. The top reservoir lies at about 10170 ft TVDs.

The amount of original oil in place is estimated to be about 38,5 Gbbl, of which up to day 782 Mbbl have been produced, resulting in a recovery factor of only 2%.[1]

Fig. 2.1: Location of Ahwaz [2]

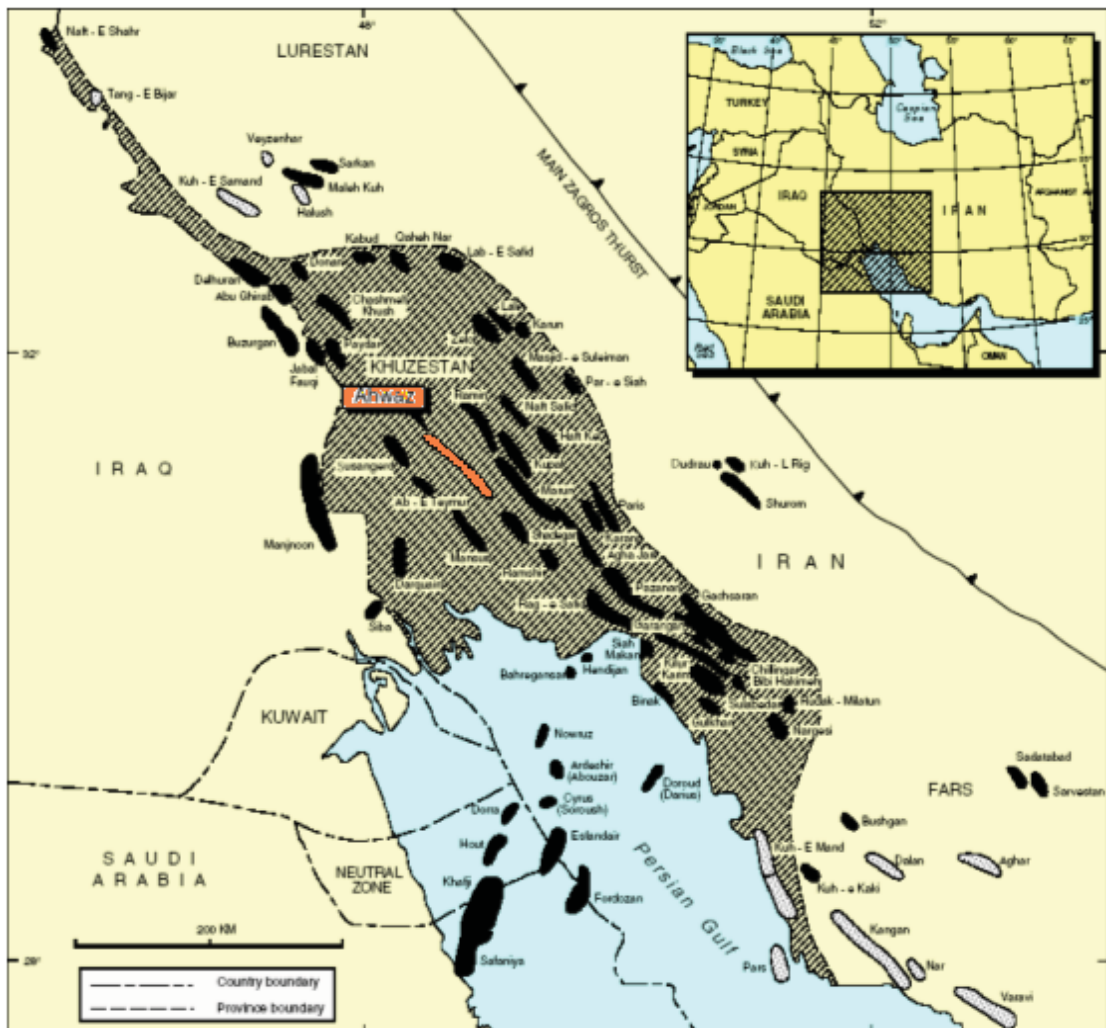
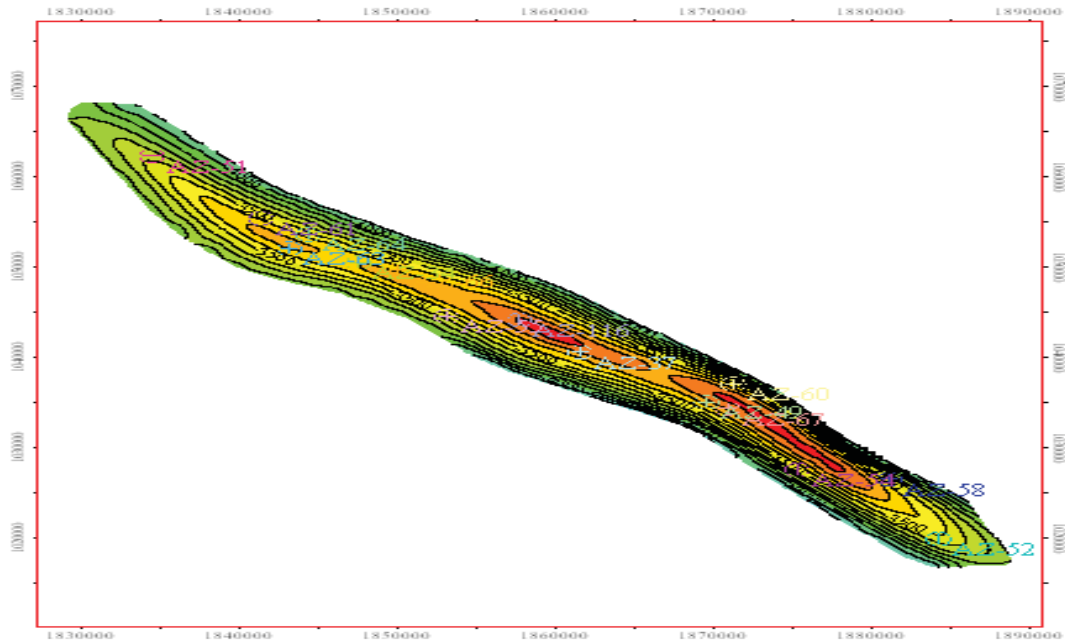


Fig. 2.2: Ahwaz geometry [2]



## 2.1. SEDIMENTOLOGY

A general shallowing of the sea in the region of Fars and Khuzestan during late Albian and Cenomanian time produced a thick interval of shallow water carbonates, which represent the Sarvak formation.

After a major event of sub aerial exposure and karstification, sedimentation of the shallow water Ilam carbonates set in the Late Cretaceous. These were then succeeded by the Gurpi sequence of deep-water shales. [2]

The structure of Ahwaz was formed by compression resulting from the closure of southern Thetys during Late Cretaceous and early Tertiary time. Further compression took place as the Afro-Arabian plates collided with the central Iranian plate during the Late Tertiary.[2]

Regionally, the Sarvak and Ilam formations are characterized by massive, rudist-bearing skeletal limestones deposited in a shallow shelf setting.

Locally in Ahwaz, the formations are composed of cyclic alternations of skeletal-peloidal packstones/grainstones and fine grained/mud-supported marly limestones.[2]

The grain dominated parts represent sedimentation in a shallow water/high energy environment during a marine regression, whereas the mud dominated parts were deposited in deeper water/ low energy setting during a marine transgression. [2]

The Sarvak formation is capped by a pronounced regional unconformity, which could have resulted in a major karst porosity development at the end of the Middle Cretaceous. However, rapid Late Tertiary



subsidence and burial caused by plate margin tectonics led to chemical compaction and cementation, which clogged significant volumes of primary intergranular and early formed secondary porosity. The Ilam reservoir consists of interbedded clayey limestone and shales and has variably but generally poor developed fracturing. [2]

The Sarvak reservoir consists of clayey limestone in its lower parts and grades upwards to massive, microporous limestone. The limestone exhibits a variable degree of secondary porosity by fracturing. In addition to the carbonate sequences, the Sarvak formation contains productive zones in fractured shales. [2]

In a “quick-look” analysis, 3 rock types could be distinguished according to their log signature. [3]

- Rock type 1 – “Fracture type”:

This rock type is a homolithic facies, non-porous ( $\Phi \leq 4\%$ ) but fractured. It shows high productivity. The oil permeability can be greater than 50 mD.

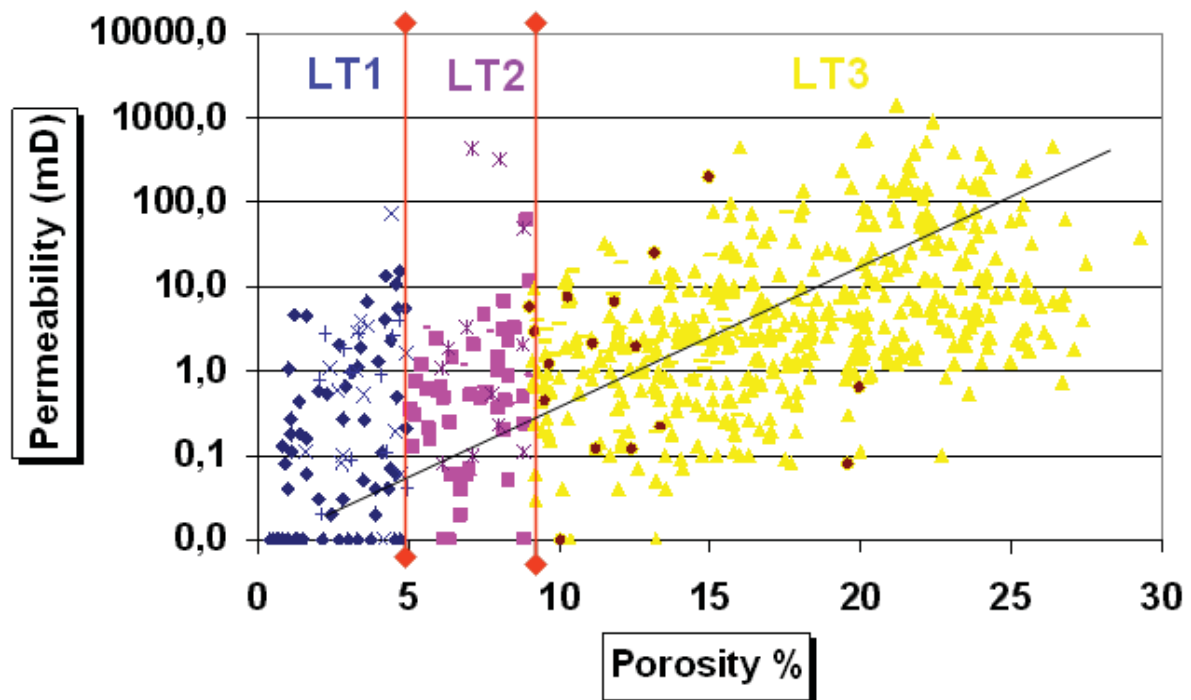
- Rock type 2 – “Intermediate type”:

Rock type 2 is a heterolithic facies with moderate porosity ( $4 \leq \Phi \leq 9\%$ ) and medium fracture occurrence. It shows fair productivity.

- Rock type 3 – “Matrix type”:

This rock type is a homolithic facies which is porous ( $\Phi > 9\%$ ) but not fractured. It is non productive (oil permeability  $< 1,5$  mD).

Fig. 2.3: Rock typing [3]



The source rock is the Middle Cretaceous Kazhdumi shale, the hydrocarbon was most likely expelled in Miocene. The Late Cretaceous Gurpi shale/marl acts as seal to the formation. [2]

Table 2.1 on the following page describes the lithology and the thereof resulting reservoir quality for each layer.

Table 2.1: Formation lithology per layer [2]

Group	Formation	Zone	Avg. Thickness	Lithology	Reservoir Quality
B A N G E S T A N	Ilam	A	60 ft 18 m	Skeletal – peloidal – oolitic wacke/packstone with marls and shales	Poor with high water saturation
		B	50 ft 15 m	Skeletal wackestone with thin bands of peloidal – skeletal Packstone	tight
		C	450 ft 137 m	Skeletal – peloidal pack/grainstone in upper part, foraminiferal wackestone in lower part	Good in upper part where intergranular and vuggy porosity is developed
	Sarvak	D	130 ft 40 m	Over-compacted pack/grainstone with thin chalky bioclastic beds	tight
		E	1050 ft 320 m	Skeletal – peloidal pack/grainstone interbedded with mudstone and wackestone	Good, in grain dominated facies where intergranular, moldic, vuggy and fracture porosity is developed
		F	150 ft 46 m	Finely crystalline marly limestone with local development of bioclastic limestone	tight
		G	300 ft 91 m	Massive, skeletal – peloidal pack/grainstone with intervals of mudstone – Wackestone	Good, in grain dominated facies where intergranular and vuggy porosity is developed
		H	280 ft 85 m	Finely- grained marly limestone with occasional Skeletal – peloidal limestone	tight
		I	400 ft 122 m	Skeletal – intraclastic limestone brecciated in part and locally dolomitic	Minor oil reservoir

## 2.2. RESERVOIR GEOLOGY

The Ahwaz field bears two reservoirs, the Upper Cretaceous Ilam and the Middle Cretaceous Sarvak. They show slightly different fluid characteristics. [2]

Based on Gamma Ray, Neutron and Porosity log correlations, the two reservoirs were subdivided into nine zones. Five of these nine zones are considered tight and non productive, four are considered porous and oil-producing. Within Ilam, this is zone C, within Sarvak this are zones E and G. The minor oil reservoir Sarvak I will not be considered further.

The barrier between Ilam C and Sarvak E is the Sarvak D; Sarvak E is separated from Sarvak G by Sarvak F. A matrix porosity cut-off of 4% has been applied to distinguish net and non-net reservoir. [2]

Within the zones the best reservoir properties can be found along the crest of the structure. This may be due to deposition in a high energy environment, or, perhaps more likely, to permeability enhancement resulting from tensional stresses occurring during the structural development of the anticlinal trap that created fissures and fractures. [2]

Fig. 2.4: Ahwaz reservoir zonation

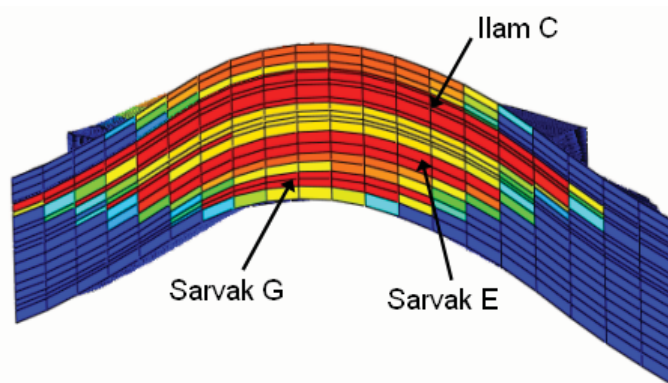


Table 2.2: Average reservoir properties field wide [1]

	Thickness (ft)	Porosity (%)	Permeability (mD)	OIP (GSTB)
Ilam C	552	11,7	5,2	19,0
Sarvak E	1212	5,6	8,9	10,4
Sarvak G & I	1048	7,2	4,0	9,3

There exist different oil - water contacts (OWC) for Ilam and Sarvak, which change over the area of the field: In the Ilam the OWC lies at 11943 ft TVDss in the eastern and central part, in the western part at 12304 ft TVDss. In the Sarvak the OWC in the eastern and central part lies at 13354 ft TVDss and at 12304 ft TVDss in the western part. [4]

The matrix porosity has an average value of about 10%; the in situ permeability is very low, in the most parts below 1 mD, the average is slightly higher (see table 2.2). [5]

Fracturing was seen at a minimum level in cores, except in low porosity rock (less than 10%). The estimated fracture porosity range is between 0,05 – 1 %.

The effective fracture permeability (product of fracture permeability and fracture porosity) was found by history matching, being in the order of 50 - 100 mD. [5]

Best production is coming from the Sarvak E reservoir, although it has the poorest petrophysical properties and not the highest OOIP.

Therefore it can be deduced that something other than the matrix properties in the vicinity of the well is contributing to production. [6] To illustrate this: the well with the best petrophysical properties in the field, which is producing mostly from the Ilam formation, is placed 17th in terms of cumulative production to date. [1]

Fractures have been detected only in one core out of fourteen cores that have been taken in total, but one has to bear in mind that core retrieval from fractured zones can often be poor.

Thus it is assumed that fractures are present to a significant degree in Sarvak E; however, due to the poor evidence in cores, no specific fracturing can be attributed.

This assumption is supported by mud loss data, production from PLT logs and production data from a controlled sample of wells, from both Ilam and Sarvak. This data suggests that production is coming from the fractured zones in Sarvak E, with only a secondary support from the matrix.

The Ilam reservoir appears much less fractured than the Sarvak. [7]

However, an alternative explanation for the enhanced productivity of Sarvak E could be the presence of distinct micro-fractured layers that act as drains.

Three possible facies types which could be acting as drains could be identified: Conglomerate, Sedimentary Breccias and nodular, bioturbated sediment.[7]

Regarding the communication within the field the non-reservoir layers of Sarvak, D, F and H act as horizontal barriers to flow. Even so, this is apparently not the case over the whole field surface, which indicates the presence of faults.

Together with the core description, one transversal fault in the western part of the field and several small normal faults in the eastern part of the field could be identified. [1]

The oil is generally undersaturated, with a gravity of 26 - 29° API, and around 3,5 weight percent sulfur content.

In the central region of Ilam and the northwestern region of Sarvak, oil quality is lighter or GOR is significantly lighter. Some asphaltene production had been observed there. [5]

There is no clear indication of significant pressure support from the aquifer, since a considerable reservoir pressure depletion of up to 2000 psi from initial reservoir pressure has been observed. As well, static pressure measurements in aquifer wells did not show any major depletion.

On the other hand, the wells were choked back after the water cut had exceeded more than 3% due to on-site water treatment capacity restrictions. [5]

There exists as well a suspicion that layers of asphaltene could stop the water. [1]

Therefore no clear statement about aquifer presence can be made at the moment.

About 124 wells have been drilled since the start of production, of which 100 were still producing at end of 2003. The cumulative production at this time point was 782 MMSTB, which corresponds to a recovery factor of 2%. [1]

Table 2.3: Oil Field Fluid Parameters [4]

		<b>Ilam</b>	<b>Sarvak</b>
<b>API gravity</b>	[°API]	29	26
<b>Viscosity</b>	[cP]	1 cP at 104,3 °C	
<b>Initial GOR</b>	[SCF/STB]	782	438
<b>FVF</b>	[RB/STB]	1,413	1,267
<b>Reservoir Temperature</b>	°C	104 °C at 11200 ft	
<b>Original reservoir pressure</b>	[psi]	5985 psi at 1200 ft	
<b>Pressure gradient</b>	[psi/ft]	0,39	
<b>OWC</b>	[ft]	- 11800	- 13650
<b>Bubble Point Pressure</b>	[psi]	1800-3000	

## 2.3. UNCERTAINTIES

The following uncertainties have been identified from Total in-house literature:

- (1) Fracture / Drain Network
- (2) Matrix Permeability
- (3) Degree of Compartmentalization
- (4) Aquifer Strength
- (5) Formation Compressibility
- (6) Horizontal Wells

### 2.3.1. Fracture / Drain Network <sup>[3],[4],[8]</sup>

Most of the oil production originates from the reservoir layer with the poorest petrophysical properties, Sarvak E. It is strongly assumed that intensive fracturing is causing this behavior.

Nevertheless, fractures have only been detected in one core, where they seem to have rather tectonic than diagenetic provenance.

However, this could be explained with poor core retrieval from highly fractured zones.

The fractures were included in the simulation model, though not in the classical way by specifying a double porosity, but as thin, high porosity - high permeability drain layers.

The fracture network is laterally more extensive in the Sarvak E than in Ilam or Sarvak G or Sarvak I. Drain layers have however been modeled also in these layers to a certain extent.

Fracture permeability was found by history matching, being in the order of 50 - 100 mD.

The “exact” value of fracture porosity could not be evaluated up to date, but the estimated fracture porosity range is between 0,05 – 1 %.

For the modelling in the reservoir simulation model a value of 0,4% was used to match high initial oil flowrate.

Nevertheless it was indicated that this values was uncertain, and that a sensitivity analysis for this parameter should be carried out.

For the sensitivity analysis, a low value of 0,05% and a high value of 1% fracture porosity were used, corresponding to a worst and best case according to the fracture porosity estimation.

### 2.3.2. Matrix Permeability <sup>[1],[3],[8]</sup>

In Ahwaz, the layer which contributes most to production has the lowest permeability, it is in general below <1 mD.

Matrix permeability was established from correlations to measured porosity from plugs and logs.

A good correlation could be established between porosity vs. air permeability for the matrix facies with a porosity of greater than 8%, thus for rock type 3.

For the facies with a porosity below 8% the correlation was found to be more random, due to the presence of fissures and dissolution.

From the standard core analysis data (SCAL), the matrix permeability to oil was found to be about ten times less than the matrix permeability to air which is an unusual result. Normally the matrix permeability to oil is no more than two thirds of the matrix permeability to air.

Also for the history matching this strongly reduced value had to be used.

Due to the heterogeneity of the formation there exists the possibility of an upside to this value.

Gas injection is envisaged as a future EOR measure, thus there is expectation to find greater permeability values. An average permeability of 1 mD would let the gas bypass the matrix and therefore be detrimental to gas injection.

In the base case model, permeability values are different for each cell but average less than 1 mD. For the sensitivity analysis, each permeability value was multiplied by 50, in order to obtain a permeability value which allows the oil to flow into the matrix.

Since 1 mD is already a very low value, only an upside sensitivity was analysed.

### 2.3.3. Degree of Compartmentalization <sup>[3],[9]</sup>

Some horizontal and vertical barriers have been identified from pressure measurements. These are:

Three barriers to vertical flow are evident from pressure measurements and production data: the layer Sarvak F in the northwest which separates Sarvak E from Sarvak G, the layer Sarvak H in the centre that acts as a barrier between Sarvak G and Sarvak I, and Sarvak D in the centre and southeast which separated Sarvak E from the Ilam reservoir.

Barriers to horizontal flow are linked to faulting: the barrier between the wells AZ-64 and AZ-34 is most likely related to presence of transverse fault, the barriers next to AZ-55 and AZ-52 suggest the presence of thrust faults along the flank of the structure.

In addition to these confirmed barriers - in order to history match pressure and production for all the wells - Ilam C had to be strongly compartmentalized in the full field model. Also in Sarvak some additional barriers were introduced, but not as strongly as in Ilam.

Since only a risk of stronger compartmentalization was indicated in the literature, only this sensitivity analysis was carried out.

The following pictures illustrate the increase in compartmentalization for each sector:

Sector West

Fig. 2.5: Transmissibility barriers in x - direction

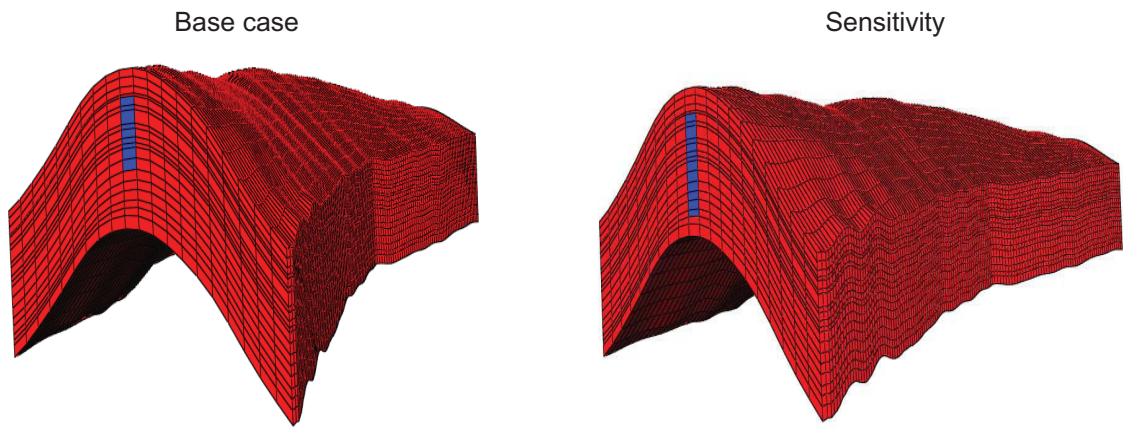


Fig. 2.6: Transmissibility barriers in y - direction

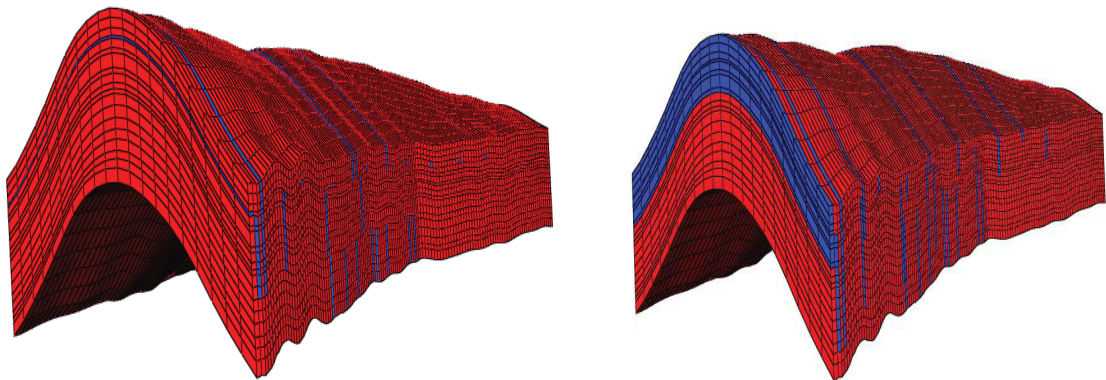
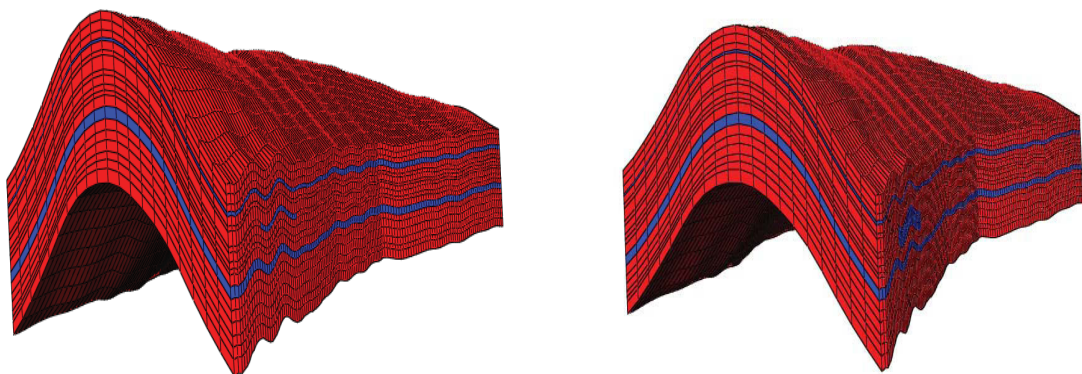


Fig. 2.7: Transmissibility barriers in z - direction





Middle Sector

Fig. 2.8: Transmissibility barriers in x - direction

Base case

Sensitivity

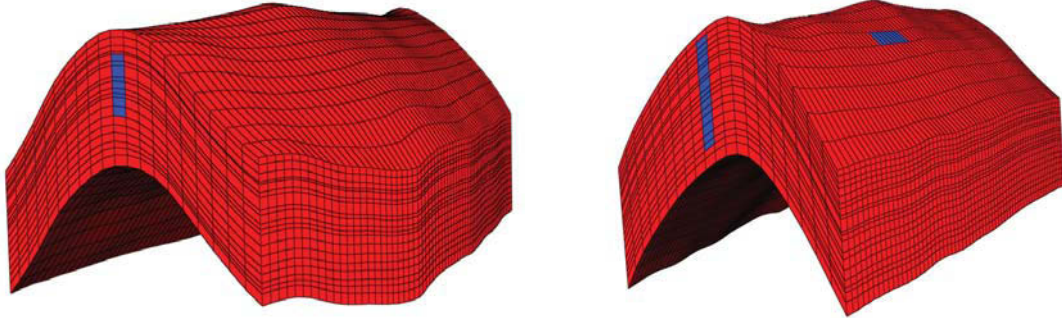


Fig. 2.9: Transmissibility barriers in y - direction

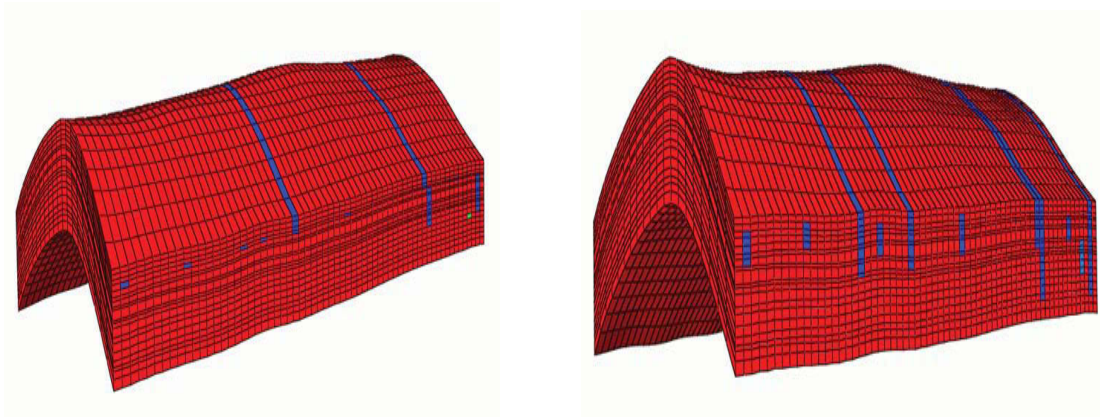
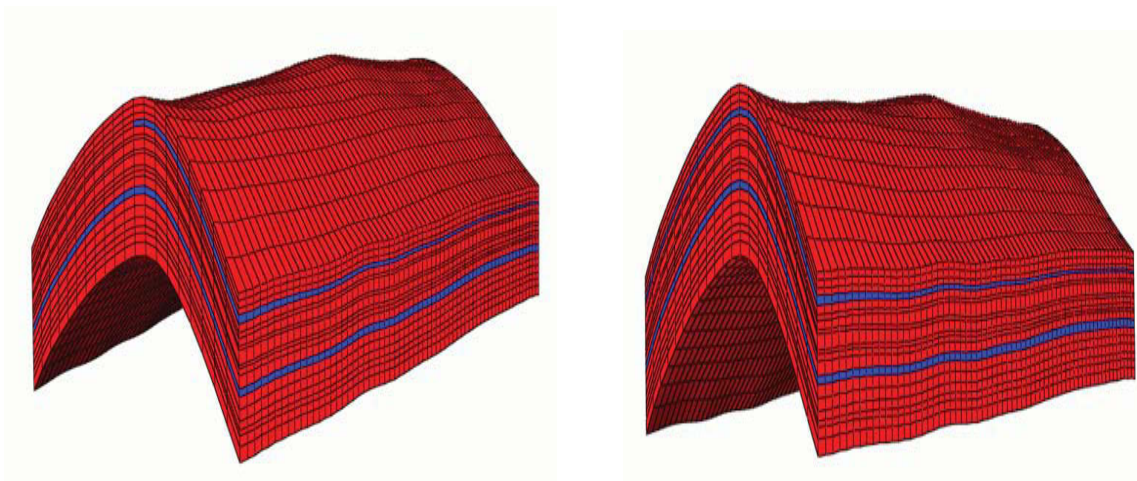


Fig. 2.10: Transmissibility barriers in z - direction



### Sector East

There are no transmissibility barriers in x- direction present in this sector.

Fig. 2.11: Transmissibility barriers in y - direction

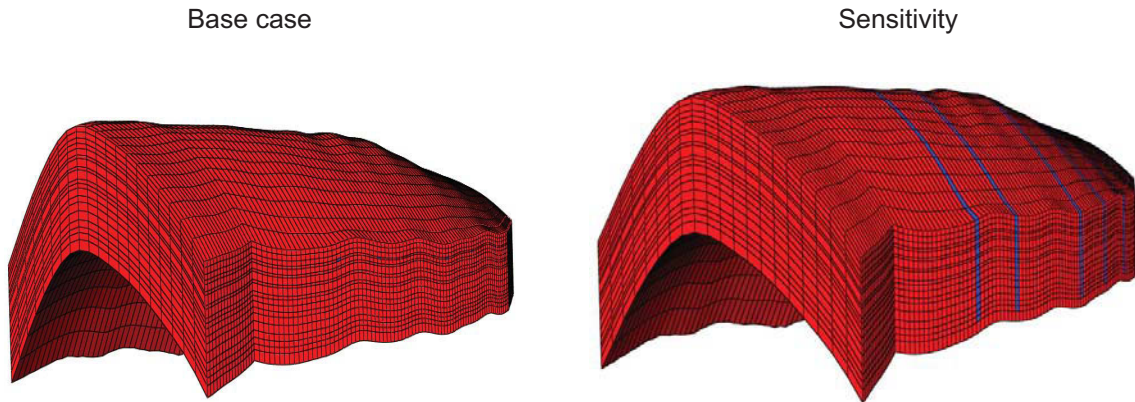
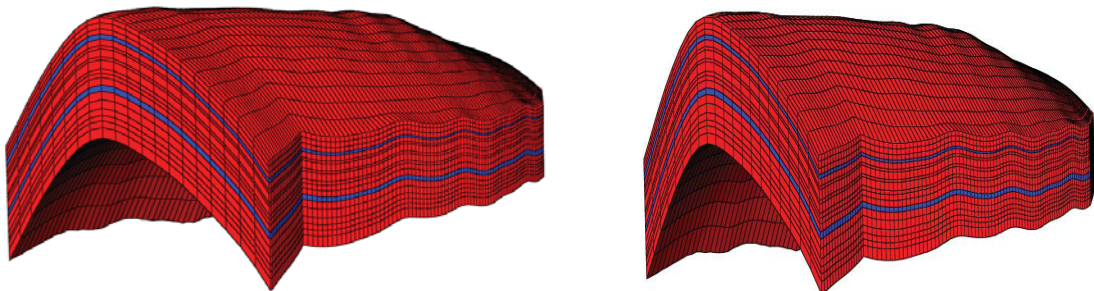


Fig. 2.12: Transmissibility barriers in z - direction



#### 2.3.4. Aquifer Strength <sup>[3],[4],[8]</sup>

The presence and force of a hypothetical aquifer could not be determined up to the present. This is due to the lack of historical water production due to water treatment capacity restrictions; wells have been choked back as soon as their water cut surpassed 3%. Moreover, whilst a significant pressure depletion of 2000 psi could be observed in the oil leg, pressure in the aquifer wells did not change considerably.

On the other hand, precipitation of asphaltenes has been observed, and there is reason to assume that also layers of asphaltene could stop the water flowing into the tubing.

In the full field reservoir simulation model the aquifer permeability had to be reduced to zero to keep the field water production below 5000 bwpd. Thus the sensitivity analysis base case does not consider an aquifer.

For the sensitivity analysis, a Carter-Tracey aquifer was added to the sector models. The aquifer properties are listed in table 2.4. The aquifer is connected to all reservoir layers.

The restriction of shutting the wells at a water cut of 3% has been suspended, as the main interest in this study is the principal, undisturbed behavior of the field.

Table 2.4: Ahwaz hypothetical aquifer properties

Radius	10000	ft
Height	1500	ft
Porosity	0,5	%
Permeability	300	mD

### 2.3.5. Formation Compressibility <sup>[3],[8]</sup>

No laboratory experiments have been carried out to determine the formation compressibility; instead reservoir analogue data of a comparable field was used.

However, for the history match it was necessary to multiply the rock compressibility by 3, compared to the value that was found in literature.

Apart from the history match there is no physical indication for a compressibility value that big.

The base case is the history matched model with the increased permeability value of  $9 \cdot 10^{-6}$  1/psi, for the sensitivity analysis the analogue value of  $3,45 \cdot 10^{-6}$  1/psi was used.

### 2.3.6. Horizontal Wells

Horizontal wells have not been mentioned in the literature, thus it is strongly assumed that no horizontal wells have been drilled up to date. Lacking obvious reasons not to drill horizontal wells, this is certainly always an interesting aspect to investigate.

Due to the tight well spacing, several existing wells were converted to horizontal wells in 2004, instead of introducing new wells.

Base Case:     Sector West    34 vertical wells  
                   Sector Middle 45 vertical wells  
                   Sector East    29 vertical wells

Sensitivity:    Sector West:   3 horizontal wells completed in Sarvak E, 2 in Sarvak G  
                   Sector Middle: the 4 horizontal wells are all completed in Sarvak E  
                   Sector East:    the 6 horizontal wells are all completed in Sarvak E

The layer of the completion was chosen according to the extent of sweep at the end of the base case simulation.

## 2.4. RESERVOIR MODEL

Due to the availability of a full field model, no sector model was ad hoc constructed. The full-field model was divided into three sector models, to reduce simulation runtime and to address the characteristics of each part.

The sector model characteristics are determined mainly by the occurrence and distribution of flow barriers and high drain layers.

As can be seen in the figures 7.2.5 - 7.2.7, the western sector features many flow barriers, particularly in y – direction, but also in x and z direction.

Drain layers are not abundant in this sector, according to table 2.6 the highest average permeability in a layer is about 7,9 mD, occurring on top Sarvak E. If a drain layer is characterized by having an average permeability > 5 mD; 4 out of 20 layers can be considered as drain layers. Two are present in Sarvak E, the other two in Sarvak G.

Figures 7.2.8 - 7.2.10 illustrate that the center sector is less compartmentalized. However, this sector is already highly fractured, the highest average permeability being 20,6 mD, on top of Sarvak E. 6 out of 20 layers can be considered as drain layers in the center part, one in Ilam C, three in Sarvak E and two in Sarvak G (see table 2.7).

In the east sector, some vertical barriers are present, but only in y – direction. Fracturing on the other hand is seen to be strongest here, as the highest average permeability per layer is 55 mD on top of Sarvak. Nine out of 20 layers can be considered as drain layers here, one in Ilam C, six in Sarvak E and two in Sarvak G (see table 2.8).

The full field model has grid dimensions of [20] [300] [20] grid cells. With the real field dimensions of about 24800 × 232300 × 2870 feet, there results an average grid block dimension of [1240][775][145] feet.

According to indications in the literature, the model was divided into the respective sectors as following: [4]

West: [20] [132] [20]

Center: [20] [63] [20]

East: [20] [105] [20]

Fig. 2.13: Ahwaz sector models side and total view

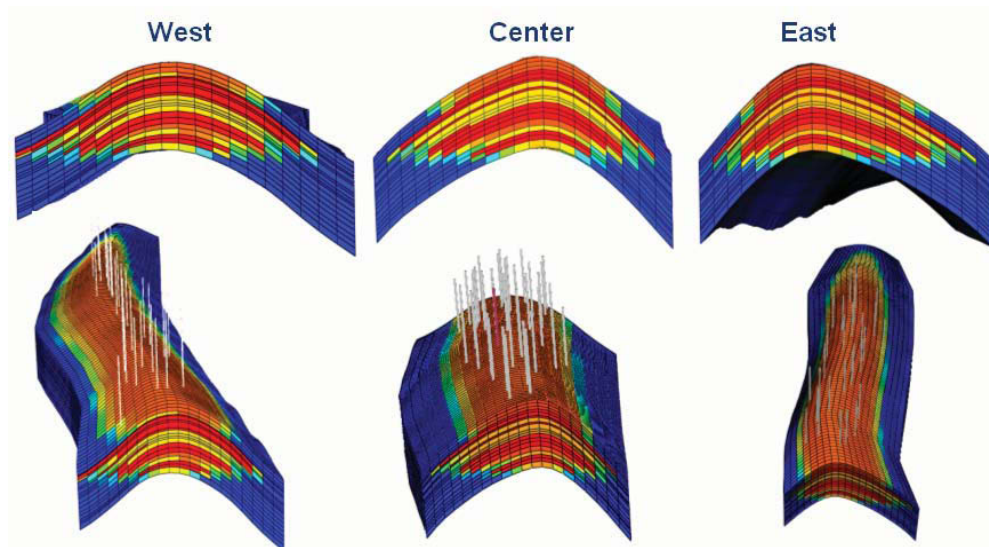


Table 2.5: Wells and completions

	West	Center	East
<b>number of wells total</b>	<b>34</b>	<b>45</b>	<b>29</b>
completed in			
<b>Ilam C</b>	12	15	5
<b>Sarvak E</b>	3	15	17
<b>Sarvak G</b>	18	7	6
<b>Ilam C &amp; Sarvak E</b>	1	1	0
<b>Sarvak E &amp; Sarvak G</b>	0	7	1

Table 2.6: Reservoir model properties – western part

Layer	h [ft] West	Porosity [-]	K(h) [mD]	$\frac{k_v}{k_h}$ [-]	Formation
1	150,3	0,12	0,623	1	Ilam C
2	129,2	0,182	1,113		
3	131,6	0,161	0,620		
4	133,3	0,113	0,140		
5	116,8	0,071	3,471	1	Sarvak E
6	123,5	0,045	7,867		
7	98,7	0,020	6,724		
8	148,9	0,071	0,252		
9	78,0	0,073	0,480		
10	120,7	0,111	0,182		
11	129,5	0,090	0,022		

12	85,4	0,083	0,249	1	Sarvak G
13	159,4	0,056	0,252		
14	138,3	0,026	0,583		
15	138,1	0,058	5,499		
16	175,1	0,119	0,051		
17	200,0	0,111	0,024		
18	167,8	0,004	5,453		
19	140,1	0,052	0,051		
20	205,6	0,106	0,008		

Table 2.7: Reservoir model properties – center part

Layer	h [ft] Center	Porosity [-]	K(h) [mD]	$\frac{k_v}{k_h}$ [-]	Formation
1	---	---	---	---	Ilam C
2	134,4	0,157	0,379	1	
3	147,3	0,147	0,221		
4	102,1	0,104	0,047		
5	81,0	0,063	5,211		1
6	140,0	0,023	16,931		
7	69,4	0,004	20,578		
8	275,7	0,099	0,051		
9	76,3	0,046	4,869		
10	151,3	0,075	0,013		
11	86,7	0,085	0,021		
12	72,2	0,065	0,846		
13	161,1	0,073	1,306		
14	194,4	0,028	9,440		
15	180,6	0,041	11,976	1	Sarvak G
16	175,6	0,108	0,051		
17	181,3	0,107	0,052		
18	135,4	0,004	8,888		
19	186,9	0,052	2,281		
20	236,7	0,112	0,026		

Table 2.8: Reservoir model properties – eastern part

Layer	h [ft] East	Porosity [-]	K(h) [mD]	$\frac{k_v}{k_h}$ [-]	Formation
1	---	---	---	---	Ilam C
2	132,0	0,131	0,078	1	
3	139,3	0,128	0,075		

4	121,7	0,105	0,175	1	Sarvak E		
5	137,9	0,041	54,945				
6	135,1	0,022	55,000				
7	110,1	0,004	51,570				
8	175,2	0,066	0,657				
9	105,8	0,049	12,398				
10	199,2	0,079	3,044				
11	96,9	0,049	16,072				
12	174,1	0,069	2,407				
13	195,4	0,037	21,240				
14	135,0	0,060	7,316				
15	187,2	0,043	11,875			1	Sarvak G
16	174,3	0,102	0,032				
17	134,6	0,107	0,041				
18	133,2	0,004	21,685				
19	129,5	0,055	4,263				
20	262,8	0,105	0,021				

The models start production on the first of February 1972. They are history matched until 2004; for prediction purpose a forecast period until 31st December 2030 was chosen.

It has to be mentioned imperatively that the original model contained production restrictions in the sense of a history file. Since these restrictions do not allow the model to produce freely and unconstrained, they were removed for the purpose of the sensitivity analysis, after the correct history match was assured.

Thus it is important to bear in mind that cumulative productions resulting from the sensitivity analysis model DO NOT correspond to values that can be found in the literature!

The following operational conditions have been implemented in the sector model for the sensitivity analysis:

- A minimum well tubing head pressure of 100 psi. The wells will shut if the tubing head pressure falls below this limit. The well bottom whole pressure is governed by a lift table.
- The wells are put under an individual liquid rate (oil, water and gas) constraint which is different for all well. Rates range from 2500 - 10000 bbl/day.
- The wells start and shut subsequently according to the indicated real production history. All of existing wells are on stream in 2005.
- There is no scheduled operation downtime for all wells at once.
- Duration of the simulation production time is 58 years.

During the simulation runs, some failure happens in the case k-50 of the Western part, due to numerical instability.

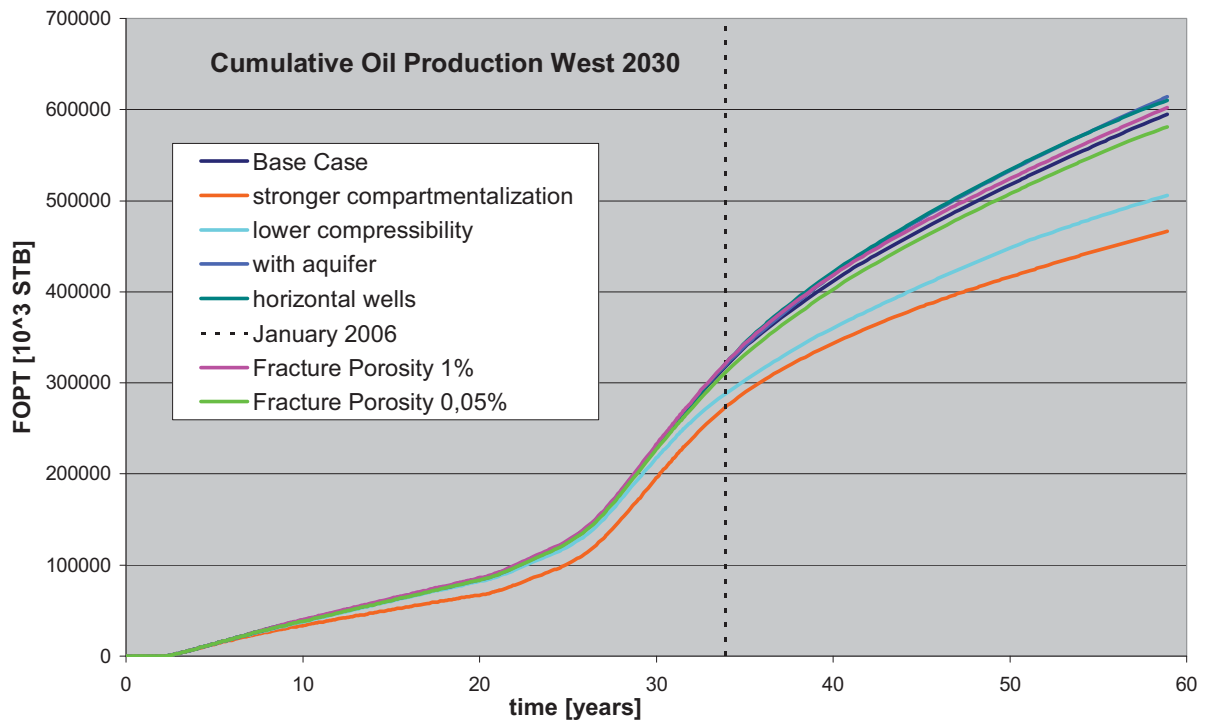
## 2.5. RESULTS AND DISCUSSION

### 2.5.1. Results West

Table 2.9: Sensitivity analysis input data west

Uncertainty	Base Case	High Case	Low Case
Fracture Network	$\Phi(\text{fracture})$ 0,4%	-----	$\Phi(\text{fracture})$ 0,05%
Matrix Permeability	$k(\text{matrix,orig.}) \sim 1$ mD	$k(\text{matrix,orig.}) \times 50$	-----
Compartmentalization	original barriers	-----	more barriers
Aquifer Strength	no aquifer	aquifer present	-----
Formation Compressibility	$9 \cdot 10^{-6}$ 1/psi	-----	$3,45 \cdot 10^{-6}$ 1/psi
Horizontal Wells	34 vertical wells	29 vertical wells + 5 horizontal wells	

Fig. 2.14: Cumulative oil production - base case and sensitivities – sector west



The main parameters to consider are the stronger compartmentalization and the lower compressibility which have a strong influence on the oil production and the pressure. The effect on oil production is negative for both parameters, as in the case for the reduced formation compressibility for the pressure, whereas the stronger compartmentalization has a beneficial effect for pressure maintenance.

The main parameters to consider are the stronger compartmentalization and the lower compressibility which have a strong influence on the oil production and the pressure. The effect on oil production is



negative for both parameters, as in the case for the reduced formation compressibility for the pressure, whereas the stronger compartmentalization has a beneficial effect for pressure maintenance.

Fig. 2.15: Water cut - base case and sensitivities – sector west

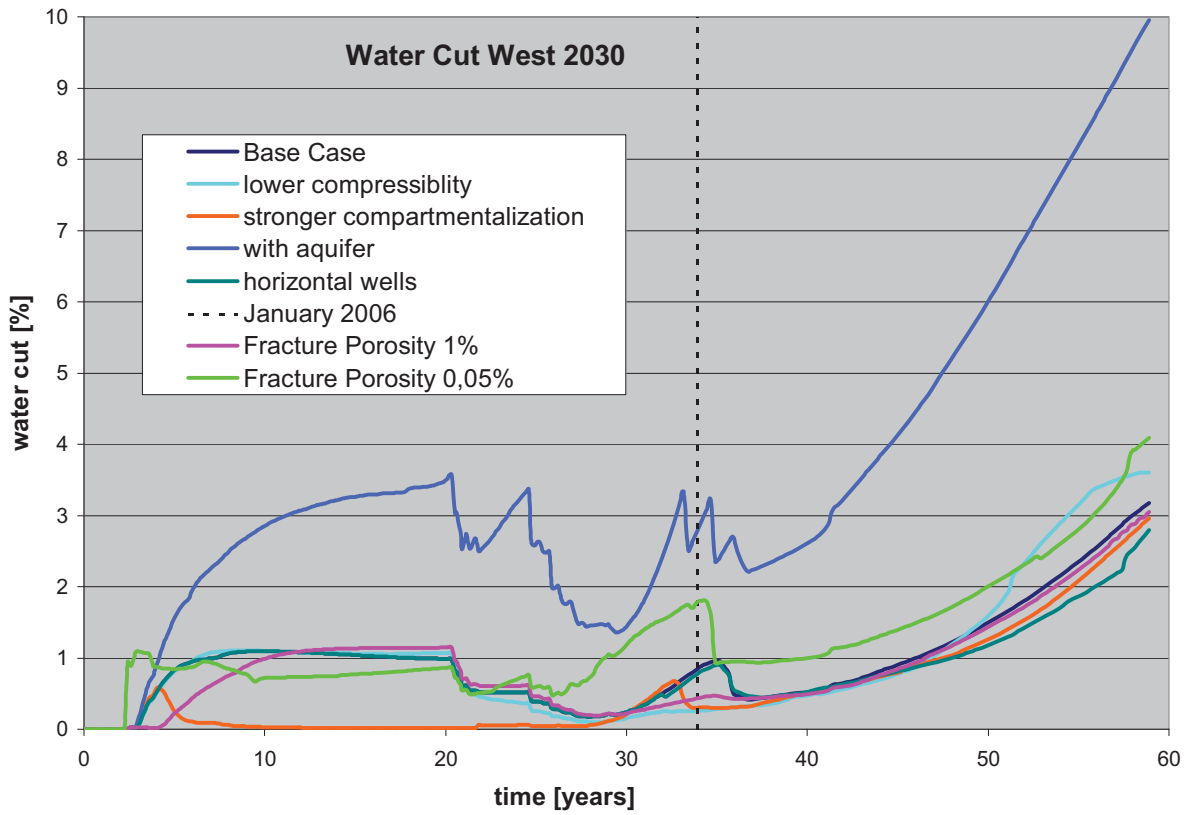
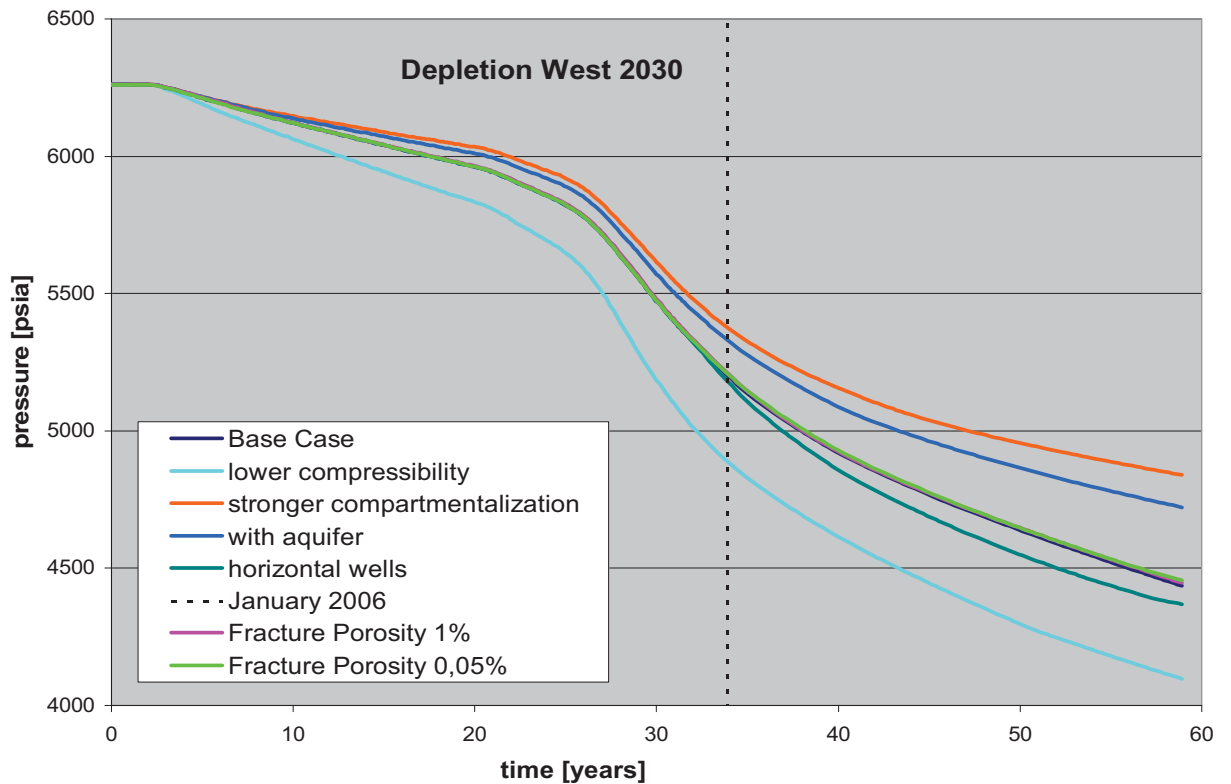


Fig. 2.16: Pressure depletion - base case and sensitivities – sector west



All other uncertainties considered have poor influence on the cumulative oil production although significant impacts are observed on pressure and water cut when an aquifer is added. This is probably due to the contrast between the high permeability drains and the low matrix permeability, the aquifer water flowing preferentially through the high permeable layers which mainly increases water production.

Another striking result is the poor gain resulting from the 5 wells converted in 2004 into horizontal wells. The conversion reduces the number of layers crossed by the well as the horizontal wells are located in one respective permeable layer only. The ability to better produce from these particular layers is balanced by the poor drainage of the other layers; sometimes they are not drained at all, due to a vertical flow barrier isolating the layers and preventing communication.

The drop in recovery factor due to lower compressibility is globally in line with the value calculated using the total compressibility in a single phase depleted reservoir.

Table 2.10: Result overview Ahwaz, western sector

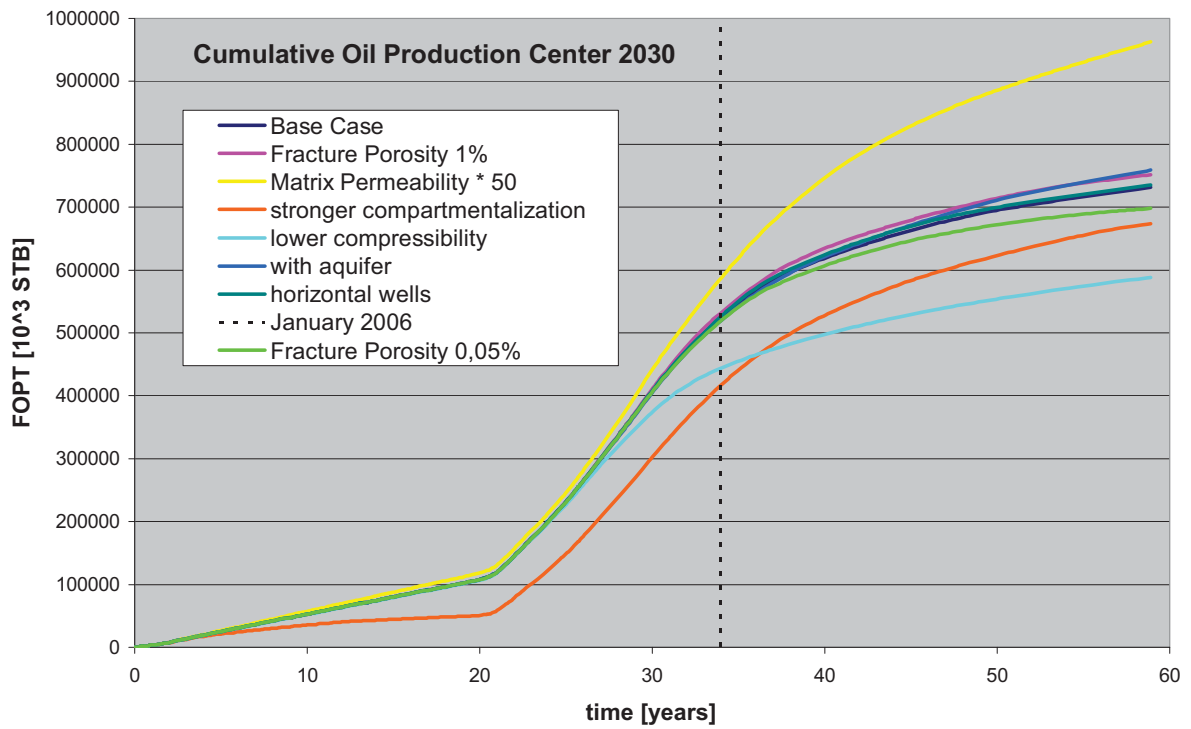
OOIP [Mbb]		13444		Np in 2030 (60 years)	RF	WC in 2030 (60 years)	Avg. reservoir pressure in 2030 (60 years)
				[Mbb]	[%]	[%]	[psi]
Base case figures	Base case			595	4,4%	3,2%	4435
0,1 to 1 mD no aquifer 34 vertical wells	High cases			convergence failure - model not running			
	Matrix permeability	k multiplied by 50		614	4,6%	10,0%	4722
	Aquifer strength	Aquifer present		610	4,5%	2,8%	4369
	Horizontal wells	5 wells converted in 2005					
	Low cases						
$\Phi$ fracture = 0,4%	Fracture network	$\Phi$ fracture = 0,05%		581	4,3%	4,1%	4457
Original barriers	Compartmentalisation	More vertical/Horizontal barriers		467	3,5%	3,0%	4840
9E-6 psi-1	Formation Compressibility	3,45E-6 psi-1		506	3,8%	3,6%	4097

### 2.5.2. Results Center

Table 2.11: Sensitivity analysis input data center

Uncertainty	Base Case	High Case	Low Case
Fracture Network	$\Phi(\text{fracture})$ 0,4%	-----	$\Phi(\text{fracture})$ 0,05%
Matrix Permeability	$k(\text{matrix,orig.}) \sim 1$ mD	$k(\text{matrix,orig.}) \times 50$	-----
Compartmentalization	original barriers	more barriers	-----
Aquifer Strength	no aquifer	aquifer present	-----
Formation Compressibility	$9 \cdot 10^{-6}$ 1/psi	-----	$3,45 \cdot 10^{-6}$ 1/psi
Horizontal Wells	45 vertical wells	41 vertical wells + 4 horizontal wells	

Fig. 2.17: Cumulative oil production - basecase and sensitivities –center sector



The presence of an aquifer has less impact than in Western part as it less powerful because it is only connected to the flanks of the reservoir; moreover the liquid offtake is higher.

The matrix permeability has a large effect on production and reservoir pressure due to the originally poor to medium permeability values and poor to medium coverage of the high permeability streaks. Lower compressibility has also a large negative influence on both oil production and reservoir pressure.

Compartmentalization leads to a lower production drop than in the West part due to weaker barriers constraints.

The conversion to horizontal wells has negligible influence for the same reason as for the western part.

Regarding the Water Cut, the real impact of the sensitivities are difficult to assess due to the very low numerical values (<3%).

Fig. 2.18: Water cut - base case and sensitivities –center sector

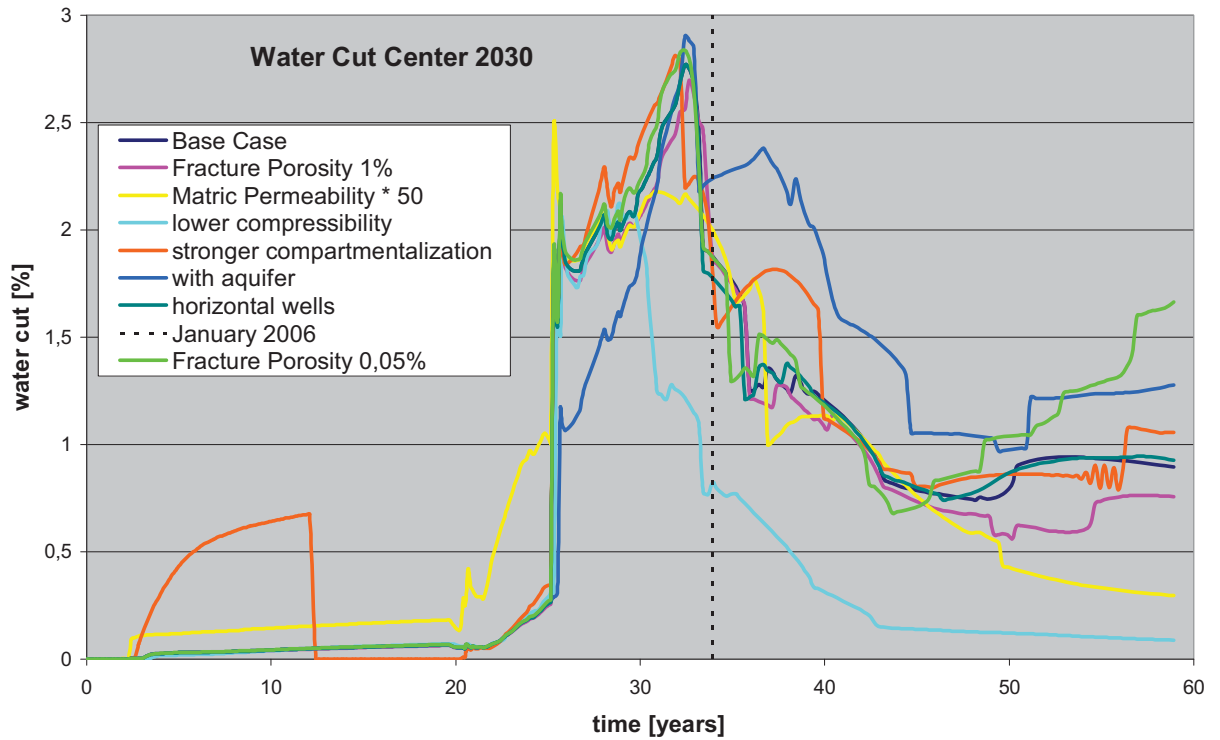


Fig. 2.19: Pressure depletion - base case and sensitivities –center sector

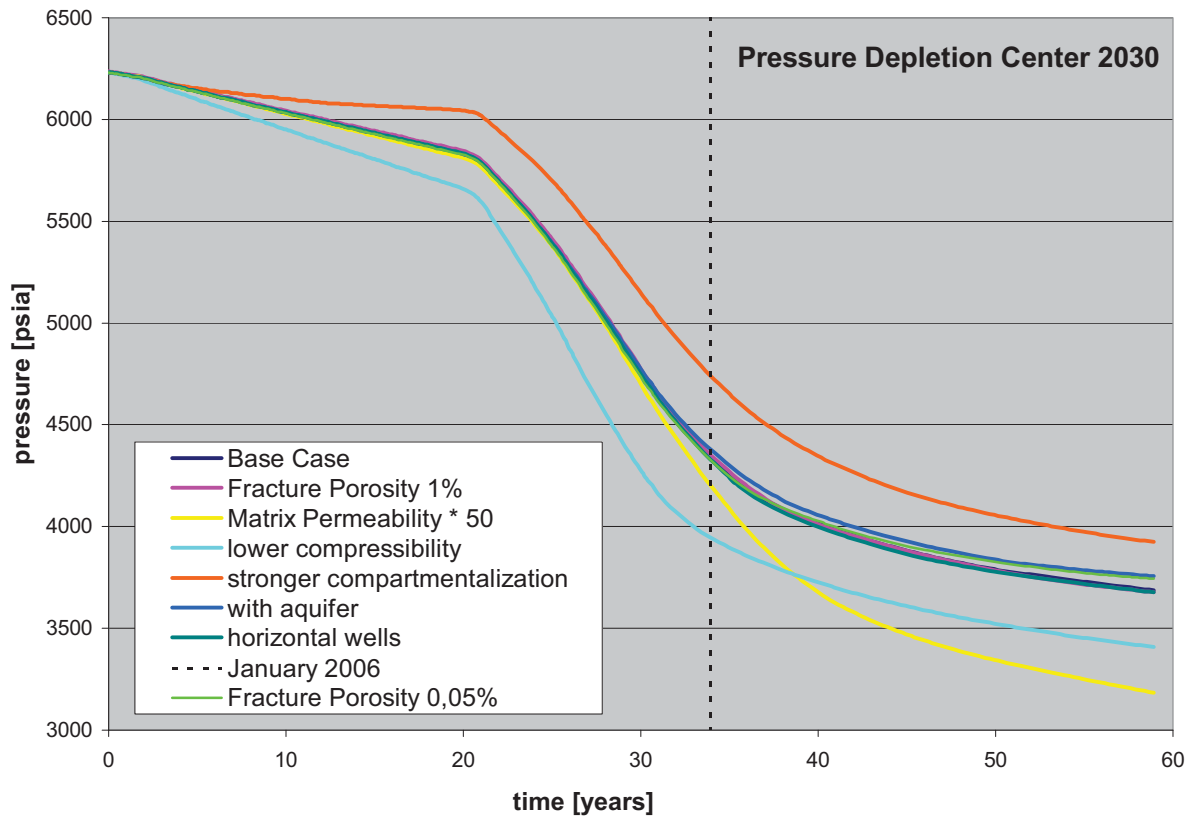


Table 2.12: Result overview Ahwaz, center sector

OOIP [Mbbbl]		13060		Np in 2030 (60 years) [Mbbbl]	RF [%]	WC in 2030 (60 years) [%]	Avg. reservoir pressure in 2030 (60 years) [psi]
Base case figures	Base case			731	5,6%	0,9%	3687
	High cases						
0,1 to 1 mD no aquifer 45 vertical wells	Matrix permeability	k multiplied by 50		963	7,4%	0,3%	3184
	Aquifer strength	Aquifer present		759	5,8%	1,3%	3756
	Horizontal wells	4 wells converted in 2005		735	5,6%	0,9%	3677
Low cases							
$\Phi$ fracture = 0,4%	Fracture network	$\Phi$ fracture = 0,05%		698	5,3%	1,7%	3743
Original barriers	Compartmentalisation	More vertical/Horizontal barriers		674	5,2%	1,1%	3924
9E-6 psi-1	Formation Compressibility	3,45E-6 psi-1		588	4,5%	0,1%	3409

### 2.5.3. Results East

Table 2.13: Sensitivity analysis input data east

Uncertainty	Base Case	High Case	Low Case
Fracture Network	$\Phi$ (fracture) 0,4%	-----	$\Phi$ (fracture) 0,05%
Matrix Permeability	k(matrix,orig.) ~ 1 mD	k(matrix,orig.)×50	-----
Compartmentalization	original barriers	more barriers	-----
Aquifer Strength	no aquifer	aquifer present	-----
Formation Compressibility	9E-6 1/psi	-----	3,45E-6 1/psi
Horizontal Wells	29 vertical wells	23 vertical wells + 6 horizontal wells	

The sensitivity cases in this sector have resulted in larger changes in oil production, reservoir pressure and water cut than in the other parts. This is due to the very poor initial compartmentalization, the more frequent occurrence of high permeability streaks and the better matrix properties.

This is particularly visible when regarding the cases with aquifer presence and the conversion to horizontal wells. The higher average permeability allows better sweeping due to the aquifer support, which also leads to a significant rise of the water cut. The effect of the conversion to horizontal wells is significant because no vertical barriers inhibit drainage and the matrix permeability is generally better.

The relative impact of the matrix permeability × 50 case is less compared to the center sector model. Because the properties were initially better, an enhancement does not show the same beneficial effect.

The effect of less compressibility is particularly detrimental on the production, but also on the pressure.

Fig. 2.20: Cumulative oil production - base case and sensitivities – sector east

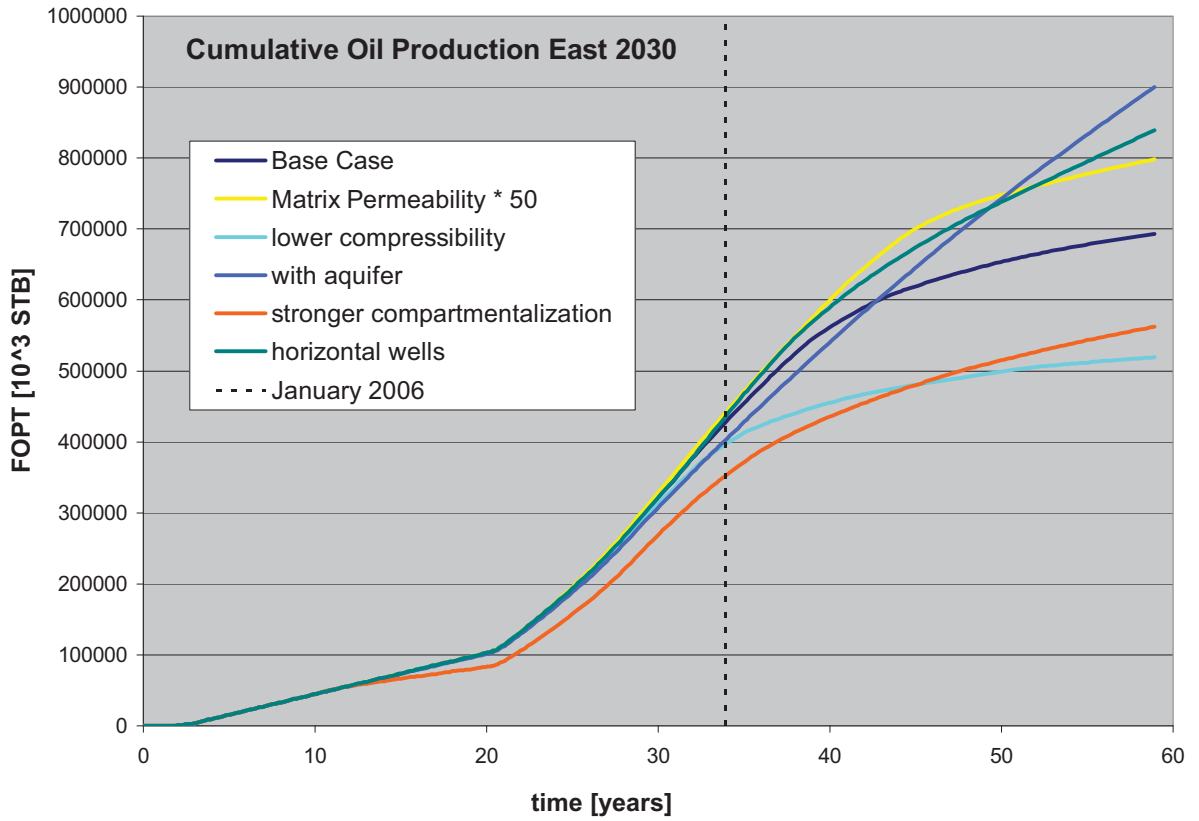


Fig. 2.21: Water cut - base case and sensitivities – sector east

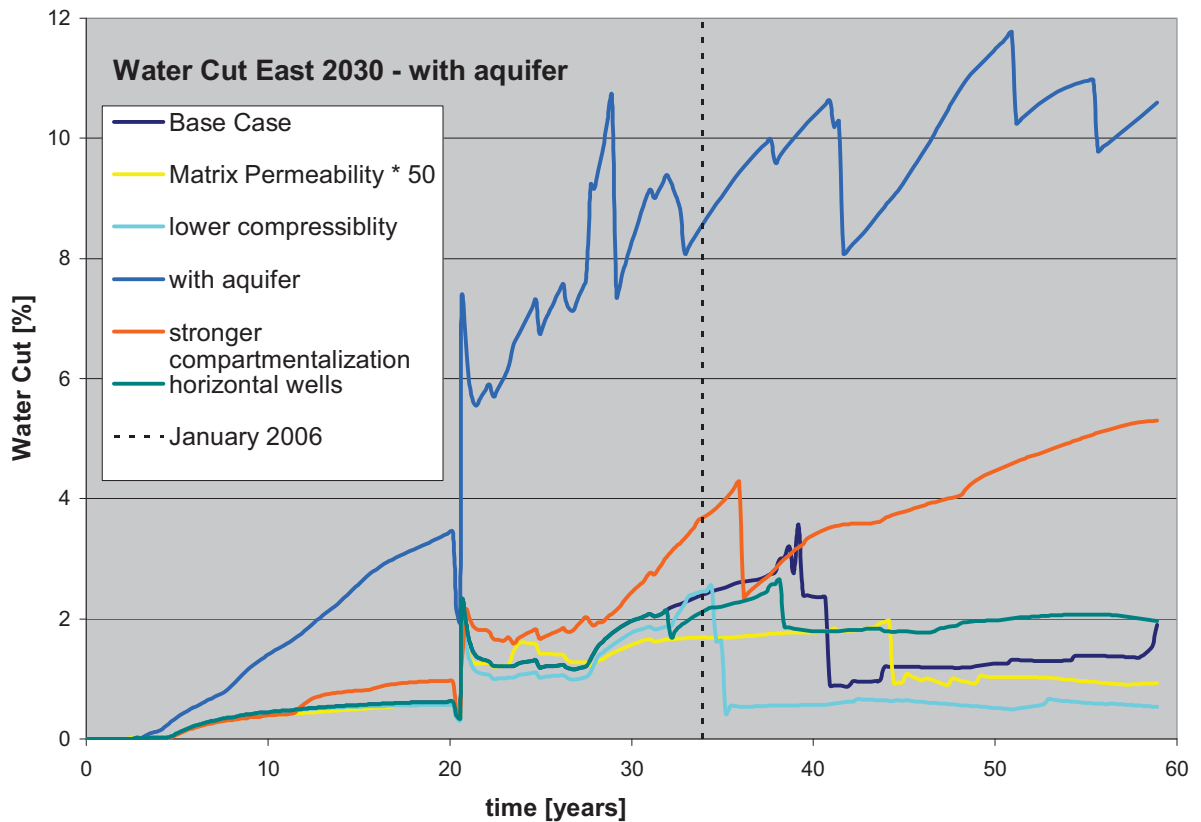


Fig. 2.22: Pressure depletion - base case and sensitivities – sector east

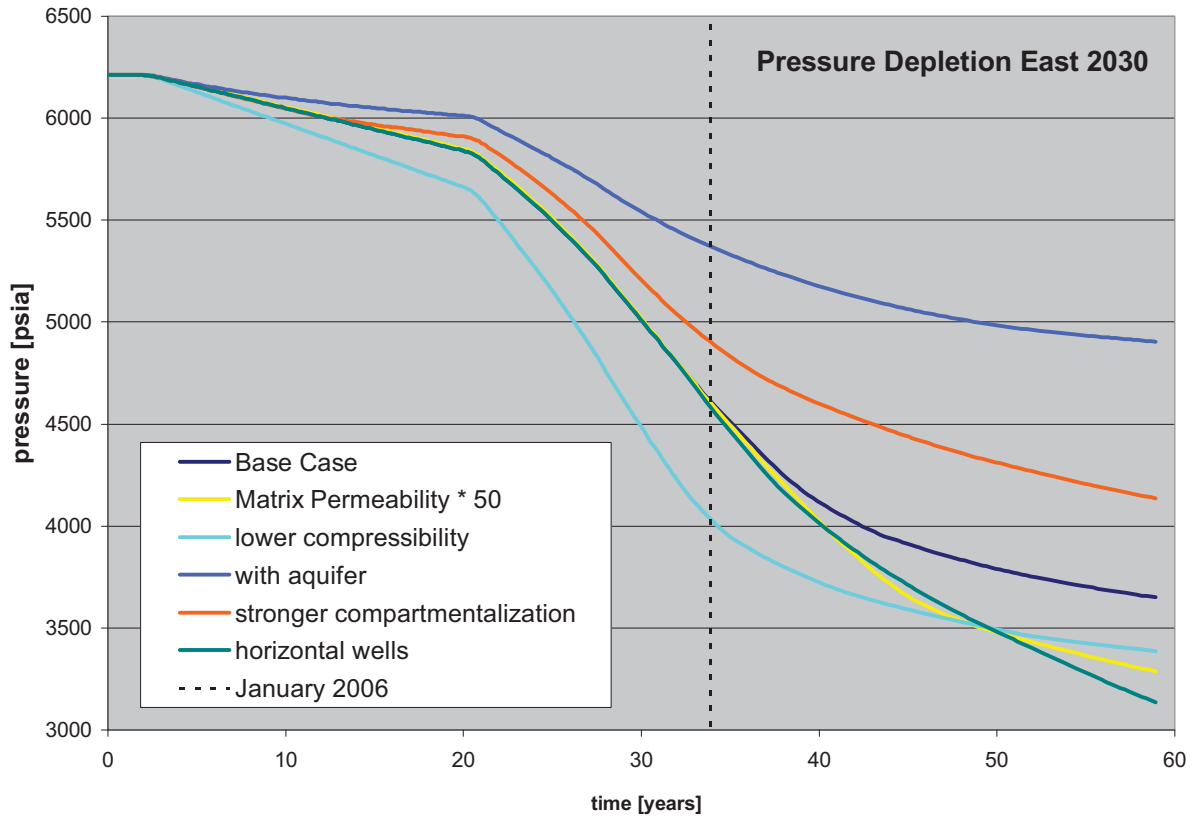


Table 2.14: Result overview Ahwaz, eastern sector

OOIP [Mbb]		12150	Np in 2030 (60 years) [Mbb]	RF [%]	WC in 2030 (60 years) [%]	Avg. reservoir pressure in 2030 (60 years) [psi]
Base case figures	Base case		693	5,7%	1,9%	3651
	High cases					
0,1 to 1 mD no aquifer 29 vertical wells	Matrix permeability	k multiplied by 50	798	6,6%	0,9%	3288
	Aquifer strength	Aquifer present	900	7,4%	10,6%	4904
	Horizontal wells	6 wells converted in 2005	839	6,9%	2,0%	3137
Low cases						
Original barriers	Compartmentalisation	More vertical/Horizontal barriers	562	4,6%	5,3%	4136
9E-6 psi-1	Formation Compressibility	3,45E-6 psi-1	519	4,3%	0,5%	3387

#### **2.5.4. General conclusions on Ahwaz results**

In a tight and compartmentalized reservoir, horizontal wells have a poor influence on production if they are completed in only one layer. Highly deviated wells that penetrate several layers should be preferred.

Adequate aquifer support or water injection require a minimum reservoir permeability to be effective.

Rock Compressibility remains a major issue for both oil production and reservoir pressure. Core measurements have to be performed, preferentially under stress conditions, especially in case of fractured reservoirs.

Compartmentalization has a strong influence, but this drawback can be mitigated through comprehensive reservoir structural and petrophysical studies to improve well locations and enable an optimized positioning of new producers.

Water cut values remain low even in case of an aquifer present. This issue is minor except in case of very strong aquifer or water injection where quick invasion of high permeability streaks could result in high water cut production.

A change in fracture porosity affects only more or less original “easy” to produce oil in the fracture system. Thus it does not affect the major oil production process involving very slow oil flow from the matrix to the high permeability streaks, which is conveying most of the oil to the well.



### 3. DOROOD

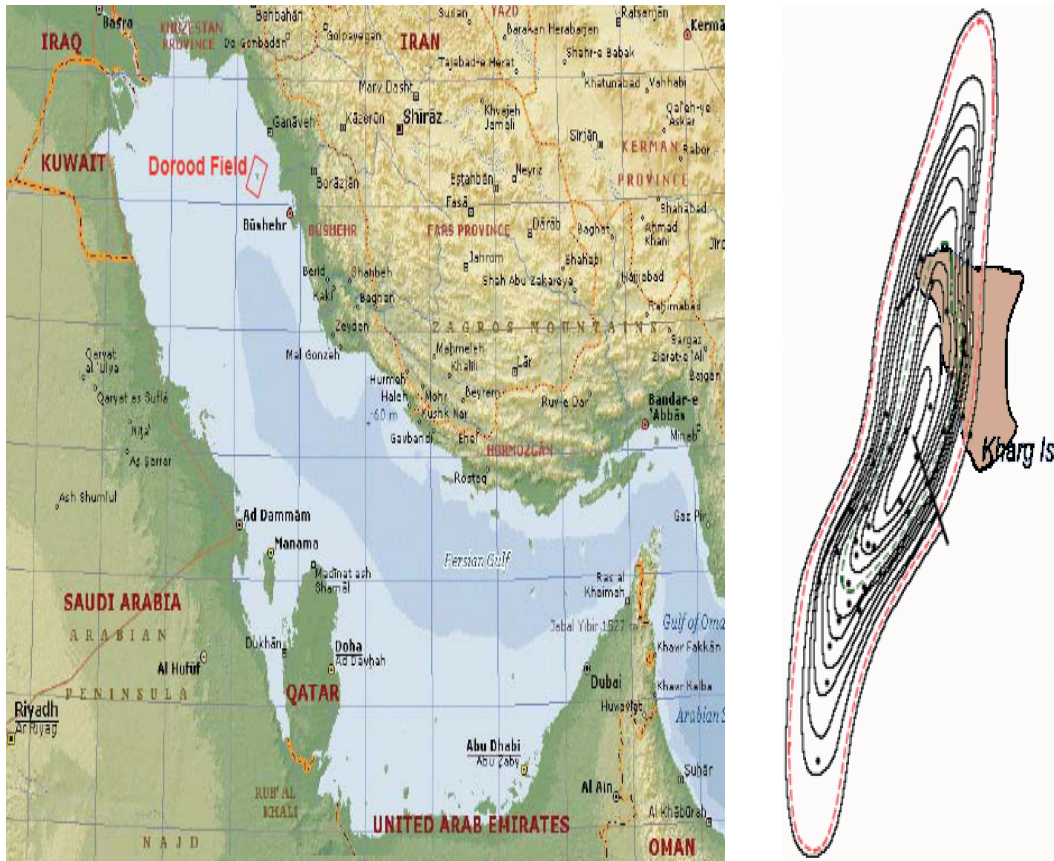
The Dorood oil field is located offshore Iran in the northern Persian Gulf area. For the most part it is an offshore oil field; a fraction however is onshore below the Kharg island.

The oil producing reservoirs lie in the Fahliyan limestone formation which has been deposited in the Neocomian stage of the Lower Cretaceous. It overlies the Late Jurassic Hith formation. The Fahliyan bears five distinct formations in this region (from top to bottom): Ratawi, Khami, Yamama, Manifa, and Arab. Ratawi, Khami and Arab are considered as non-productive due to their poor reservoir properties, therefore this study is only concerned with the reservoirs Yamama and Manifa. The overlying Khalij and Gadvan formations act as seals of the reservoirs.

The field geometry is a NNE/SSW elongated anticline; its dimensions are approximately 15,5×3,7 miles. The dip of the flanks increases from south (10°) to north (25°). The top of the Yamama reservoir is lying at 11950 ft TVDs. Original oil in place is estimated to be 8,5 billion bbl.

Dorood was discovered in 1961 and put on stream in September 1964. Since then, 1,41 billion bbl have been produced, which corresponds to a recovery factor of approximately 17 %. [10],[11]

Fig. 3.1: Location and geometry of Dorood [12]



### 3.1. SEDIMENTOLOGY

The depositional timeframe of the Fahliyan, the Lower Cretaceous was a rather quiet period. Carbonate was deposited relatively undisturbed in very shallow water; this led to a flat platform topography. This kind of platform is also called intra-cratonic platform. Especially in the Manifa a very large extent of shallow carbonate shelf can be seen. [13]

The structure of Dorood was defined by two major folding events: the Arabian plate folding in the Late Cretaceous and the Zagros belt folding in the Plio-Pleistocene. [14]

The compression caused by the Arabian plate folding formed a long, northeast oriented anticline. Several faults were formed by the tensions created. During the later Zagros folding, these faults were reactivated with a different stress.

Interestingly, the oil charge of Dorood occurred before the Zagros folding, which resulted in a significant change of the reservoir fluid PVT properties. [15]

Three different structural styles are recognizable within Dorood, which naturally partition the field into a northern, center and southern part.

North Dorood is a high asymmetric anticline which was highly tilted in the Tertiary through an uplift of the east flank. Gently dipping normal faults are present which have a highly variable throw and tectonic pattern. Possible communication through the fault throws is assumed.

South Dorood on the contrary is a gentle symmetric anticline; the faults are subvertical. This zone has been only slightly uplifted during Tertiary folding.

Central Dorood is an intermediate triangular zone, with both vertical and dipping faults. The east flank was also highly uplifted during Tertiary. [15]

The Yamama formation, which overlies Manifa, is the major reservoir interval. It is grouped in two units, the Middle and Upper Yamama.

The Upper Yamama, which has a thickness of about 330 feet has not been cored or logged. The vertical evolution is marked by an increase in muddy facies, probably corresponding to a global eustatic trend.

Middle Yamama is marked by major flooding surface, which is characterized by outer-shelf muddy facies (Mudstone to Wackestone). Afterwards progradational parasequences of bioclastic Wackestone to Packstone appear. Very different facies are deposited after the maximum flooding surface; during the downward shift shallow-marine aggrading sequences in a global shallowing up context are deposited. The top of Middle Yamama was deposited in a supralittoral environment; the sub-emersive facies which are mainly cemented oolitic grainstones have been called beach-rocks.

Manifa, which is a Late Jurassic interval, consists of very shallow marine evaporitic to dolomitic sediments. These are for example bioclastic Grainstone or Packstone-Grainstone with peloids and bioclasts. In a sequence stratigraphic sense, Manifa shows a shallowing upwards trend, and it is strongly assumed that it came to an exposure at the end of Manifa deposition.

Therefore the facies were affected by strong dissolution, which led to the creation of vugs and interconnected pore space.

Yamama is sealed by the overlying Khami and Ratawi formations which are muddy - shaly limestones.

Core information is just available from one well; this core has been the reference for all subsequent geological interpretation. Sequential layering is based on thin section and  $\Phi/k$  core measurement interpretation. For the base Manifa and Upper Yamama, which have not been cored, the geological interpretation is based on wireline log interpretation. [13]

Seven rock types, that is packages with similar  $\Phi/k$  – characteristics could be distinguished in Dorood according to their  $\Phi/k$  – characteristics. They are classified in vuggy and non-vuggy; no ties to lithofacies have been calibrated yet. [16]

Fig. 3.2:  $\Phi/k$  – relationship in Upper Yamama [12]

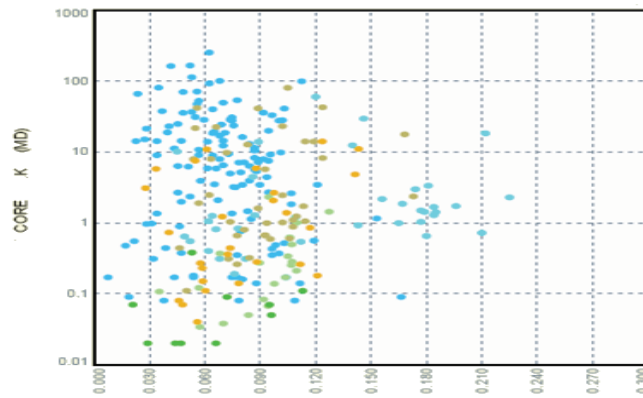


Fig. 3.3:  $\Phi/k$  – relationship in Lower Yamama [12]



Fig. 3.4:  $\Phi/k$  – relationship in Manifa [12]

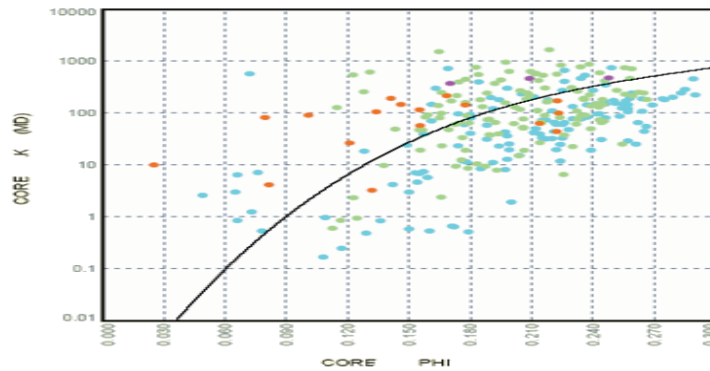


Table 3.1: Formation layering [17]

Group	Formation	Zone	Avg. Thickness	Lithology	Rock Type	Reservoir Quality
F A H L I Y A N	Upper Yamama	CD	161 ft 49 m	Packstone with peloids	Rock Type 2 non – vuggy	poor
		E	82 ft 25 m	Wackestone/Mudstone with small shells		
		F1	49 ft 15 m	Wackestone with algae debris	&	
		F2	52 ft 16 m	Mudstone with miliolids	Rock Type 3 vuggy	
	Middle Yamama	G1	56 ft 17 m	Rudstone with intraclasts	Rock Type 4 non – vuggy	generally poor  but excellent in some parts  ( high permeability streaks)
		G2	49 ft 15 m	Grainstone/Rudstone with shells, peloids		
		G3	52 ft 16 m	Grainstone/Rudstone coarse grained		
		H1	95 ft 29 m	Fine grained Grainstone, well sorted	&	
		H2	82 ft 25 m	Fine grained Grainstone, structureless	Rock Type 5 vuggy	
		I1	66 ft 20 m	Packstone/Floatstone	Rock Type 6  n/a	
		I2	62 ft 19 m	Coarse peloidal Packstone		
		J	108 ft 33 m	Peloidal Packstone		
	Manifa	L1	L2	72 ft 22 m	Fine peloidal Packstone	Rock Type 7  Vuggy
				128 ft 39 m	n/a	
			39 ft 12 m			

Layers A and B represent the Ratawi and Khami layers, which are not included in the reservoir model and thus also discarded here. [16]

In the Middle Yamama, several high permeability (10-100 mD) streaks were recognized from the wireline log signature.

These high permeability zones were found to be preferably developed at depositional sequence tops. They are believed to result from aerial exposure and meteoric dissolution.

From the core interpretation the high permeability streaks were found to be associated to Rudstone facies which are interpreted as “short lived storm events”. The vugs found in the Rudstone beds are up to several millimeters wide, but they are very heterogeneously distributed.

The sequences in which the high permeability streaks could be interpreted are pinching out northwards; they are therefore not considered present in the northern part of the field. [17]

### 3.2. RESERVOIR GEOLOGY

The Dorood field consists of two reservoirs, the Lower Cretaceous Yamama and the Late Jurassic Manifa.

Based on core and log information, the Dorood field was divided into a 17 layer model (see table 3.1) Layers 1 and 2 represent the non-reservoir Ratawi and Khami formations. The Upper Yamama is represented by four layers, the Lower Yamama by nine layers and Manifa by two layers. [16]

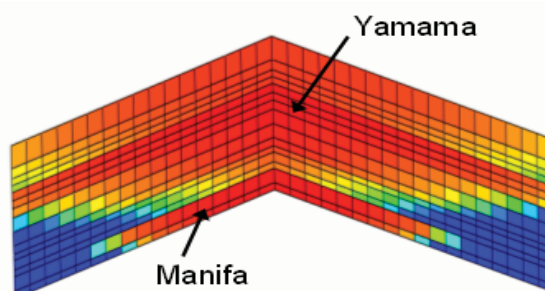
It is important to note that the fieldwide correlation of the reservoir layers is based only on very scarce data. It is mainly based on log correlation since core description was only available for one well at that time. Three additional cores that were taken have confirmed the reservoir zonation, even though they were taken in the vicinity of the first core, which does not completely validate the result.

There exists a significant risk that not all the reservoir heterogeneity was captured by the reservoir description as it exists now. [12]

Yamama and Manifa are separated by a transmissibility barrier, which acts as seal in the south but, according to RFT/MDT data, layer communication was observed in the northern part. The communication is believed to be enhanced by contact through the fault throws. In the center part both of the two phenomena are encountered. [16]

There exist two different Oil-Water contacts. For the Yamama reservoir it lies at 11920 ft/TVDss, for Manifa at 12055 ft/TVDss. At this depth the common free water level is supposed. [10]

Fig. 3.5: Dorood reservoir zonation



The Dorood field contains numerous faults; more 150 were interpreted from seismic sections, of which the 34 biggest and supposedly most important were retained for the full field model.

Faults are present everywhere, although the retained faults in the simulation model are located only in the center and northern part. They are believed to have only small throws and thus no impact in the south. [16]

During the reservoir correlation work some very low porosity/permeability zones were interpreted particularly at the top of the Middle Yamama and traced over significant distances of up to 10 km in the field. These zones have been interpreted as cemented sand related to exposure and lithification. These facies were thus named “beach rocks”.

In some cases they coincided with offsets in pressure data from RFT/MDT measurements, thus it can be assumed that they act as flow barriers to a certain extent. [12]

On the basis of log signatures, high permeability drains were associated with the vuggy facies found in Middle Yamama, especially in the southwestern part. They are associated with dissolution by meteoric water of the top Manifa, which is believed to having been subaerially exposed at that time. Permeability values in these drain layers range from 10 to 100 mD.

The sections containing these streaks pinch out northwards, therefore they are only recognized in the southern and center part of Dorood. [17]

Table 3.2: Average reservoir properties fieldwide [10]

	Thickness (ft)	Porosity (%)	Permeability (mD)	OIIP (MMSTB)
Upper Yamama	344	9 - 12	1	2272
Middle Yamama	642	12 - 17	0,5 - 5	5061
Manifa	167	16 - 20	> 100	1169

The three sectors, north, center and south, generally own the same petrophysical properties for a given layer. Difference occurs only in case of the occurrence of high permeability streaks.

It is not sure if an initial gas cap existed; in any case a strong bubble point pressure gradient was found which is not compatible with thermodynamic equilibrium. At the top of Yamama, the oil is nearly saturated; at the bottom it is strongly undersaturated.

A theory considers an initial gas cap existed before after the Arabian plate folding which was then redissolved by diffusion through rapid burial during the Zagros folding. However, this will remain a hypothesis since it is not possible to prove this theory due to the depletion level of Dorood. [16]

The Manifa reservoir is connected to four different aquifers, namely in the center part on the west and east flank, and in the northern part on the north flank. On the east flank of the center part two different aquifers can be distinguished. The following table details their properties, as derived from history matching of the full field model: [16]

Table 3.3: Dorood aquifer properties [16]

		Manifa North	Manifa West	Manifa South-East 1	Manifa South-East 2
Connection length	[ft]	20900	36650	19280	12550
Height	[ft]	150	150	150	150
Permeability	mD	50	200	200	200
Porosity	-	0,1	0,2	0,15	0,25
Ratio	-	1,5	infinite	infinite	1,5
Connection Angle	°	60	120	180	180

Table 3.4: Oil Field Fluid Parameters [18]

		Yamama	Manifa
<b>API gravity</b>	[°API]	36	32
<b>Viscosity</b>	[cP]	0,17	0,6
<b>Initial GOR</b>	[SCF/STB]	1130	820
<b>FVF</b>	[RB/STB]	1,6	1,4
<b>Reservoir Temperature</b>	°C	112	125
<b>Original reservoir pressure</b>	[psi]	5670	5860
<b>Formation compressibility</b>	[1/psi]	$2 \cdot 10^{-5}$	$2 \cdot 10^{-5}$
<b>Bubble Point Pressure</b>	[psi]	5469	3626

Production started in September 1964 and was temporarily suspended during the Islamic revolution in early 1979 and again, as a result of the Iran-Iraq war, between 1981 and 1988.

The field is producing by natural depletion, however it was planned to implement water injection by August 2005. There exists no information if this intention was accomplished. [16]

The cumulative production in February 2006 was 1,42 Billion bbl, which yields a recovery factor of 17%. [10]

### 3.3. UNCERTAINTIES

The following uncertainties have been identified from Total in-house literature:

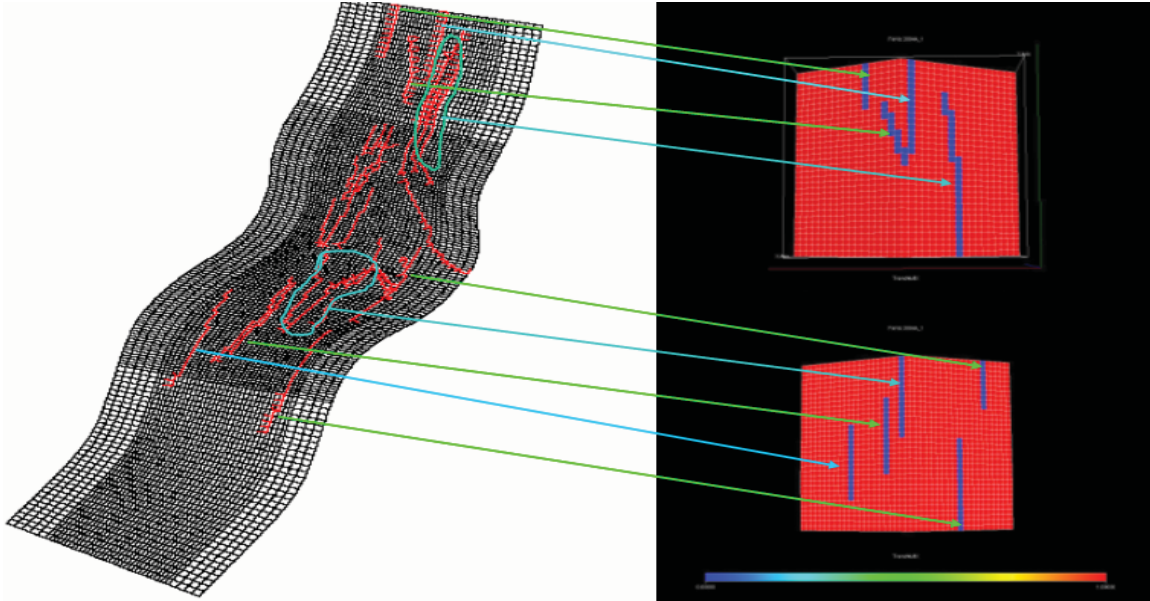
- (1) Fault Transmissibility
- (2) Layer Transmissibility
- (3) Extension of high k streaks
- (4) Rock type distribution
- (5) Different relative permeability curves
- (6) Impact of horizontal wells
- (7) Impact of water injection

### 3.3.1. Fault Transmissibility <sup>[12],[16]</sup>

More than 150 faults could be interpreted from the seismic data, of which the 34 biggest and supposedly most important were adopted for the full field model. The retained faults are present in the northern and center part.

Due to a lack in dynamic data, their importance and impact on the flow behavior are unclear.

Fig. 3.6: Fault mapping into sector model [16]



The 34 faults of the full field model were merged into 9 faults in the sector model as shown in Fig. 3.6. This was necessary on one hand because of the imprecise specification of the fault location, on the other hand it was due to the coarseness of the sector models.

The flow through the fault throw was modeled as fault transmissibility. In the base case the faults are intransmissible; consequently they do not enhance any communication between layers in different PVT regions.

In the sensitivity analysis the faults were modeled with full transmissibility. This case evaluates the option that the faults do not have any impact on flow behavior because they oppose zones with the same properties.

### 3.3.2. Layer Transmissibility <sup>[11],[12],[16]</sup>

Very low porosity/permeability zones that have been detected from their log signatures were interpreted as early lithified beach rocks. During correlation work some of these zones could be followed distances of several kilometers.

Nevertheless, their occurrence and connectivity remains unclear due to lack of core and log data.



These zones are potential transmissibility barriers, but if so, the extent and degree can only be found by integration of dynamic data, which is also sparse in Dorood.

For the full field model the extension of the beach rock zones was found by history matching, and the results of that were adopted for the sector models.

The tight zones are particularly present between the layers 4 and 5, which is the top of Middle Yamama, between layers 6 and 7 and between the layers 13 and 14. The latter is not necessarily a beach rock, it is rather the barrier between Yamama and Manifa, whose origin has however not been mentioned in the literature.

On the other hand, it was deduced from RFT/MDT data that this barrier is fully sealing in the south part, but that there is some communication in the center and northern part. The degree of communication in the center north was suggested with a MULTZ value of 0,3 which was adopted for the sector model.

In the base case all tight layers which are classified as beach rocks are completely intransmissible (MULTZ 0) in all three sector models.

The barrier between Yamama and Manifa is completely intransmissible in the south part, in the northern part it is modeled with a MULTZ value of 0,3. Since the boundary of the transmissible barrier in direction south is not well defined, approximately half of the Yamama/Manifa barrier in the center part was also modeled with transmissibility.

For the sensitivity analyses, following scenarios were modeled.

For the northern part the possibility of less communication than anticipated between Yamama and Manifa was modeled. A MULTZ value of zero was used for that.

The same was carried out for the center part, yet not for the whole area of the layer boundary but for approximately the half.

Another sensitivity analysis was intended for a high case, namely to model the beach rock layers as fully transmissible, in order to simulate no impact on flow behavior. Unfortunately this case is not running due to unresolved numerical instabilities in the model.

Fig. 3.7: distribution of tight layers, southern sector

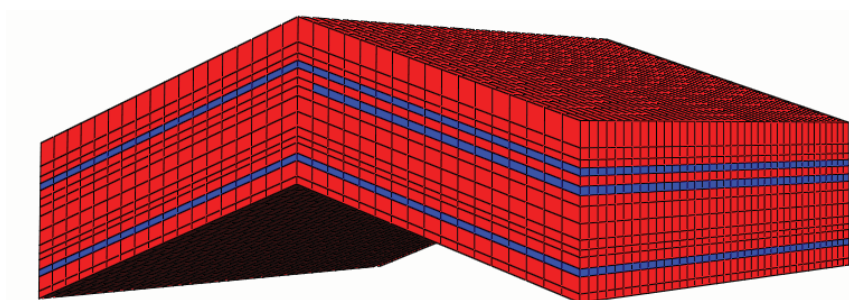


Fig. 3.8: distribution of tight layers, center sector, left basecase, right sensitivity

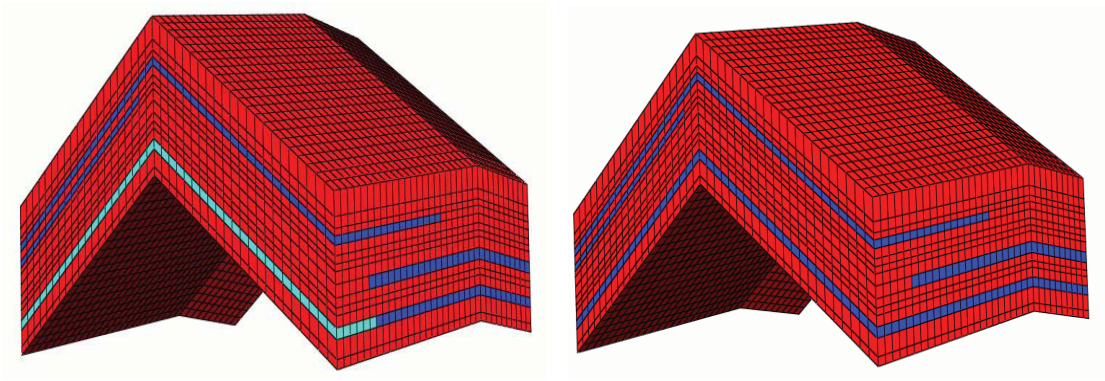
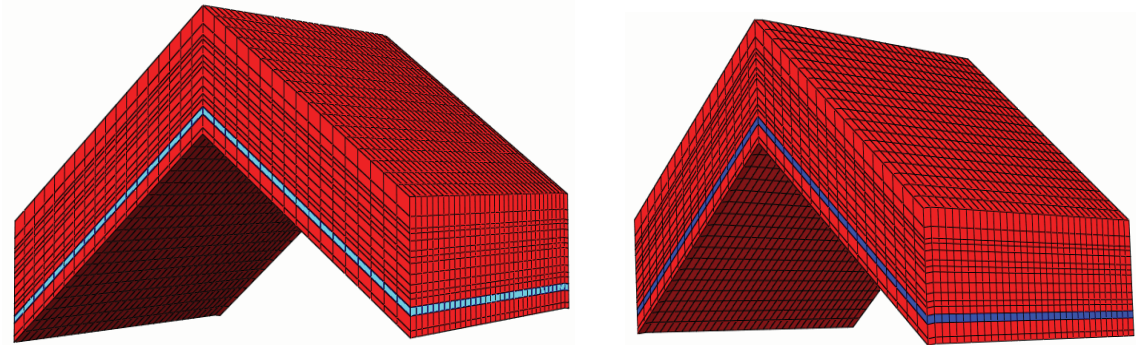


Fig. 3.9: Yamama/Manifa barrier, northern sector, left base case, right sensitivity



### 3.3.3. Extension of high k streaks <sup>[12],[16],[17]</sup>

High permeability streaks associated with vuggy facies were detected on log signatures in the southern and central part of Dorood..

They occur most likely due to enhanced dissolution through meteoric water influx, mainly in upper Middle Yamama. The presence of these high permeability drains could explain the good productivity from some wells.

However, the existence of these zones could not be physically proven due to the lack of core data. Therefore the extension and connectivity of the high permeability streaks are unknown (cp. with section on layer transmissibility).

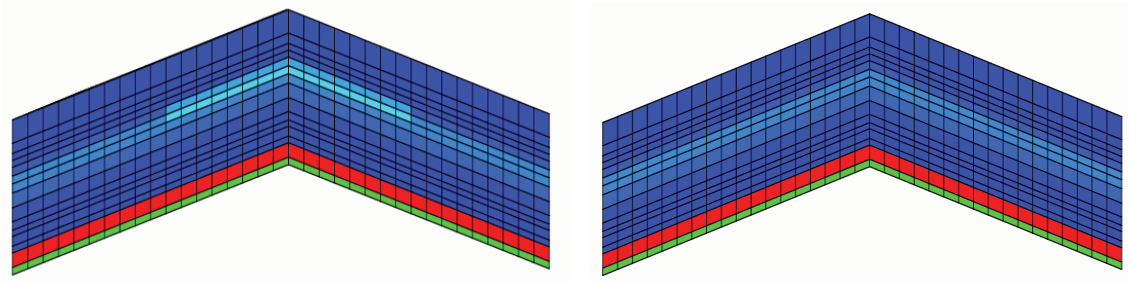
In the base case the high permeability streaks are modeled as being present in the south and center sector model.

For the base case the drain layers were modeled with an average permeability of 20–40 mD. This is lower than the before mentioned 100 mD, but the lower value was chosen to compensate for the different layer thickness.

In the sector model the average layer thickness is about 20 m, whereas the hypothetical physical thickness of the high permeability streaks is rather in the order of less than one meter.

For the sensitivity analysis this value was reduced to 10 mD – not to zero because this would be too close to matrix permeability – and there are indications of the drain layers from the log signature.

Fig. 3.10: high k streaks, southern sector, left base case, right sensitivity



### 3.3.4. Rock type distribution <sup>[11],[16]</sup>

Seven different rock types can be distinguished in Dorood according to their  $\Phi/k$  behavior. Rock type 1 is referring to the Ratawi/Khami layers, which are not modeled for the sensitivity analysis.

There exists no tie to a certain lithofacies, rather to a group of lithofacies (cp. Table 3.1).

There exists only a classification into vuggy and non-vuggy facies. Alike the high permeability streaks and the tight layers, also here the extension, respectively heterogeneity of the different rock types is unclear, especially in the Middle Yamama.

As base case it was, as indicated in the literature, modeled that the Middle Yamama contains vuggy and non vuggy facies. Since the presence of vuggy facies is physically confirmed from core interpretation, only an upside sensitivity analysis was carried out. The whole Middle Yamama was modeled as vuggy facies.

Table 3.5: rock type distribution, left base case, right sensitivity [12]

Rock type	Reservoir layers	Description	Rock type	Reservoir layers	Description
2	Upper Yamama	non vuggy	2	Upper Yamama	non vuggy
3	Upper Yamama	vuggy	3	Upper Yamama	vuggy
4	Middle Yamama	non vuggy	4	Middle Yamama	vuggy
5	Middle Yamama	vuggy			
6	Lower Middle Yamama	n/a	6	Lower Middle Yamama	n/a
7	Manifa	vuggy	7	Manifa	vuggy

### 3.3.5. Different relative permeability curves <sup>[11],[16]</sup>

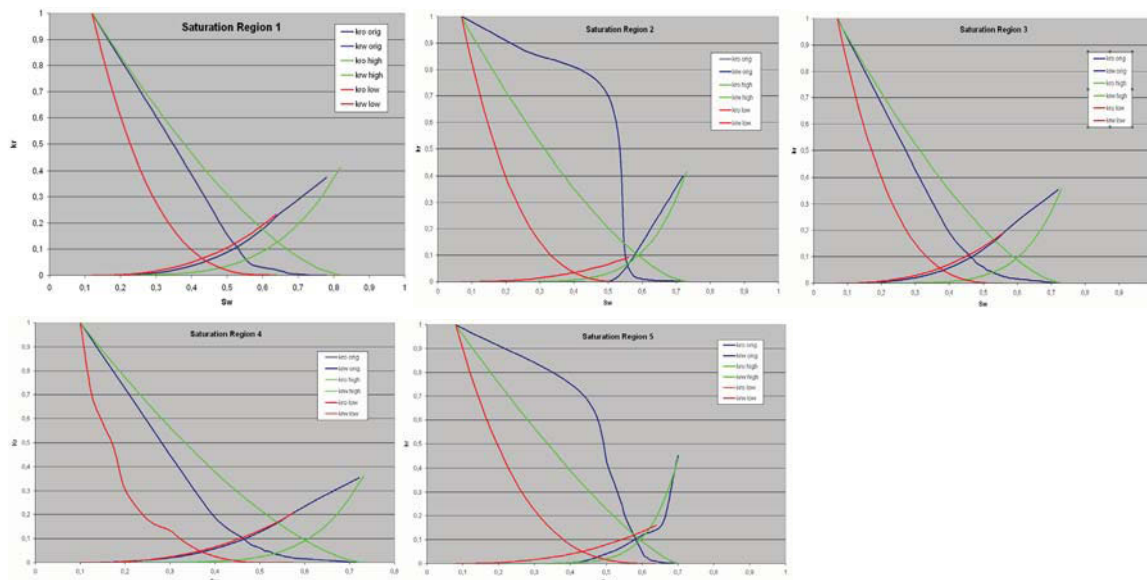
As mentioned before, there exists a strong saturation gradient from the top to the bottom of Dorood. Moreover it is reported that the lab measurements of Dorood plugs show a wide range of residual oil saturations.

The relative permeability curves are particularly mentioned as one of the greatest uncertainties in Dorood. The curves employed in the full field model were only found by history matching.

For the base case the same curves as in the full field model were used. There exist five different saturation regions, thus five different relative permeability curves. The lower/higher oil relative permeability curves for the sensitivity analysis were generated by changing the Corey coefficient and the residual oil saturation to water.

In the following there is an illustration of the different curves:

Fig. 3.11: Basecase and sensitivity relative -k curves for each saturation region



### 3.3.6. Impact of horizontal wells <sup>[10],[19]</sup>

Horizontal wells were considered from the beginning as a possible way to increase well productivity. In spite of that they have never been implemented.

The apparent reason for that were problems to drill high inclination boreholes in the unstable shale formations Kazhdumi and Gadvan, which are overlying Dorood.

Two different scenarios were modeled for the sensitivity analysis, in one scenario there exist horizontal wells from the beginning on; in the second scenario additional horizontal wells are drilled after the end of the history matching period, in 2005.

While the second sensitivity model refers directly to Dorood, the first one gives a hint of the benefits of horizontal wells for future analogue data use. To illustrate the particular benefit of horizontal wells, the number of wells was not changed, but rather some wells from the base case were converted to horizontal wells for the sensitivity analysis.

In the base case there are no horizontal wells present.

- Sensitivity analysis with horizontal wells from the beginning on:

From 16 vertical oil wells (18 completions), 2 single completion wells were converted to horizontal wells in southern sector.

From 15 vertical oil wells (18 completions), 4 single completion wells were converted to horizontal wells in center sector.

From 17 vertical oil wells (25 completions), 4 single completion wells were converted to horizontal wells in northern sector.

- Sensitivity analysis with horizontal wells starting in 2005:

3 horizontal wells were added to 16 vertical wells in the southern sector.

4 horizontal wells were added to 18 vertical wells in the center sector.

2 horizontal wells were added to 25 vertical wells in the northern sector.

### 3.3.7. Impact of water injection <sup>[16],[19]</sup>

Dorood was producing by natural depletion since the start of production. According to literature it is/was contemplated to implement water injection by August 2005. The intended injector well locations were reported. Yet there is no information is available if this intention was accomplished or if it had to be delayed.

In the base case no water injection is taking place. For the sensitivity analyses water injection is implemented according to the reported plan.

Sensitivity:      2 water injectors for 16 production wells in southern sector  
                      3 water injectors for 18 production wells in center sector  
                      6 water injectors for 25 production wells in northern sector

All water injectors are completed over both the Yamama and Manifa reservoirs.

### 3.4. RESERVOIR MODEL

Three sector models have been built for Dorood in order to properly address the different structural styles, for the southern, center and northern part, respectively.

The models are based on, for this purpose utilizable, information about the reservoir that has been gathered from various reports. The degree of complexity of the model is a function of the amount and detail of information that could be obtained.

In the southern sector there are, contrary to the other two sectors, no faults and no aquifer present. High permeability streaks could be detected there.

The center and northern part are both faulted and supported by an aquifer, the high permeability streaks however are only present in the center part, they have not been found in the North.

All the models consist of 15 reservoir layers, 13 for the Yamama and 2 for the Manifa. The sector models have the following real and grid dimensions: [16],[17]

Table 3.6: Dorood sector models dimensions

	South		Center		North	
real sector length [ft]	19685-19685-994		19685-16400-1024		19685-16400-935	
number of grid blocks	[35] [38] [15]		[42] [34] [15]		[35] [33] [15]	
length/grid block [ft/grid block]	X	562	X	469	X	562
	Y	518	Y	482	Y	497
	Z	66	Z	68	Z	62

Fig. 3.12: Dorood sector models side and total view

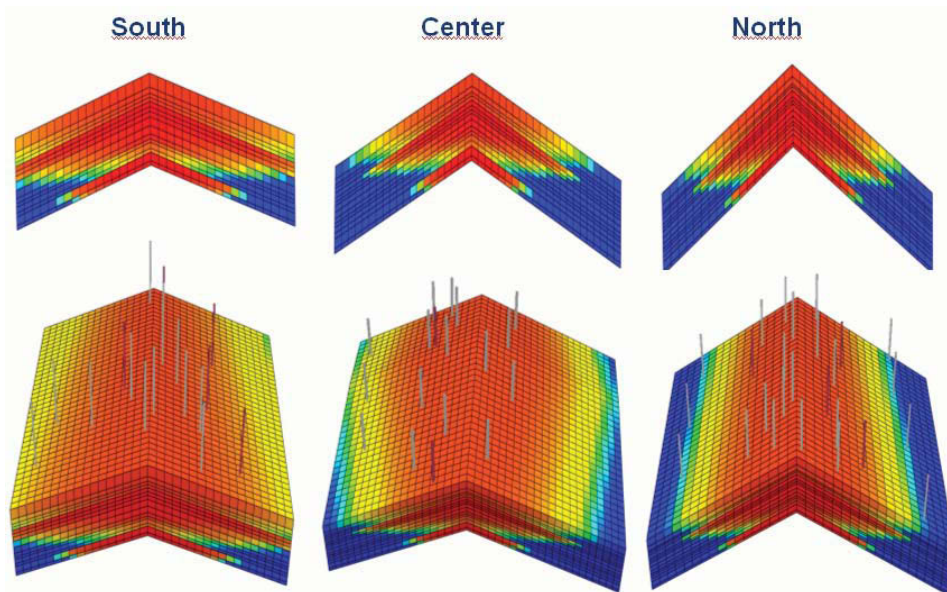


Table 3.7: Wells and completions [16]

	South	Center	North
<b>number of production wells total</b>	<b>16</b>	<b>15</b>	<b>17</b>
<b>number of injection wells total</b>	<b>2</b>	<b>3</b>	<b>8</b>
completed in			
<b>Upper Yamama</b>	0	0	1
<b>Middle Yamama</b>	6	4	8
<b>Manifa</b>	2	0	1
<b>Upper &amp; Middle Yamama</b>	6	0	1
<b>Middle Yamama &amp; Manifa</b>	4	14	14

Table 3.8: Reservoir Model petrophysical properties

Layer	h [m] South	h [m] Center	h [m] North	$\Phi$ [-]	$k_h$ [mD]	$\frac{k_v}{k_h}$ [-]	Formation
1	45,8	45,9	40,1	0,090	1,150	0,1	Upper Yamama
2	20,0	20,8	24,7	0,102	1,380	0,1	
3	13,5	13,0	9,8	0,118	1,790	0,1	
4	13,5	16,3	14,8	0,118	1,870	0,1	
5	17,0	18,8	20,5	0,150	9,820	0,3	Middle Yamama
6	15,5	14,5	13,0	0,170	20,950	0,3	
7	18,1	13,0	12,1	0,166	20,470	0,3	
8	28,6	22,3	22,1	0,171	13,850	0,3	
9	27,4	23,7	21,0	0,164	3,820	0,1	Lower Middle Yamama
10	16,6	17,1	17,1	0,145	1,710	0,1	
11	12,1	13,7	11,6	0,140	1,240	0,1	
12	19,1	20,7	16,3	0,153	2,080	0,1	
13	13,3	20,5	17,7	0,116	0,840	0,1	
14	28,3	34,4	29,6	0,193	159,840	1,0	Manifa
15	14,5	17,5	14,1	0,160	79,070	1,0	

Production begins on first of September 1964 and ends September 2031. The model has been history matched until 2003, the year from which the latest production data is available.

The following operational conditions have been implemented in the sector model for the sensitivity analysis: [16]

- A minimum well bottom hole pressure of 1450 psi. The wells will shut if the bottom hole pressure falls below this limit. A well tubing head pressure limit could not be set due to the lack of lift tables.
- The wells are put under an individual oil rate constraint which is different for all wells and an average of the historical production rates. Rates range from 314 - 10375 bbl/day.

- The wells start and shut subsequently according to the indicated real production history. In the year 2005, 4 production wells are on stream in the south part, 11 in the center part and 9 in the north part. The reason why there are so few wells in the south part is operational (well damages and problems of moving the rig to the southern part of the field). There is no scheduled operation downtime for all wells at once.
- Duration of the simulation production time is 76 years.

### 3.5. RESULTS AND DISCUSSION

#### 3.5.1. Results South

Table 3.9: Sensitivity analysis input data south

Uncertainty	Base Case	High Case	Low Case
Horizontal wells from beginning	16 vertical wells, 0 horizontal wells	14 vertical wells, 2 horizontal wells	---
Relative permeability curves	lab and history matching curves	favorable Corey coefficient and $S_{or,w}$	unfavorable Corey coefficient and $S_{or,w}$
Less extension of high permeability streaks	$k = 20 - 40$ mD	---	$k = 10$ mD

Due to numerical instabilities, the water injection and additional horizontal wells cases could not be run. In view of the lower coverage of oil producers compared to the center part, new horizontal wells would have probably brought significant additional production (compare center part results)

It is also noted that due to the very low water cut values for all cases (2% maximum), the impact of the sensitivities is considered non conclusive.

Only the relative permeabilities sensitivities show significant change in oil production outputs.

The absence of high permeability streaks has a poor consequence on both oil and reservoir pressure due to the relatively similar permeability ratio between this facies / rock type and the normal matrix.

Horizontal wells from beginning have a minor influence on oil production and on reservoir pressure; this is because the conversion to horizontal wells results in a negligible change in their productivity. Draining several vertical layers or one long horizontal section seems to have in this case a minor effect on production. The drilling of horizontal wells will have to be decided based on economic indications.



Fig. 3.13: Cumulative oil production, basecase and sensitivities – sector south

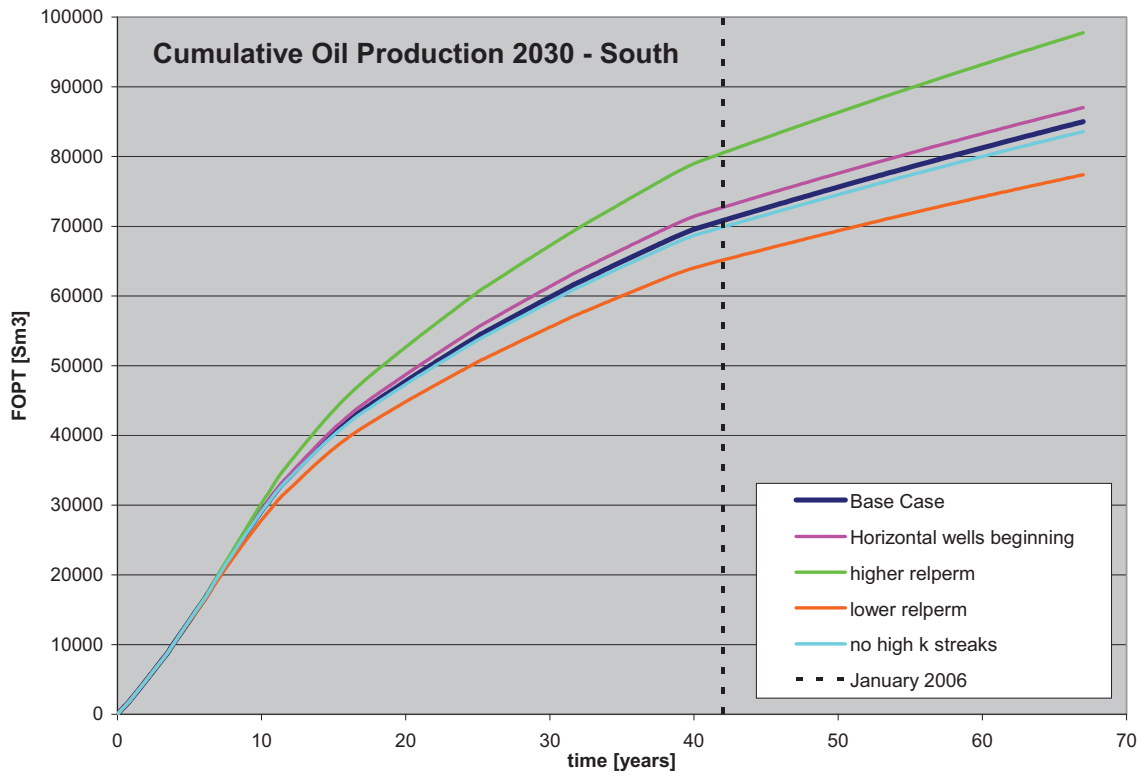


Fig. 3.14: Water cut, basecase and sensitivities – sector south

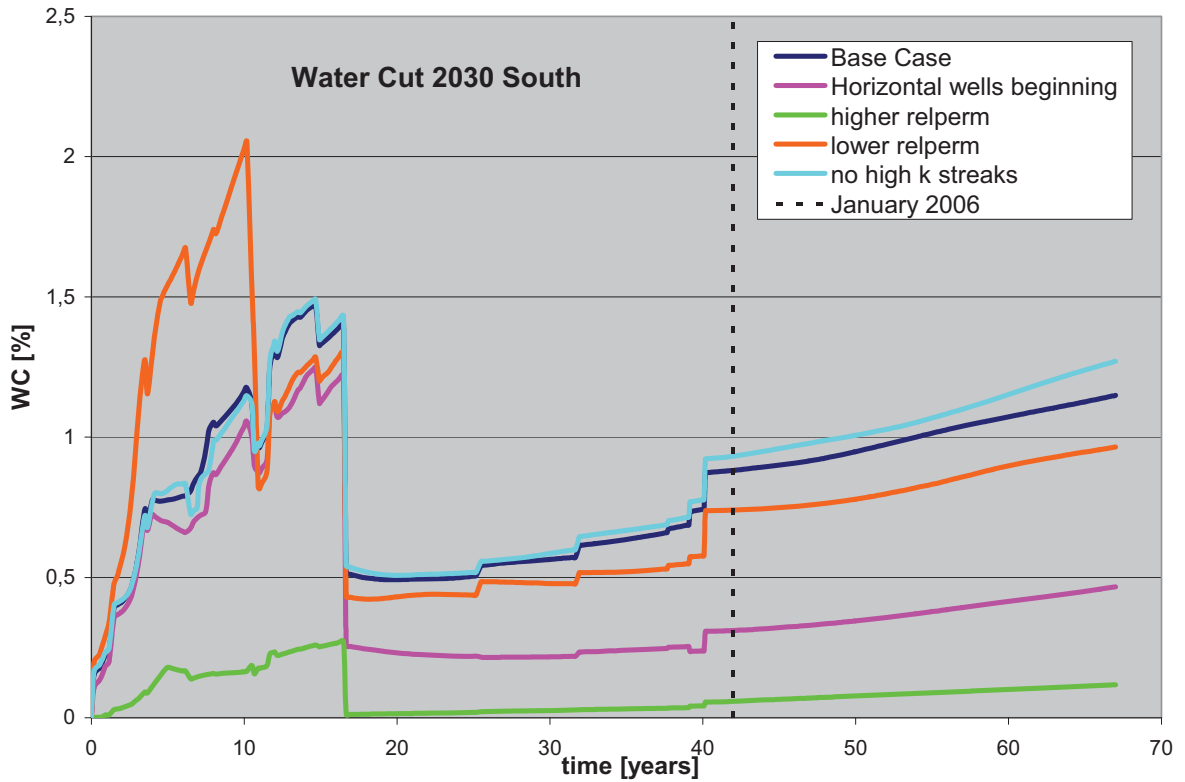


Fig. 3.15: Pressure depletion, basecase and sensitivities – sector south

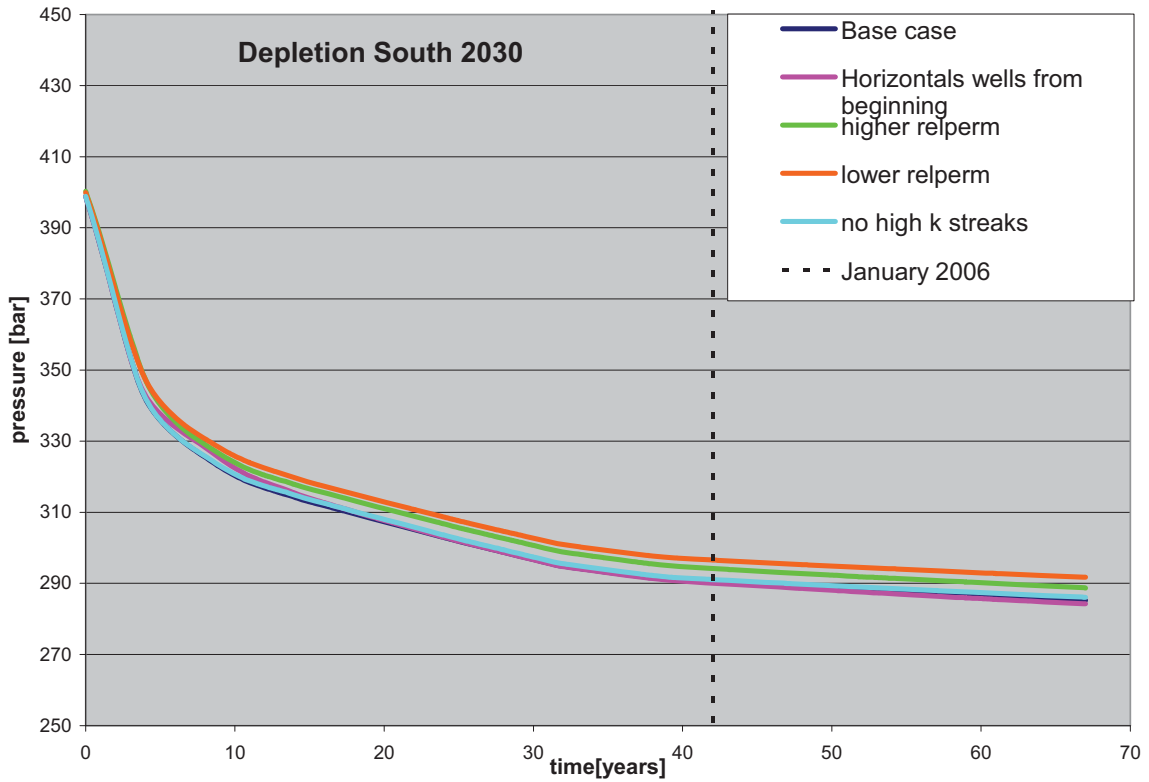


Table 3.10: Result overview, Dorood sensitivity study, southern sector

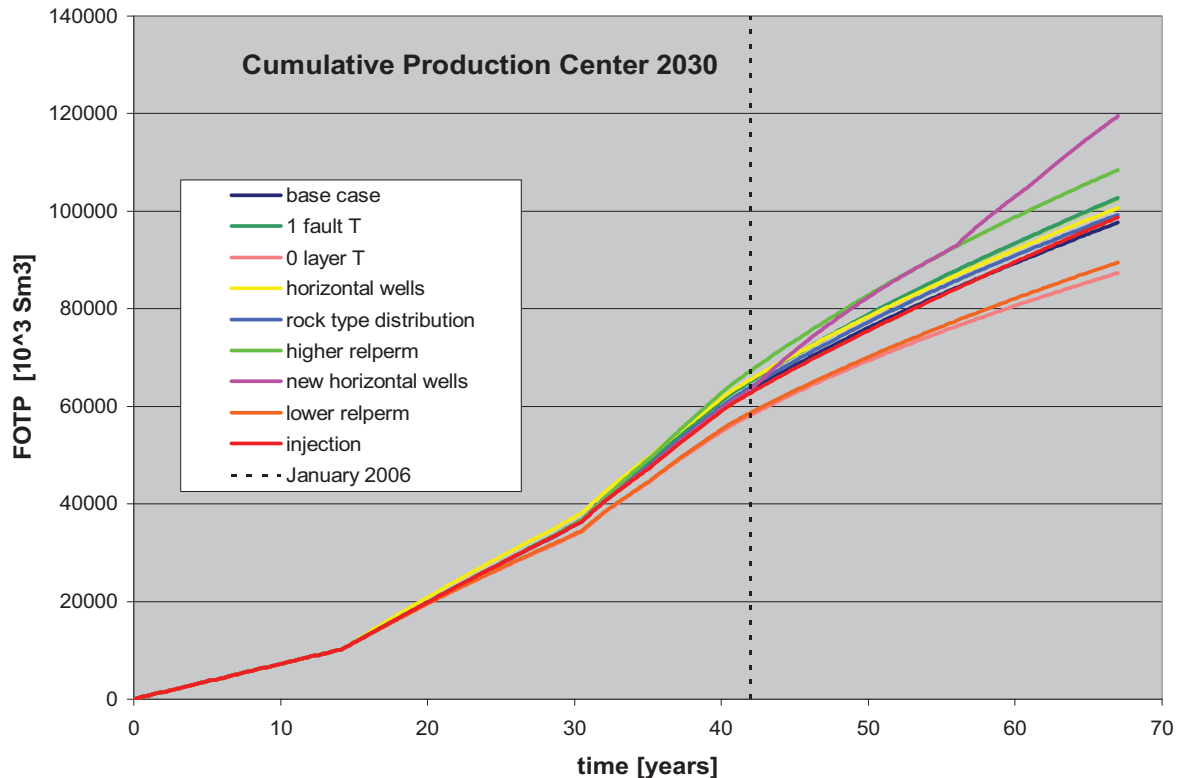
OOIP [Mbb]	3622	Np in 2030 (66 years) [Mbb]	RF [%]	WC in 2030 (66 years) [%]	Avg. reservoir pressure in 2030 (66 years) [bar]	
16 vertical wells (18 completions) no aquifer, no water injection Curves from lab tests and history matching 16 vertical wells (18 completions)	Base case	535	14,8%	1,1%	285,2	
	High cases					
	Horizontal wells	2 Hor well-completions over 18 from the beginning	547	15,1%	0,5%	284,2
	Water injection	2 inj (inj in Yamama and Manifa)	Convergence failure - model not running			
	High Kr	High case curves from changing Corey coefficients and Sorw.	615	17,0%	0,1%	288,7
Some layer steaks with K 20-40 mD Curves from lab tests and history matching	Additional Horizontal wells	3 new H wells in 2005	Convergence failure - model not running			
	Low cases					
	No high K streaks	reduce K to 10 md	526	14,5%	1,3%	286,1
	Low Kr	Low case curves from changing Corey coefficients and Sorw.	487	13,4%	1,0%	291,7

### 3.5.2. Results Center

Table 3.11: Sensitivity analysis input data center

Uncertainty	Base Case	High Case	Low Case
Horizontal wells from beginning	26 vertical completions, 0 horizontal completions	22 vertical completions, 4 horizontal completions	---
Relative permeability curves	lab and history matching curves	favorable Corey coefficient and Sor,w	unfavorable Corey co- efficient and Sor,w
Water injection	No injection	3 injection wells In Yamama and Manifa	---
Fault transmissibility	all faults completely sealing	All faults fully passing	---
Additional horizontal wells	26 vertical completions, 0 horizontal completions	26 vertical completions, 4 horizontal completions from 2005 on	---
Layer transmissibility	some layers communicate	---	No communication between layers
Rock type distribution	Middle Yamama is vuggy and non - vuggy	all Middle Yamama is vuggy	---

Fig. 3.16: Cumulative oil production, basecase and sensitivities, center sector



Considering the large gain obtained by adding four new horizontal wells from 2005, it seems that the well coverage of the center part is not optimized with 15 vertical wells, since the recovery factor is only 22% after 60 years.

Oil production and pressure are very sensitive to layer vertical transmissibility reduction as it results in a complete seal between Yamama formation, which is bearing most of the oil, and the Manifa formation. This does not allow the relatively strong water aquifer in Manifa to give pressure support to the Yamama reservoir. This leads to a dramatic drop in field water cut during the production history. The third parameter showing large impact on oil production outputs is the relative permeability.

As for the southern part of the field, horizontal wells from the beginning of production have a minor influence on cumulative production and on reservoir pressure.

Water injection also has a poor influence, due to the fact that the aquifer support is already strong and only three water injectors are implemented. The impact is only visible through slightly higher water cut and reservoir pressure.

Allowing the reservoir fluids to flow through the 9 modeled faults results in a minor rise in oil production but in a more considerable decrease of the water cut. This might be due to the fact that these faults, when impermeable, tend to prevent water from moving to the top of the reservoir and also trap water in flank wells. When the faults become transmissible, the water is more diffuse, which reduces the water cut in the flank wells tends while wells at the top reservoir are still producing at very low water cut.

The rock type distribution has almost no effect as difference in permeability remains small compared to matrix.

Fig. 3.17: Water cut, basecase and sensitivities, center sector

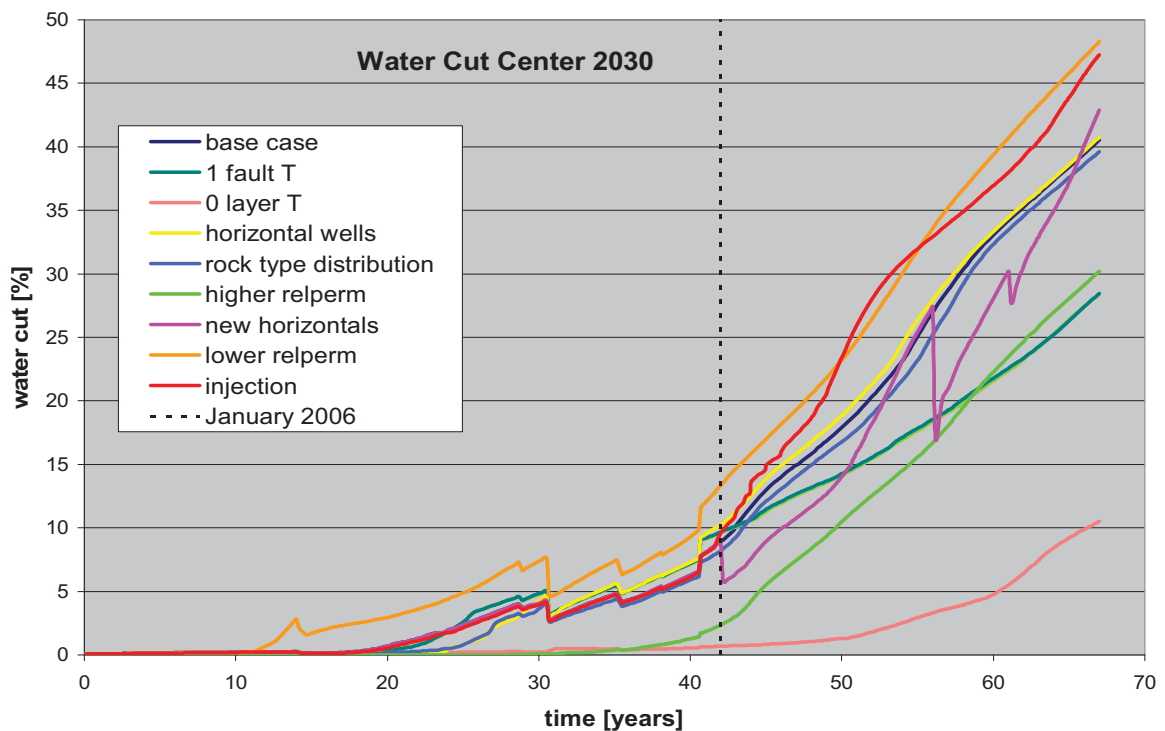


Fig. 3.18: Pressure depletion, basecase and sensitivities – center sector

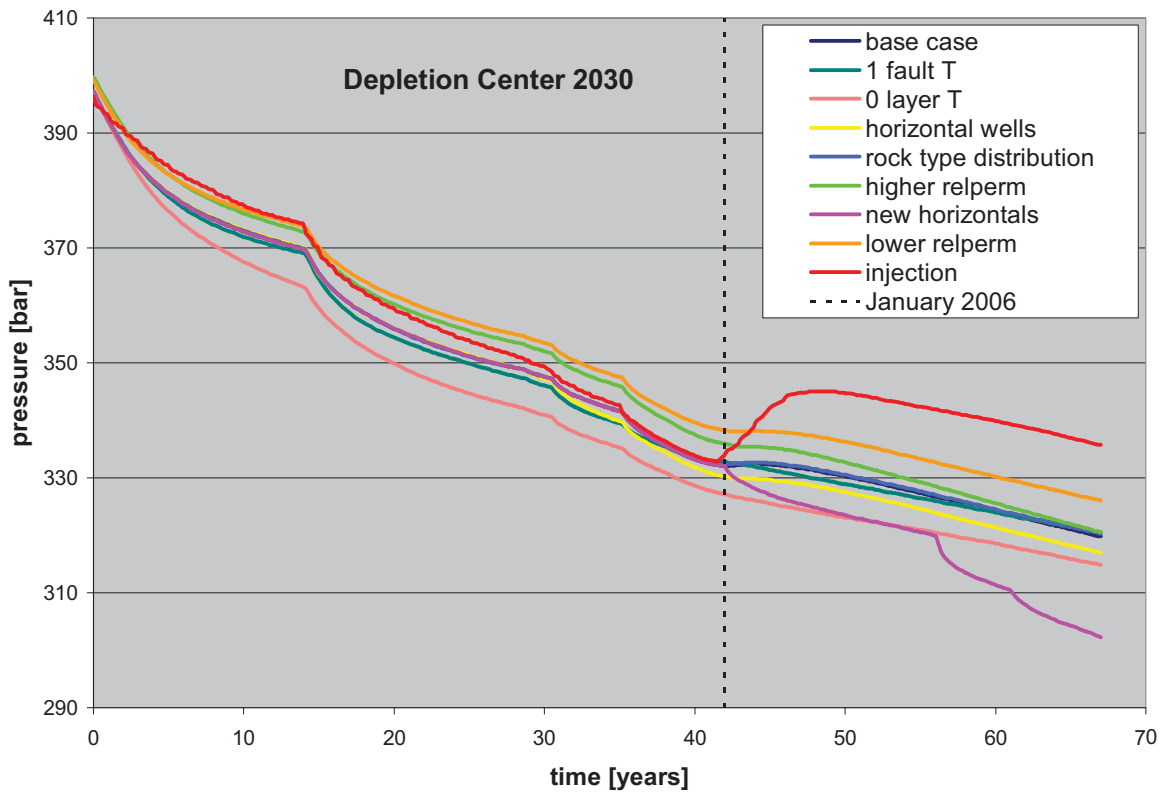


Table 3.12: Result overview, Dorood sensitivity study, center sector

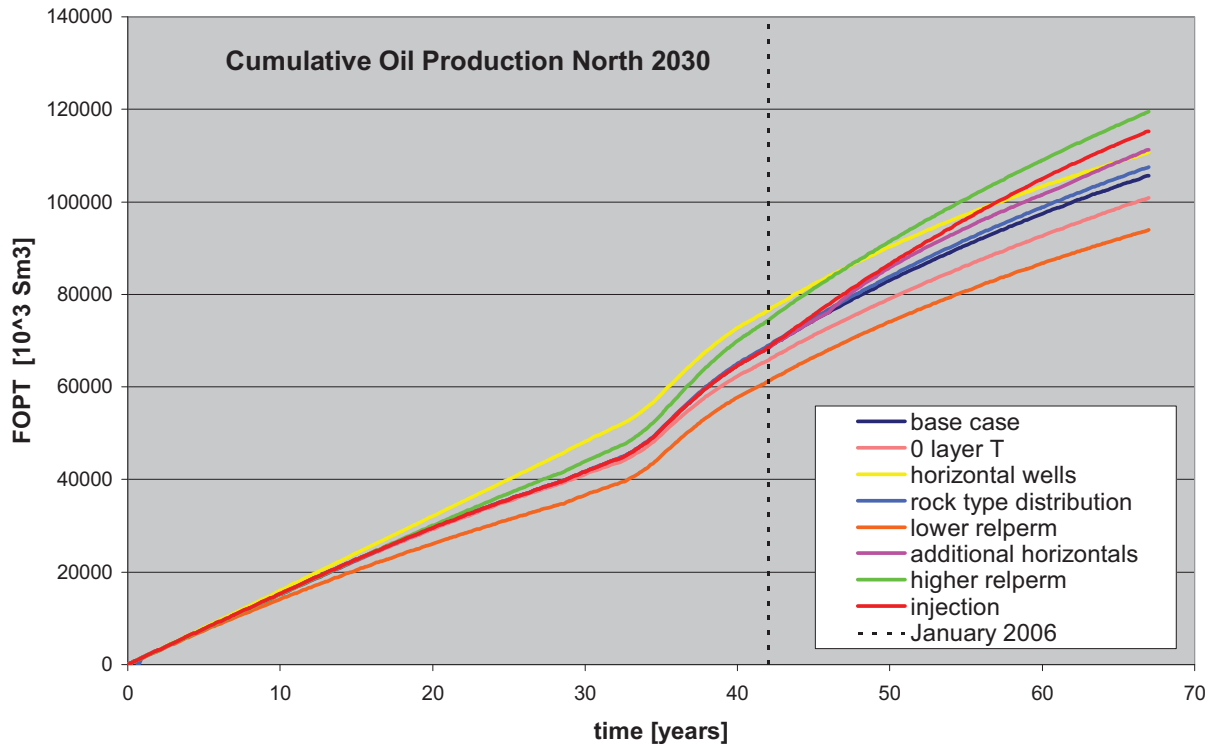
OOIP [MbbJ]		2776		Np in 2030 (66 years) [MbbJ]	RF [%]	WC in 2030 (66 years) [%]	Avg. reservoir pressure in 2030 (66 years) [bar]
Base case figures	Base case		614	22,1%	40,5%	319,8	
	High cases						
15 vertical wells (26 completions) poor aquifer, no water injection all Faults (34) are sealing Curves from lab tests and history matching	Horizontal wells from beginning	4 hor. well completions out of 26 in base case	633	22,8%	40,7%	317,0	
	Water injection	3 inj (inj in Yamama and Manifa)	623	22,4%	47,3%	335,7	
	Faults	All Faults fully passing	646	23,3%	28,4%	320,4	
	High kr	High case curves from changing Corey coefficients and Sorw.	682	24,6%	30,2%	320,5	
15 vertical wells (26 completions)	Additional Horizontal wells	4 new H wells in 2005	752	27,1%	42,9%	302,3	
Some layers allow communication Curves from lab tests and history matching	Low cases						
	0 Layer Transmissivity	no communication between layers	549	19,8%	10,5%	314,9	
	Low kr	Low case curves from changing Corey coefficients and Sorw.	563	20,3%	48,3%	326,1	

### 3.5.3. Results North

Table 3.13: Sensitivity analysis input data north

Uncertainty	Base Case	High Case	Low Case
Horizontal wells from beginning	23 vertical completions, 0 horizontal completions	19 vertical completions, 4 horizontal completions	---
Relative permeability curves	lab and history matching curves	favorable Corey coefficient and $S_{or,w}$	unfavorable Corey coefficient and $S_{or,w}$
Water injection	No injection	2 injection wells In Yamama and Manifa	---
Additional horizontal wells	23 vertical completions, 0 horizontal completions	23 vertical completions, 3 horizontal completions from 2005 on	---
Layer transmissibility	some layers communicate	---	No communication between layers
Rock type distribution	Middle Yamama is vuggy and non - vuggy	all Middle Yamama is vuggy	---

Fig. 3.19: Cumulative oil production, basecase and sensitivities, sector north



The adding of four new horizontal wells in 2005 results in a moderate increase in oil production. It appears that, in opposition to the center part, the northern part seems adequately covered with its 17 vertical wells.

Oil production and pressure are also less sensitive to layer vertical transmissibility reduction than the center part due to the weaker aquifer support from Manifa.

On the other hand, the impact of water injection involving 6 injectors is massive and has influences on oil production and especially on both water cut and reservoir pressure. Nevertheless, the cost of this water injection implementation has to be balanced against the gains.

The second parameter showing large impact on oil production outputs is again the relative permeability.

As for the other parts of the field and for the same reasons, the case of horizontal wells from the beginning has a minor influence on oil production and on reservoir pressure.

As for the center part, rock type distribution has almost no effect.

As a conclusion, it is pointed out that the sensitivity runs have generally less impact in the northern than in the center part. This might be due to the better well coverage especially in Yamama (17 wells for 2169 MMBbl oil versus 15 wells for 2776 MMBbl oil) and the lack of high permeable streaks.

Fig. 3.20: Water cut, basecase and sensitivities, sector model north

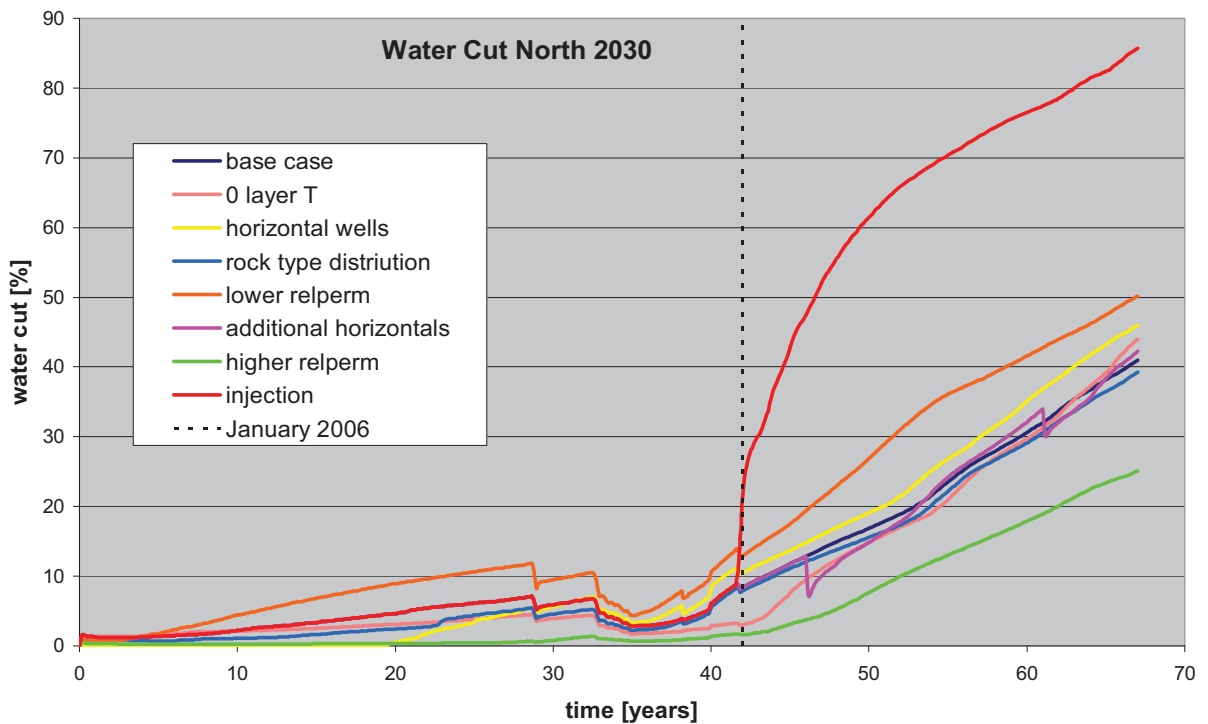


Fig. 3.21: Pressure depletion, basecase and sensitivities, sector north

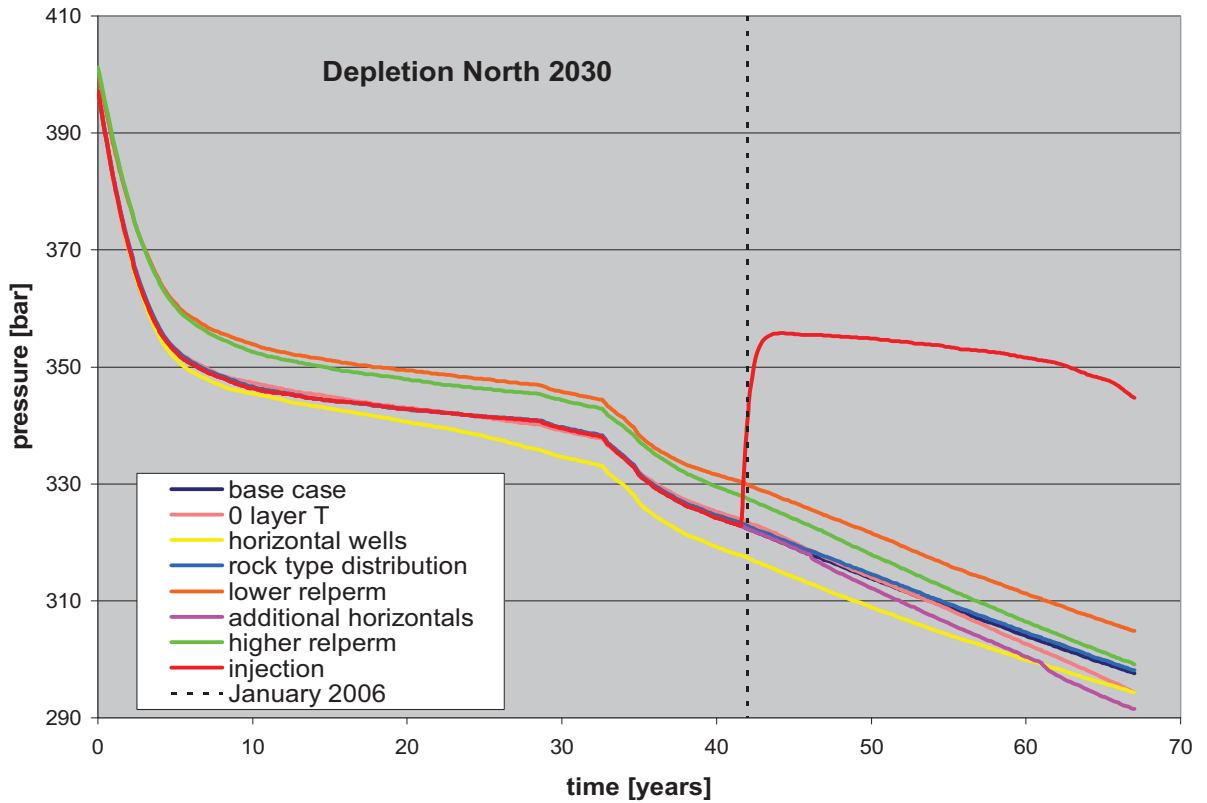


Table 3.14: Result overview, Dorood sensitivity study, northern sector

OOIP [Mbb]	2169		Np in 2030 (66 years) [Mbb]	RF [%]	WC in 2030 (66 years) [%]	Avg. reservoir pressure in 2030 (66 years) [bar]
Base case figures	Base case		665	30,7%	41,0%	297,6
	High cases					
17 vertical wells (23 completions) medium aquifer, no water injection Curves from lab tests and history matching Middle Yamama Vuggy or non vuggy	Horizontal wells from beginning	4 hor. well completions out of 23 in base case	696	32,1%	45,9%	294,3
	Water injection	2 inj (inj in Yamama and Manifa)	725	33,4%	85,7%	344,7
	High kr	High case curves from changing Corey coefficients and Sorw.	752	34,7%	25,0%	299,2
	Rock type distribution	all Middle Yamama is vuggy	677	31,2%	39,3%	298,1
17 vertical wells (23 completions)	Additional Horizontal wells	3 new H wells in 2005	700	32,3%	42,2%	291,5
Some layers allow communication Curves from lab tests and history matching	Low cases					
	0 Layer Transmissivity	no communication between layers	635	29,3%	44,0%	294,3
	Low kr	Low case curves from changing Corey coefficients and Sorw.	591	27,2%	50,2%	304,8



### 3.5.4. General conclusions on Dorood results:

The different relative permeability curves and endpoints have a significant impact on the cumulative oil production and the water cut. It is recommendable to carry out further SCAL measurements to get more reliable data. This might require new core taking.

In this moderately heterogeneous reservoir, horizontal wells have a minor to medium impact on cumulative production, due to a relatively weak horizontal to vertical permeability anisotropy and a relatively little permeability difference between layers where drains are located and layers above and below. In the tightest part of the reservoir, highly deviated wells that penetrate several layers should be preferred.

The adding of new wells, either vertical, horizontal or deviated ones, is of significant importance in the southern and central part of the field where the coverage with existing original oil producers is low and the situation is worsening as wells are shut-in due to operational reasons.

Barriers to vertical flow generally have a poor impact, except if they are significantly restraining the communication with a downdip aquifer. Log measurements to better define the position of these layers are advisable, in order to be able to assess the aquifer impact and to optimize the position of new producers.

The rock type distribution, including high permeable streaks, is of minor importance due to the poor permeability difference between these facies and normal matrix. The limited number of grid blocks in the model makes the modeling of very thin highly permeable layers difficult.

Water injection has a moderate impact on oil production as parts of the reservoir are already supported with the Manifa aquifer and reservoir pressure remains high except in the southern part with no aquifer present. Injection could have significant impact if implemented rigorously, as in the northern part, and efficiently. Nevertheless, the involved costs, i.e. equipment and higher water treatment costs have also to be balanced against the gain in production. This is highly dependent on the oil price.

In general, it appears that the well situation in 2006 does not allow an optimized field development. It is strongly recommended to add new wells, especially in the south and center part, to accelerate field development.

## 4. MAJNOON / MISHRIF

The Mishrif reservoir is part of the Majnoon oil field. It is located near the river Tigris in southwest Iraq, approximately 70 km north of the city Basrah, at the border with Iran. [20]

Majnoon was discovered in 1976, but appraisal was interrupted in 1980 due to the Iran-Iraq war. 24 appraisal wells have been drilled, but up to day the reservoir has never been put on stream. [21]

The field geometry is a north/south anticline of the dimensions 31 × 6,8 miles and covers an area of 98850 acres (400 km<sup>2</sup>). The top reservoir lies at about 7710 ft TVDss.

Majnoon bears five distinct reservoirs, from top to bottom: Hartha, Mishrif, Bin Umr, Zubair and Yamama. Apart from Zubair and Bin Umr which are sandstone formations, the other three reservoirs are carbonates.

This study will only be concerned with the Mishrif reservoir, since it has the greatest reserves, which estimated to be 17500 Mbbl. [22]

Fig. 4.1: Location of Majnoon [20]

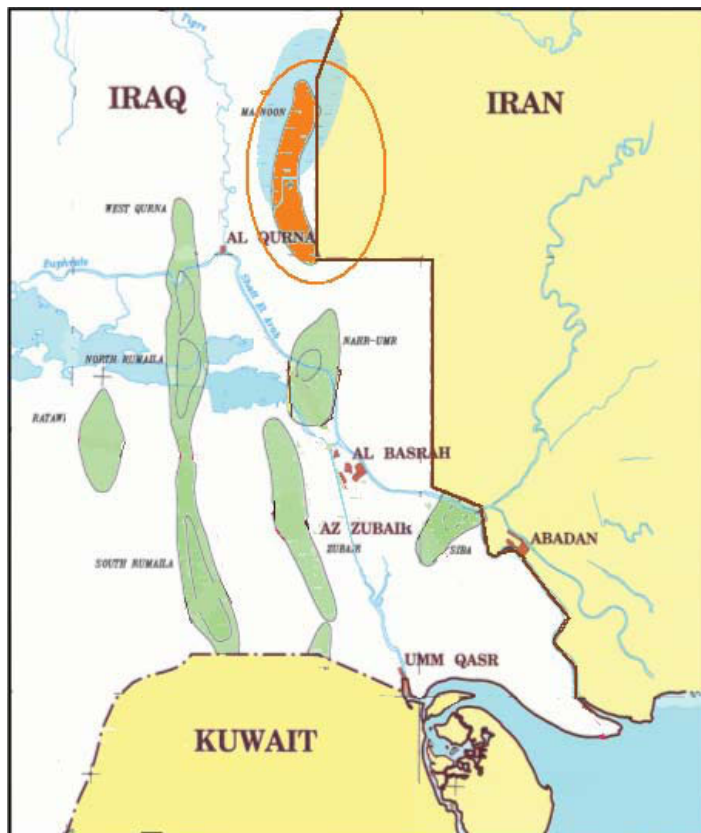
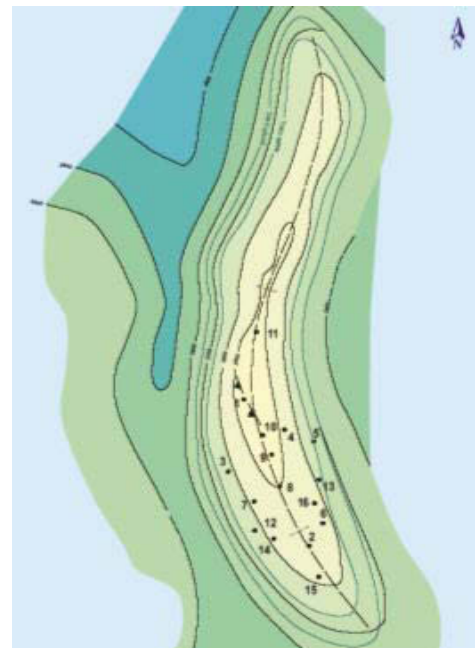


Fig. 4.2: Top Mishrif [20]



## 4.1. SEDIMENTOLOGY

The Majnoon field has been interpreted as a stable Arabic platform, whose evolution was linked to the evolution of the Thetys ocean.

Deposition is believed to have taken place in three cycles: first a retrograde cycle in which delta structures were formed, interrupted by phases of carbonate production. The second cycle is characterized by the deposition of a large carbonate platform in a quiet period with alternating deposition of more shaly facies. Through inspection of the shales it can be determined if deposition took place in a retrogradational or progradational period of the cycle. The third cycle is globally regressive; in which shoal and rudist carbonated platforms were deposited, again interrupted by more shaly deposits. [23]

Various sequence boundaries and maximum flooding surfaces were recognized:

The Sb3b sequence boundary is an erosional contact between a prograding and an aggrading grain-dominated platform; the facies shift to being muddier.

The Sb5 sequence boundary is an erosional contact between a grain and a mud dominated platform: a toplap erosive surface is clearly observed on seismic lines, and there occurs a drastic jump from muddy facies to facies in the outer shelf area.

The Sb7 sequence boundary is the top of a porous lagoonal facies clearly observed on well logs.

Maximum Flooding Surfaces are MF3, which is a tight and discontinuous level on the grain dominated platform, and MF7 which is tight and continuous on the mud dominated platform. [24]

The platform is a thick carbonated shelf which was deposited in environments varying from bathyal to intertidal.

Low thickness variations are found, but strong lateral changes of facies and important vertical heterogeneities. [22]

The structure of the field is a 31 × 6,8 miles north-south anticline with a vertical closure of about 1500 feet. The crest of the structure lies at about 7710 TVDss.

Hydrocarbon trapping is controlled by the structural closure, it is unknown if there exists a fault network.

Interbedded baffles and overlying tight or dense carbonates and shales seal the formation. [21]

The Majnoon field consists of five different major oil reservoirs, which are shortly presented in the following. Average reservoir petrophysical and fluid properties which show the main contrasts of the different reservoirs are detailed in table 4.1.

The Hartha reservoir is the topmost formation and corresponds to a carbonate wedge of a thickness of about 330 ft. It was deposited in a west-southwest to east-northeast prograding ramp setting. The

facies are prevailingly outer and inner shelf and lagoon facies with local shale development (cp. with facies types in the following chapter).

Hartha contains about 6% of the total Mishrif OOIP. [20],[22],[23]

The Mishrif reservoir is about 725 ft thick and contains the biggest fraction of OOIP in the Mishrif field, about 65%. Oil in Mishrif is heavy crude oil with some content of asphaltenes. A more detailed description of the Mishrif reservoir can be found in the following chapter. [20],[22],[23]

The Bin Umr reservoir has a thickness of about 570 ft and can be divided into two different lithological units. The upper unit consists of about 420 ft of shale, marl and tight carbonates in thick beds. This zone has a poor reservoir potential. The lower unit is an up to 250 ft thick sandstone layer with interbedded shales. The sandstone was deposited in a prograding deltaic setting. OOIP constitutes only about 3% of total Mishrif OOIP. [20],[22],[23]

The Zubair formation is about 960 ft thick. Although it is the second thickest layer in the Majnoon field it contains only about 7% of the OOIP.

There are strong lithology variations to be found, even within single layers, lithology ranging from thick shales, siltstones, limestones and sandstones to cemented carbonates.

The depositional environment has been interpreted as a prograding wave dominated delta.

The Yamama reservoir is the thickest reservoir with a thickness of about 1150 ft. A separate study describes the Majnoon Yamama reservoir in detail; also a simulation model has been built. Interest in Yamama is high since it contains the second largest portion of OOIP in Majnoon with approximately 20%. [20],[22],[23]

Fig. 4.3: Majnoon field zonation [20]

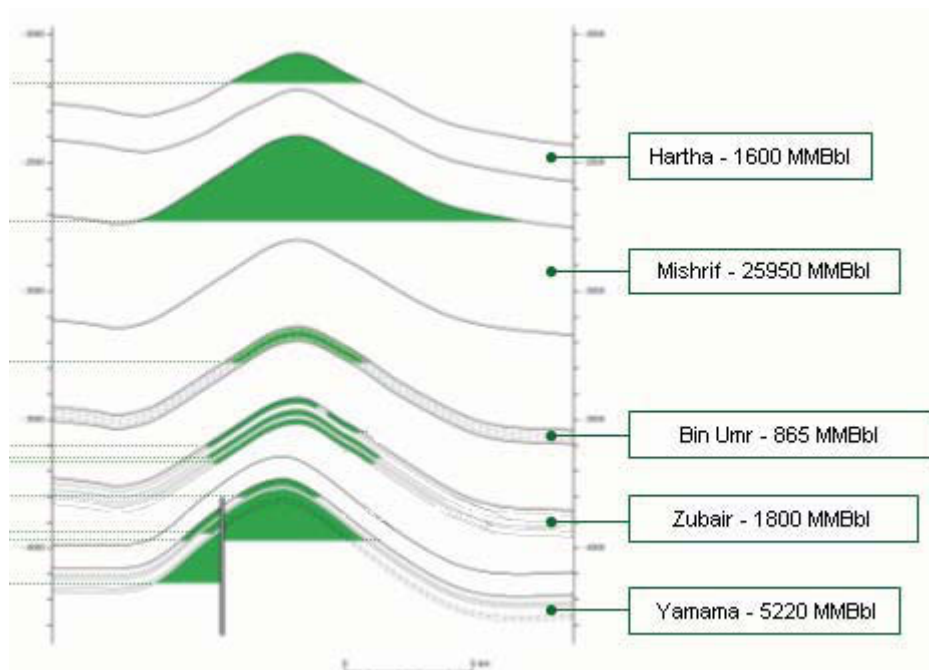


Table 4.1: Majnoon reservoir properties [22]

	<b>Hartha</b>	<b>Mishrif</b>	<b>Bin Umr</b>	<b>Zubair</b>	<b>Yamama</b>
<b>Lithology</b>	Limestone	Limestone	Sandstone	Sandstone	Limestone
<b>Thickness [ft]</b>	331	725	571	985	1150
<b>Avg. Porosity [%]</b>	20	13	16 - 20	14 - 17	14
<b>Avg. Permeability [mD]</b>	600- 5000	5 - 500	170 - 700	60 - 350	0,01 - 250
<b>Oil Gravity [°API]</b>	29,5	22,5	30,2	31,5	39,8

## 4.2. RESERVOIR GEOLOGY

Since Mishrif contains the most OOIP of the five reservoirs in Majnoon, it was chosen for the sensitivity analysis. [22]

The Mishrif reservoir is an about 985 ft thick carbonate formation. It consists of nine distinguishable reservoir units, which are named as following: Khasib B, mA, mB11, mB12, mB21, mB23, mC1 and Ahmadi. [21]

Khasib B and Ahmadi are considered as different reservoirs but there is an excellent pressure communication with the six units in between belonging to the Mishrif reservoir. It is believed that they shared an initial fluid column. [25]

The depth of the top reservoir lies at 7710 ft TVDss, the original oil in place is estimated to be between 17350 and 25950 MMSTB. This large variation is due to the fact that only the south of the field has been appraised and the results extrapolated to the north. [26]

The Mishrif reservoir is supposed to have a tilted oil-water contact. The tilt gradient is estimated to be about 15 m/km from west to east, and it is supposed to result from strong hydrodynamics in the past. The oil-water contact lies at about 8925 ft TVDss in the west of the field and at about 8450 ft TVDss in the east. [25]

As mentioned before, the reservoir lithology is carbonate, with interbedded porous and dense carbonates or shaly beds. These intra reservoir tight beds are discontinuous at field scale and they are potential future flooding barriers. [21]

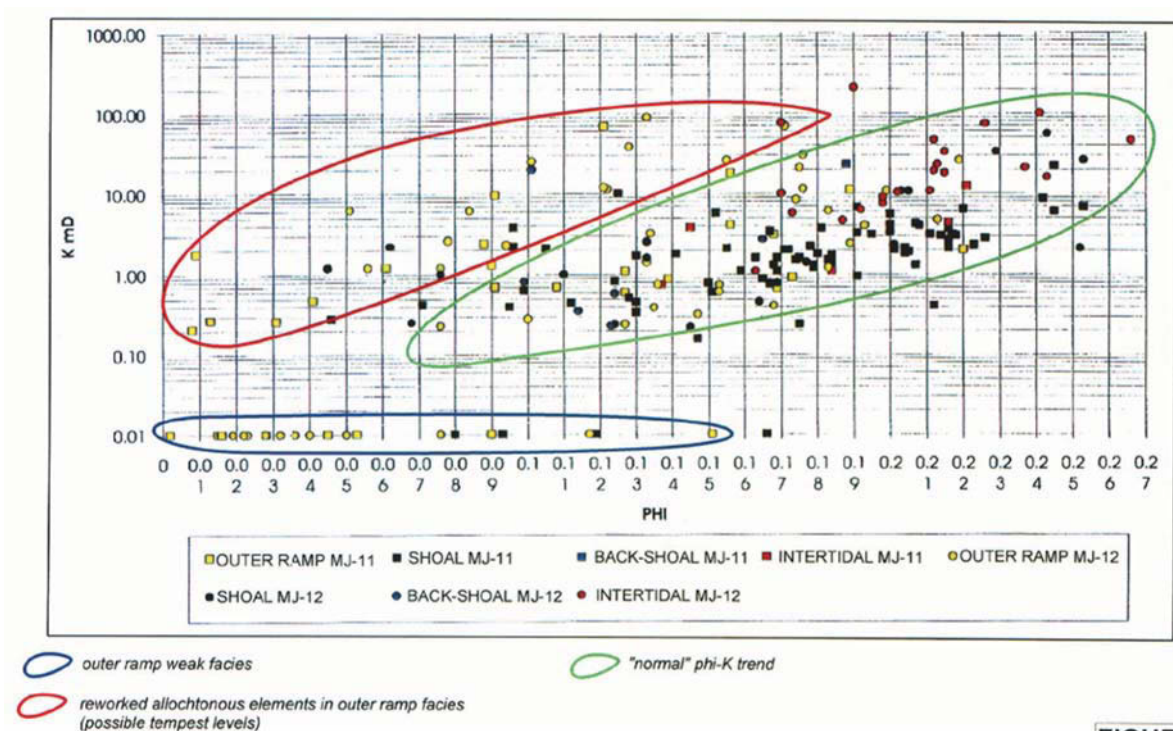
Six main facies which are related to their depositional environments can be clearly distinguished in Mishrif: [25]

“Basin” facies: the so called basin facies were deposited during the major platform flooding. This facies has not been observed on cores.

- “Outer shelf” facies: this facies was deposited in a subtidal environment. Clayey Mudstones, Wackestone and Packstones are observed in this facies.
- “Shoal” facies: the Shoal facies consists of tidal high energy grainstones
- “Black shoal rudist” facies: Black shoal Packstones are observed. However, the rudists are diversified, they occur as well on the platform as in open marine settings.
- “Inner shelf” facies: this facies was deposited in a low energy environment; it consists of Wackstones and Packstones.
- “Intertidal” facies: this facies corresponds to sediments under influence of subaerial exposure.

This six facies were grouped into three rock types according to their  $\Phi/k$  trend, as illustrated in the following figure.

Fig. 4.4: Mishrif rock types [25]

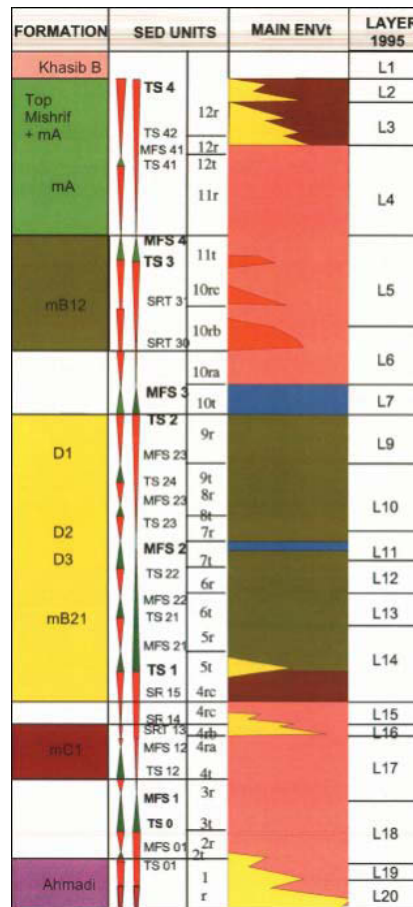


The units mA, mB2.1/ mB2.2 and mC1 constitute the major drain layers. [21]

Table 4.2: Mishrif average reservoir properties [25]

Field	Reservoir	Zone	% OOIP	OIIP (MMSTB)	Porosity (%)	Permeability (mD)	Reservoir Quality
M A J N O O N	M I S H R I F	Khasib B	7	220	7 - 12	0,1 - 50	rather poor
		Mishrif mA	22	402,5	6 - 17	0,1 - 1000	very good drain layer
		Mishrif mB1	22	490,5	5 - 17	0,1 - 70	rather poor
		Mishrif mB2.1/2.2	32	723	9 - 17	0,1 - 600	very good drain layer
		Mishrif mB2.3/mC1	7	220	7 - 23	0,1 - 1000	very good drain layer
		Ahmadi	9	195	4 - 23	0,1 - 600	rather poor

Fig. 4.5: Zonation of the Mishrif reservoir [27]



The oil is heavy oil (19,5 – 26 ° API°) with some asphaltene, sulfur (3-4%) and metal content. The oil characteristics are subject to strong variations concerning gravity, viscosity and GOR, most likely due to gravitational segregation. The oil is undersaturated; no initial gas cap exists in Mishrif. [22]

The Mishrif reservoir is sealed by overlying tight, respectively dense carbonates and shales. [21]

Table 4.3: Average oil field fluid parameters Mishrif [22]

		<b>Mishrif</b>
<b>API gravity</b>	[°API]	19,5 - 26
<b>Viscosity</b>	[cP]	1,1 – 6,5
<b>Initial GOR</b>	[SCF/STB]	55 - 85 m3/m3
<b>FVF</b>	[RB/STB]	1,15
<b>Reservoir Temperature</b>	°C	86
<b>Original reservoir pressure</b>	[psi]	4400 @ 8950 ft
<b>Formation compressibility</b>	[1/psi]	4,8E-08
<b>Bubble Point Pressure</b>	[psi]	1700

### 4.3. UNCERTAINTIES

Following uncertainties were identified from Total in-house literature:

- (1) Horizontal wells
- (2) Artificial Lift methods
- (3) Permeability anisotropy
- (4) Relative permeability curves
- (5) Permeability field

It has to be noted that, since the field was not put on production up to now and information only comes from the appraisal wells, the uncertainties apply only to the vicinity of the wells and cannot be generalized without caution to the whole field !

#### 4.3.1. Horizontal wells <sup>[28]</sup>

No horizontal wells have been drilled up to date. In the literature it is shortly mentioned that the Mishrif zone does not fall into the classical applications for horizontal wells, although it is not explained why this would be so.



Nevertheless there exists interest to evaluate the performance of horizontal and subvertical wells. Especially in the flanks of the field where the oil bearing layers are sparse and thin, horizontal wells could decrease water coning.

The base case contains 28 vertical producers and 4 vertical injectors in a sector model that covers about one seventh of the field.

The well configuration for the sensitivity analysis was chosen according to a proposition in a study about horizontal wells in the Mishrif formation.

22 sub-horizontal producers and 4 sub-horizontal injectors are present, the deviation is 87°. The drain of the sub-horizontal wells covers five grid blocks, which equals about 3600 ft.

#### **4.3.2. Artificial Lift methods** <sup>[28]</sup>

An extensive regional aquifer is believed to be present in Mishrif and Ahmadi, but former sector model simulation results indicate that is not sufficiently able to provide the necessary pressure support which leads to rapid dying of the wells.

Therefore artificial pressure maintenance is envisaged. The possibilities are either water or gas injection; former simulations have however suggested a detrimental effect of gas injection. Consequently water injection is the preferred option at the moment.

Nevertheless, both possibilities and their combination were re-investigated for the sensitivity analysis.

In the base case four water injection wells are present which inject with a flexible rate in order to replace the production voidage.

Three different sensitivity analyses were carried out. One investigates the production behavior if water injection was not implemented. A second analysis examines the behavior under only gas lift; the third one considers the option of combined water injection and gas lift.

In the gas lift option applies in principle to all wells. It is defined in a way so that an increment of 2000 Sm<sup>3</sup>/day of oil production from the sector is the target. To achieve that a target gas injection rate is set at 50000 SCF/day for three different well clusters. However, the exact rates that are employed in each iteration are subject to a gas lift optimization algorithm within Eclipse.

The whole sensitivity analysis with the three options was carried out one time for the base case with the vertical wells, and a second time for the case with horizontal wells which was described in the previous section, in order to inquire if the behavior was different.

#### **4.3.3. Permeability anisotropy** <sup>[25],[27]</sup>

No data is available to characterize the vertical to horizontal permeability anisotropy in Mishrif. It was calculated as averages from the core data for the different facies.

Especially for the implementation of horizontal wells it would be important to better estimate the impact of vertical permeability anisotropy.

The  $k_v/k_h$  values are relatively scattered and heterogeneously distributed both throughout the field and within the layers. It can generally be said that the permeability in vertical direction is a factor of either 0,01 / 0,1 / 0,5 or 1 of the permeability in horizontal direction.

In the sensitivity analysis, the original anisotropy distribution was kept because the different multiplication factors were difficult to separate in a practical sense. Instead the values were multiplied as a whole with a certain factor.

For the low case the original PermZ values were multiplied by 0,1; for the high case they were multiplied by 1,5.

#### 4.3.4. Relative permeability curves <sup>[25],[27]</sup>

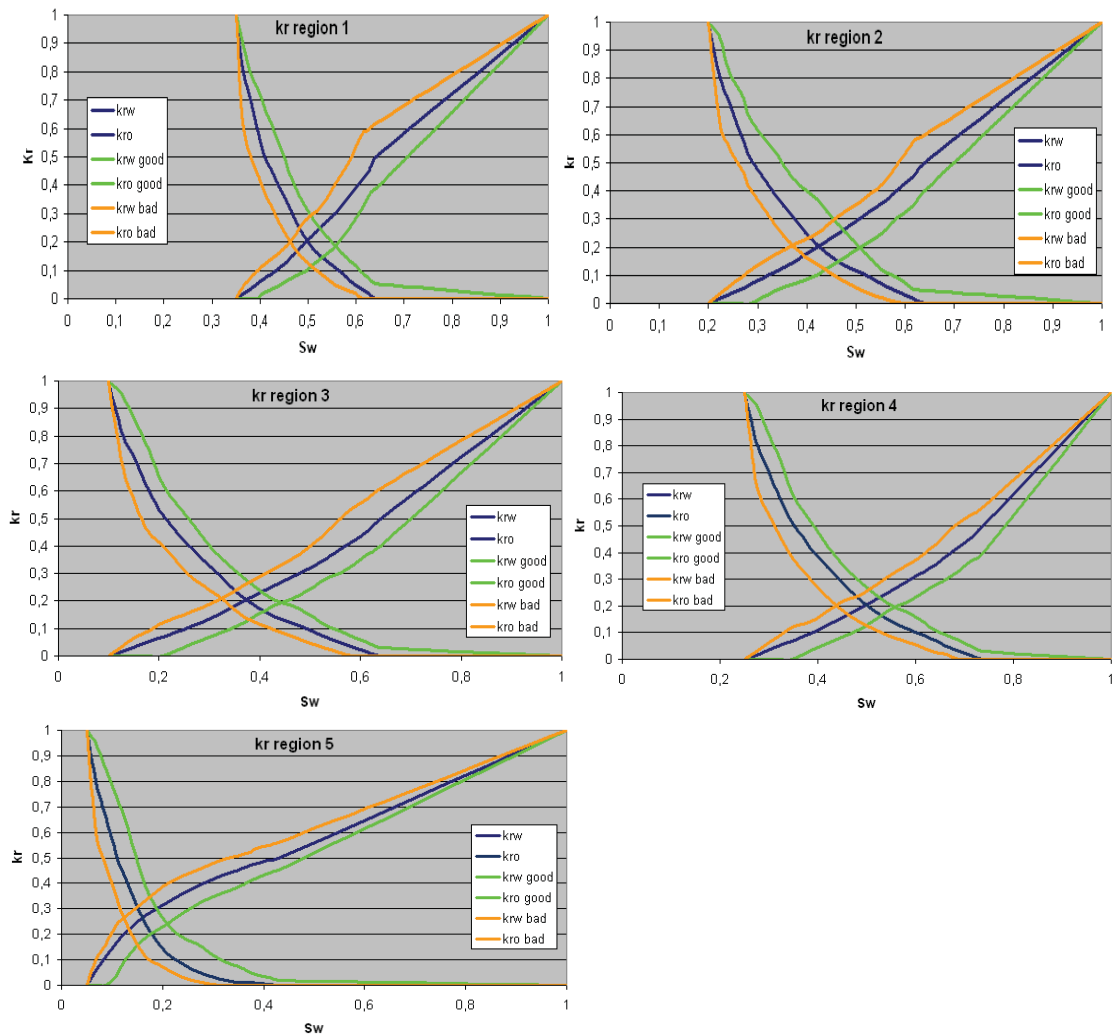
The relative permeability curves derived from Special Core Analysis (SCAL) laboratory data are considered unreliable. The reasons for that are very small horizontal plugs and a high sweeping velocity.

In the end a pair of curves from an analogue field was selected and adjusted in the course of the history matching process.

Due to the poor production history, chances exist that curves found from a SCAL analysis of a Mishrif core from the Majnoon field are slightly different.

As base case, the original relative permeability curves, based on analog field values, from the sector model were used for each of the five saturation regions. They are illustrated together with the curves for more, respectively less favorable relative permeabilities in Fig. 4.6.

Fig. 4.6: Original and sensitivity relative – k curves for every region



### 4.3.5. Permeability field <sup>[27]</sup>

For the establishment of the permeability field only very scarce data was available. The data consists of twelve reinterpreted short duration well tests, of 52 not interpreted test results from the data room and 177 pairs of  $\Phi/k$  data from plugs.

Consistency analyses between the well test and the  $\Phi/k$  plug data led to the insight that the plugs did not represent the diagenetic effects. Subsequently the permeability field was correlated using production rates and productivity indexes.

In spite of this, the actual magnitude and heterogeneity of the permeability field remain undetermined.

For the base case, the original permeability field from the sector model was used. For the sensitivity analysis the permeability values in the three drain layers; 2, 11 and 12, were the subject of modification, since these layers are assumed to be most crucial for production.

For the low case the permeability values were divided by 3, for the high case they were multiplied by 3.

## 4.4. RESERVOIR MODEL

A sector model of the Mishrif reservoir was already available from an earlier reservoir study; therefore no new simulation model was built.

The sector model is based on an east/west cross-section representing 1/7<sup>th</sup> of the full field. The dimensions are about 9380 feet in width and 164042 ft (31 miles) in length. [26]

As can be seen in Figure 7.4.7, the reservoir is connected to a large aquifer at the base of the oil pool. The size of the aquifer is  $1,7 \cdot 10^{11}$  bbl of water, compared to  $2,25 \cdot 10^9$  bbl of oil in place. The communication of the aquifer with the oil reservoir is weak, although it is not possible to quantify the degree of communication exactly, due to the manual input of the connection data in the Eclipse model and no exact statements in the literature.

28 vertical oil producers and 4 vertical water injectors have been implemented for the base case.

The tilted oil-water contact in the model has been created by implementation of a water injector and a water producer 45000 years before the start of the simulation. The result of this run was the input data for the initial conditions of the sector model. [28]

Fig. 4.7: Mishrif sector model side view

A 3D side-view visualization of the Mishrif sector model. The model is represented as a series of blue horizontal layers forming a basin. In the center, there is a dome-shaped structure representing the oil reservoir. The top of this dome is colored with a gradient from red to green, indicating different fluid layers. A label 'tilted Oil-Water contact' with an arrow points to the boundary between the oil and water layers, which is shown as a curved, tilted surface. Several vertical lines representing wells are shown extending from the top of the dome down into the reservoir.

Fig. 4.8: Mishrif sector model length and side view

A 3D perspective view of the Mishrif sector model, showing both its length and side profile. The model consists of blue horizontal layers forming a long, narrow basin. In the center, there is a dome-shaped structure representing the oil reservoir. The top of this dome is colored with a gradient from red to green. The view shows the model's extent in the horizontal plane as well as its vertical structure.

64

Table 4.4: Sector model dimensions

	<b>Mishrif</b>	
real sector length [ft]	2800 · 164042 · 1437	
number of grid blocks	[13] [71] [20]	
length/grid block [ft/grid block]	X	21,5
	Y	2310
	Z	72

Table 4.5: Sector model properties - from Eclipse PRT file

Layer	h [ft]	avg. $\Phi$ [-]	Avg. K(h) [mD]	$\frac{k_v}{k_h}$ [-]	OOIP [MMBbl]	Formation
1	132	0,094	22,6	0,50	220,4	Upper Mishrif
2	80	0,096	370,2	0,02	260,2	
3	70	0,087	8,1	0,47	142,7	
4	79	0,084	18,2	0,50	221,7	
5	72	0,088	6,4	0,02	124,3	
6	69	0,086	0,6	0,26	106,3	
7	39	0,089	0,6	0,10	38,2	Lower Mishrif
8	49	0,093	2,3	0,04	36,6	
9	51	0,107	36,5	0,93	129,0	
10	67	0,116	1,2	0,17	150,5	
11	39	0,138	134,0	0,50	98,3	
12	65	0,116	63,3	0,26	101,3	
13	31	0,120	22,9	0,40	71,4	
14	39	0,150	160,3	0,50	137,0	
15	68	0,089	24,3	0,02	39,6	
16	33	0,113	235,1	0,50	118,9	
17	46	0,134	35,5	0,40	63,0	
18	112	0,082	0,6	0,33	58,2	
19	106	0,122	10,2	0,48	106,5	
20	209	0,121	233,2	0,50	29,6	
<b>FIELD AVERAGE</b>	<b>73</b>	<b>0,108</b>	<b>88,3</b>	<b>0,11</b>	$\Sigma$ <b>2,25·10<sup>9</sup></b>	

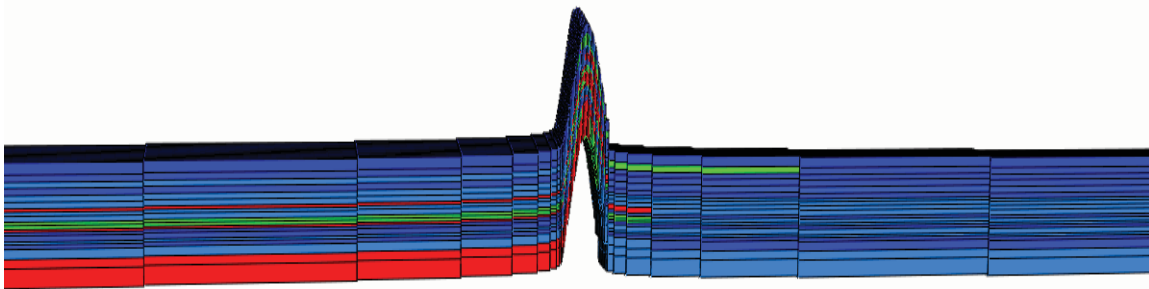
Table 4.6: Wells and completions [28]

	<b>Mishrif</b>
<b>number of wells total</b>	<b>28</b>
<b>producers</b>	22
<b>injectors</b>	4
completed in	
<b>Lower Mishrif</b>	0
<b>Upper Mishrif</b>	22
<b>Lower &amp; Upper Mishrif</b>	10

As can be seen in table 4.5, the Mishrif formation shows strong vertical heterogeneities. The model can be divided into upper Mishrif which is represented by the layers 1 to 6 and lower Mishrif, represented by the layers 7 to 20. [26]

There exist strong barriers to vertical flow between Khasib B and Mishrif; this is between layers 1 and 2, and between Mishrif mB2.1 and mB2.3, respectively layers 14 and 15, as well as within the layers mB2.3 and mC1. [28]

Fig. 4.9: Transmissibility barriers in Mishrif



The following operational conditions have been implemented in the sector model for the sensitivity analysis:

- A minimum well bottom hole pressure of 2248 psi and a minimum well tubing head pressure of 217,5 psi. The wells will shut if the respective pressure falls below either of these two values.
- The wells are put under a group target rate, where the cumulative well production cannot exceed 37740 bbl/day of reservoir fluids, this includes water and gas; the group oil target rate is set to 16430 bbl/day in the first two years and is then elevated to 32860 bbl/day.
- Water injection maximum target rate is 12500 bwppd for the four wells together.
- All wells start at the same time at the beginning of the simulation.
- There is no scheduled operation downtime.
- Duration of the simulation production time is 30,5 years.

The basecase conditions are as follows: vertical wells only, water injection and no gas lift.

## 4.5. RESULTS AND DISCUSSION

In order better compare the results and for clearer illustration purposes, two types of sensitivity analyses have been made.

One is concerned with the reservoir aspects like relative permeability curves or permeability anisotropy. The second sensitivity analysis evaluates the different lift methods; it consists of one case where the different options are compared for just vertical wells, in the other case the same options are applied to horizontal wells.

The base case for the horizontal wells is the horizontal well case described in the reservoir uncertainty section.

### 4.5.1. Reservoir parameters

Table 4.7: Sensitivity analysis input data, reservoir parameters

Uncertainty	Base Case	High Case	Low Case
Horizontal Wells	28 vertical wells, 0 horizontal wells, 4 vertical injectors	0 vertical wells, 22 subhorizontal wells, 4 subhorizontal injectors	---
Permeability anisotropy	0,01 - 1	PermZ-1,5	PermZ-0,1
Relative permeabilities	analogue and history matching curves	favorable Corey coefficient and $S_{or,w}$	unfavorable Corey coefficient and $S_{or,w}$
Matrix permeability	lab and history matching values	Values in layers 2,11,12 multiplied by 3	Values in layers 2,11,12 divided by 3

The figures 7.4.10 - 7.4.12 on the following pages illustrate the simulation outcomes of the sensitivity study. All the sensitivity parameters have large influences on the cumulative oil production.

The multiplier for the matrix permeability has a big influence in both directions although it has only been applied in three of twenty layers. However, the increased production also leads to an increased water cut.

Permeability anisotropy change has also a significant impact on oil production. The low case has not only a large negative impact on oil production but also on water cut as this reduction in vertical flow ability resulted in more water produced in wells completed over only one of few layers .

Due to the strong vertical heterogeneity of the Mishrif reservoir, subhorizontal wells were rather implemented than horizontal wells. They are beneficial for an increased production but also enlarge the water cut disproportionately.

The relative permeability curves have a big impact in spite of a relative little change compared to the changes that have been applied in other fields with the same sensitivity parameter.

Pressure decline has proved to be relatively poor (10% of initial pressure and reservoir is still above bubble point pressure) due to water injection providing significant support after several years. The difference between the cases is no more than 10 bar for an average decline of about 30 bar. In the depletion diagram, figure 7.4.12, one can very well see when the impact of water injection sets in.

Fig. 4.10: Cumulative oil production, basecase and sensitivities – reservoir case

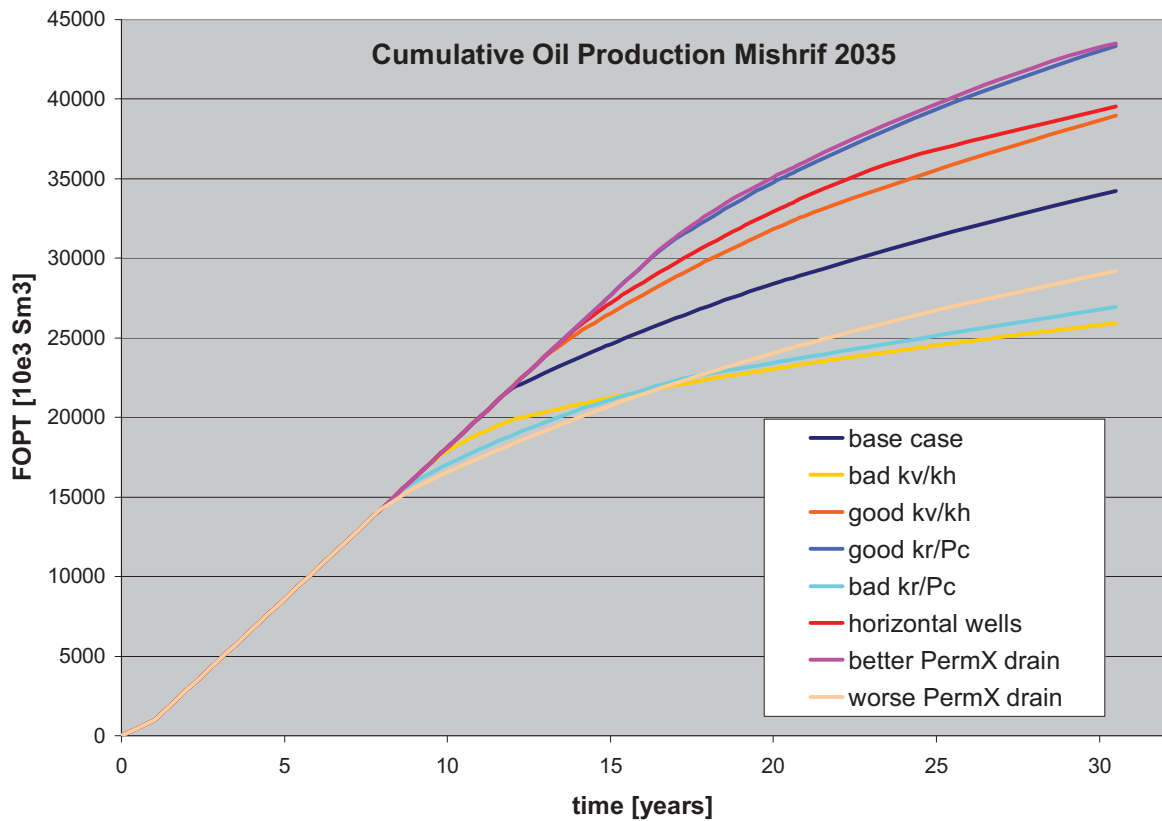




Fig. 4.11: Water cut, basecase and sensitivities – reservoir case

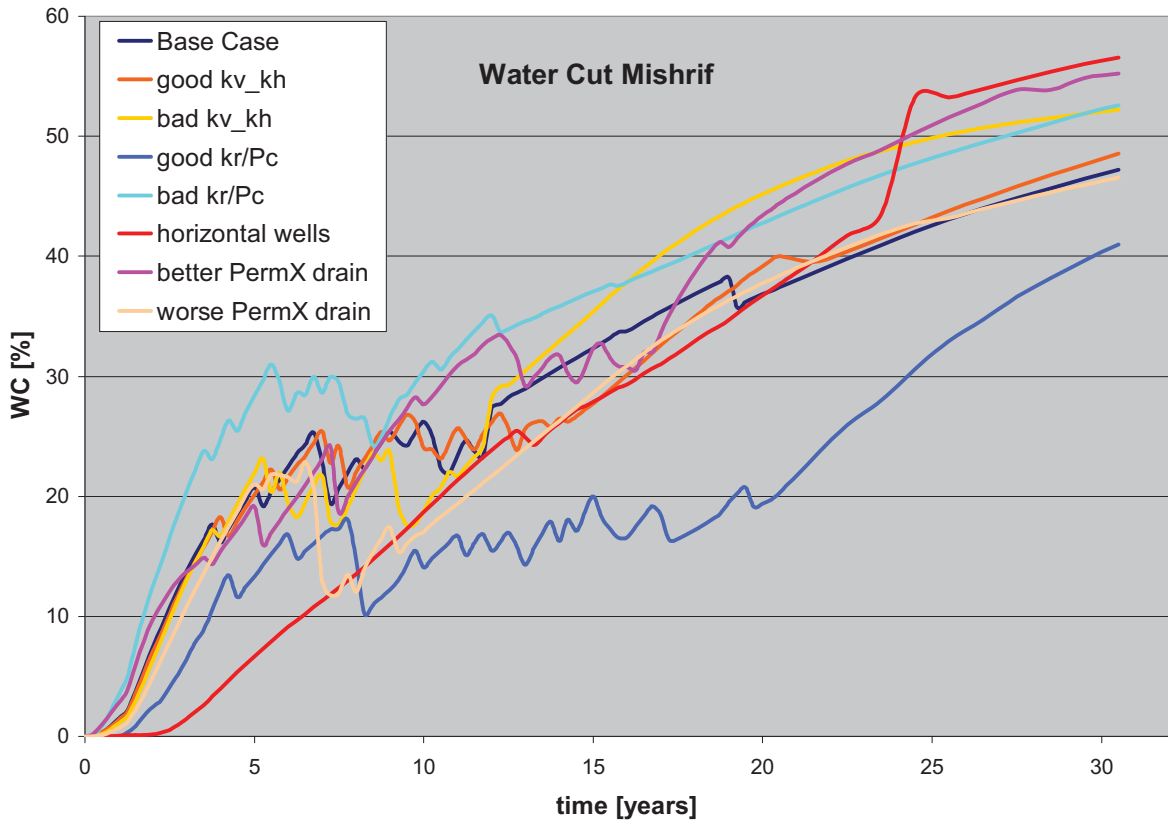


Fig. 4.12: Depletion, basecase and sensitivities – reservoir case

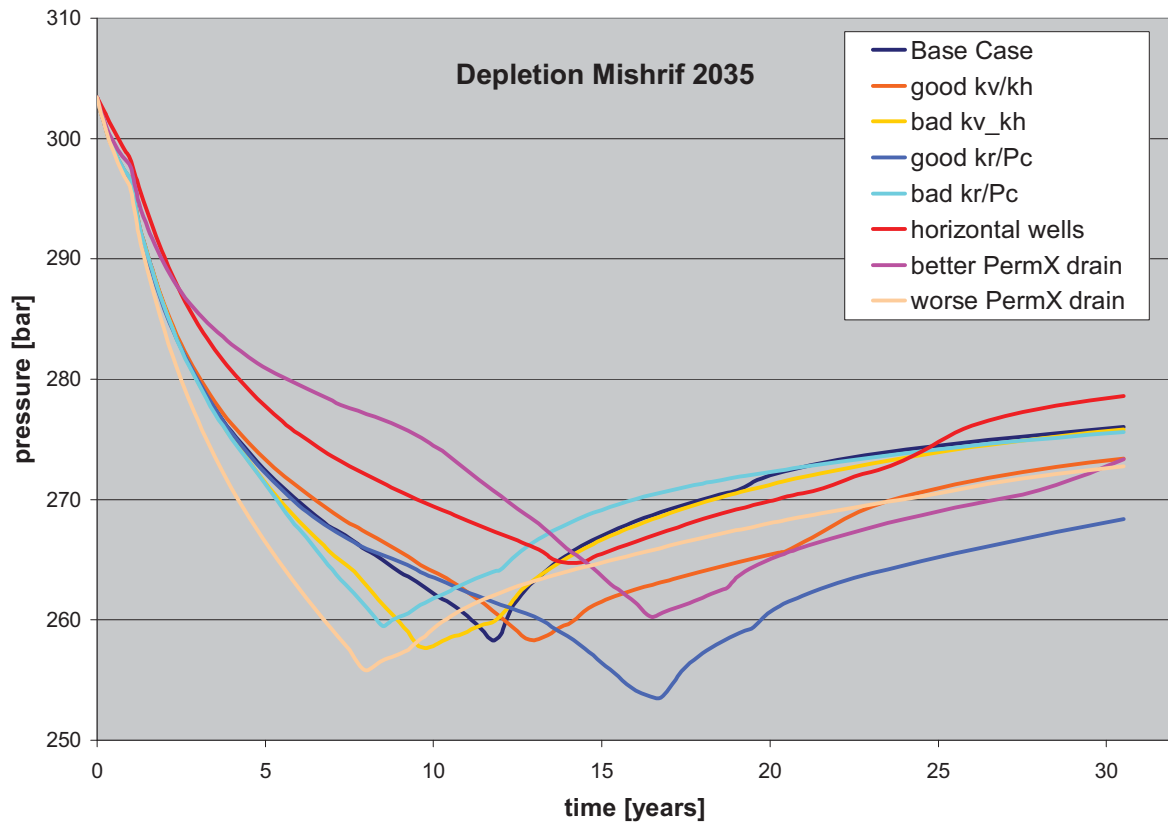


Table 4.8: Result overview Majnoon sensitivity study, reservoir properties

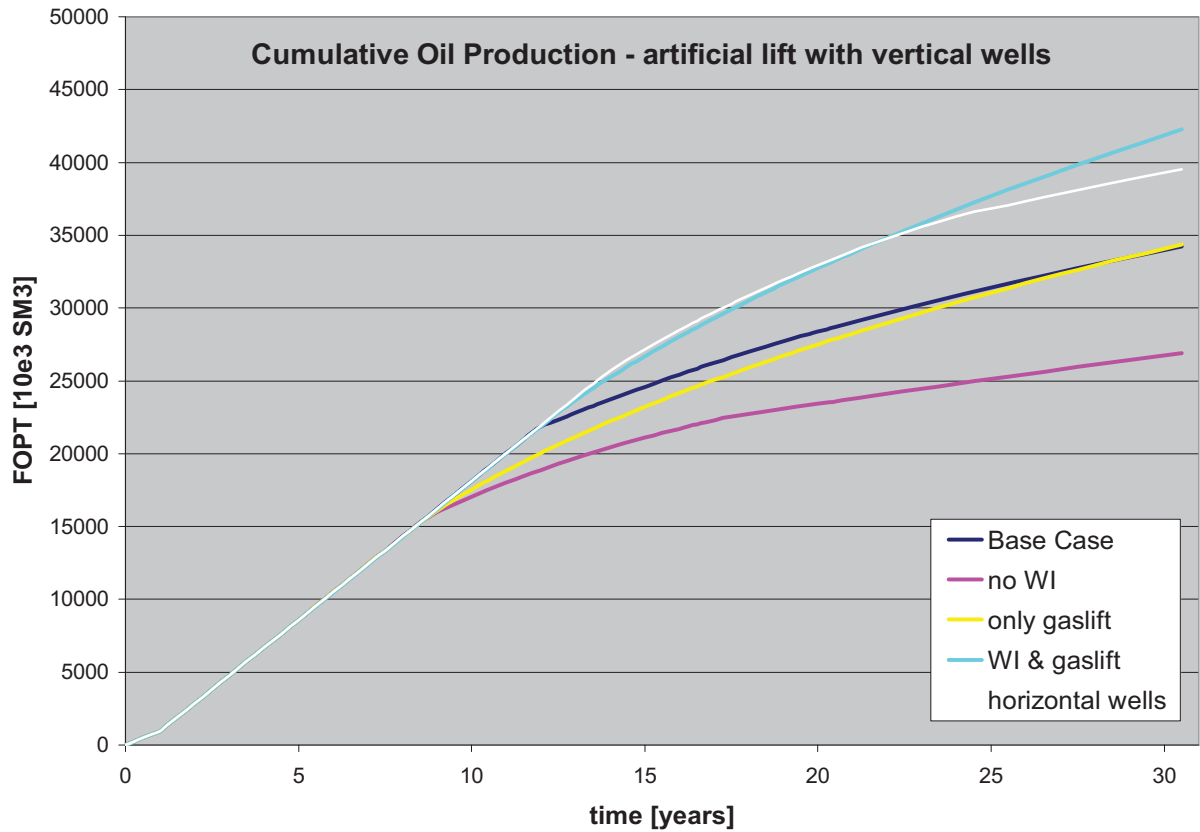
OOIP [Mbb]	2253	Np in 2035 (30,5 years) [Mbb]	RF [%]	WC in 2035 (30,5 years) [%]	Avg. reservoir pressure in 2035 (30,5 years) [bar]	
Base case figures  28 oil vertical wells +4 WI  variable from 0,01 to 1  Curves from analog and history matching from lab tests and history matching  variable from 0,01 to 1  Curves from analog and history matching from lab tests and history matching	Base case		215	9,6%	47,2%	276,0
	High cases					
	Horizontal wells	22 oil and 4 water injectors sub-horizontal wells from the beginning	249	11,0%	56,6%	278,6
	High Kv/Kh	PermZ +50% from base case figures	245	10,9%	48,5%	273,4
	High Kr	High case curves from changing Corey coefficients and Sorw. values multiplied by 3 in layers 2,11 and 12	273	12,1%	41,0%	268,4
	High permeability		274	12,1%	55,2%	273,4
	Low cases					
low Kv/Kh	PermZ 1/10th of base case figures	163	7,2%	52,2%	275,8	
Low Kr	Low case curves from changing Corey coefficients and Sorw.	186	8,3%	52,6%	275,6	
low permeability	values divided by 3 in layers 2,11 and 12	184	8,1%	46,6%	272,8	

### 4.5.2. Artificial lift with vertical wells

Table 4.9: Sensitivity analysis input data, artificial lift, vertical wells

Uncertainty	Base Case	Sensitivity
artificial lift method	28 vertical wells,  4 vertical water injectors,  no gas lift	28 vertical wells, water injection suppressed, no gas lift → no artificial lift
		28 vertical wells, water injection suppressed, gas lift
		28 vertical wells, 4 vertical water injectors, gas lift

Fig. 4.13: Cum. oil prod., basecase and sensitivities – artificial lift, vertical wells



Only the combination of water injection and gaslift yields a satisfactory result. No artificial lift at all is detrimental for the production, as lift alone gives only the same production as the base case with water injection. Nevertheless, the combination of water injection and gaslift increases the water cut significantly.

The case without water injection shows a pressure stabilization at around 215 bar while production is running at about 20,000 bwpd, this is an indication of the strength of the aquifer.

The thin white curve illustrates the base case with horizontal wells, in order to facilitate comparison between the case horizontal wells without gas lift and the case vertical wells with two artificial lift methods.

Fig. 4.14: Water cut, basecase and sensitivities – artificial lift, vertical wells

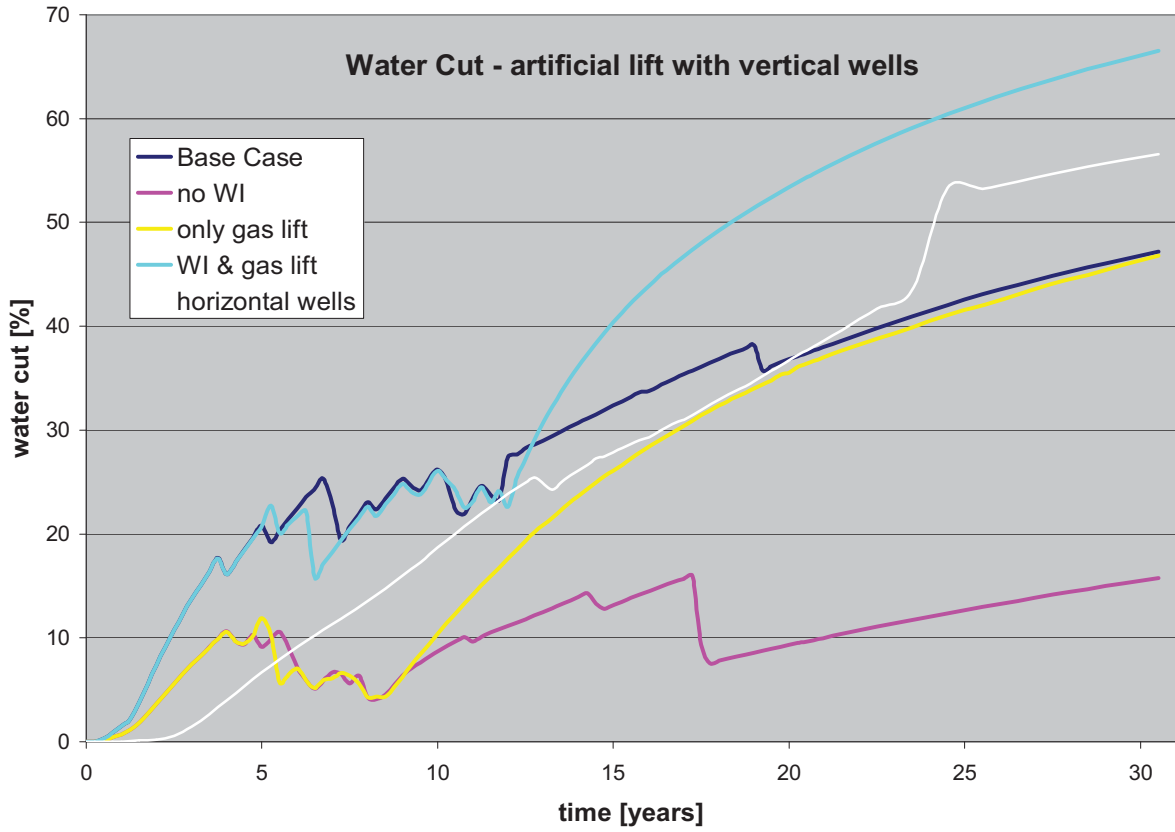
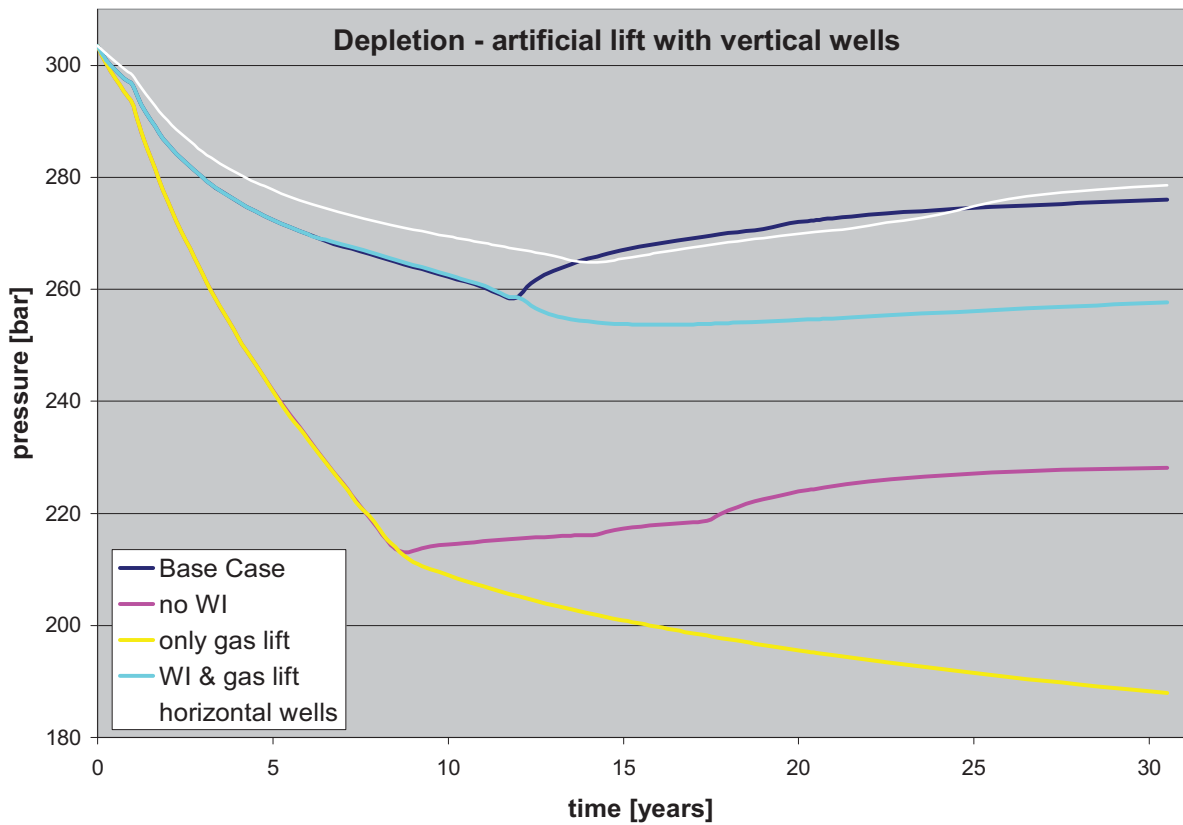


Fig. 4.15: Depletion, basecase and sensitivities – artificial lift, vertical wells

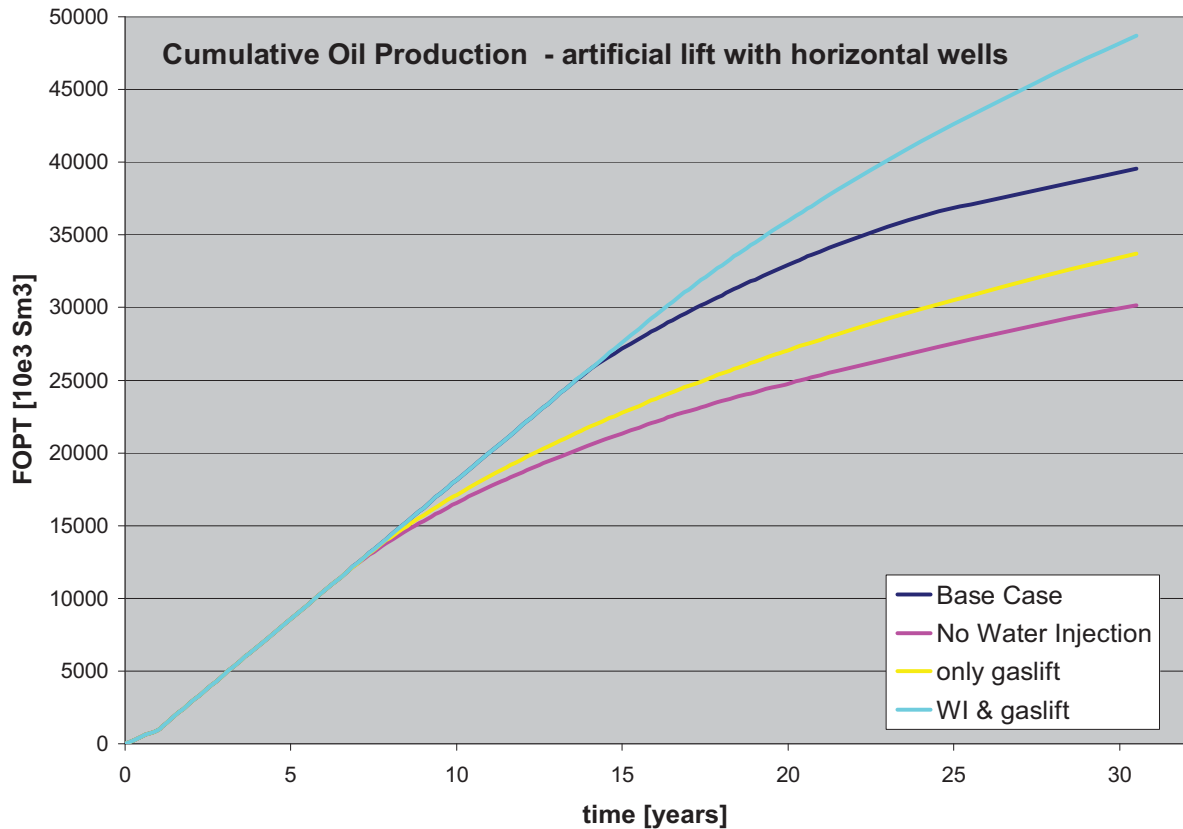


### 4.5.3. Artificial lift with horizontal wells

Table 4.10: Sensitivity analysis input data, artificial lift, horizontal wells

Uncertainty	Base Case	Sensitivity
artificial lift method	22 subhorizontal wells, 4 subhorizontal water injectors, no gas lift	22 subhorizontal wells , water injection suppressed → no artificial lift
		22 subhorizontal wells , water injection suppressed, gas lift
		22 subhorizontal wells, 4 subhorizontal water injectors, gas lift

Fig. 4.16: Cum. oil prod., basecase and sensitivities, artificial lift, horizontal wells



As in the sensitivity runs with the vertical wells, only the adding of gaslift yields more production than the base case with water injection.

The water cut is also higher than in the cases with vertical wells, as the sub-horizontal wells are completed in a lower number of layers and produced at higher rates. In this relatively low  $k_v/k_h$  ratio reservoir this facilitates earlier water breakthrough.

Here, gas lift alone gives even slightly less production than in the base case. This is because pressure losses (deviated hole is longer than vertical one) and water cut are slightly higher in sub-horizontal wells than in vertical ones. When reservoir pressure has declined and is coming close to the well dying limit, well productivity is of minor importance compared to pressure losses during production.

The water cut is significantly increased by all artificial lift methods.

Fig. 4.17: Water cut, basecase and sensitivities, artificial lift, horizontal wells

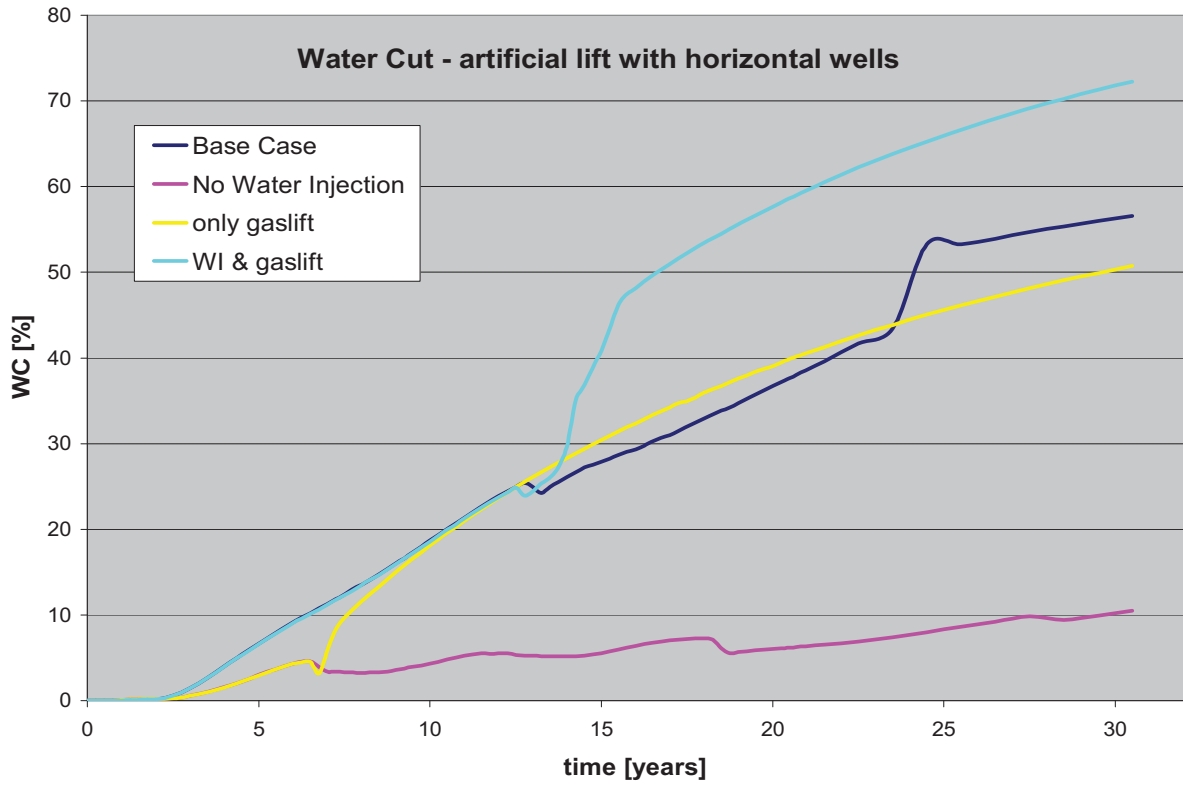


Fig. 4.18: Depletion, basecase and sensitivities, artificial lift, horizontal wells

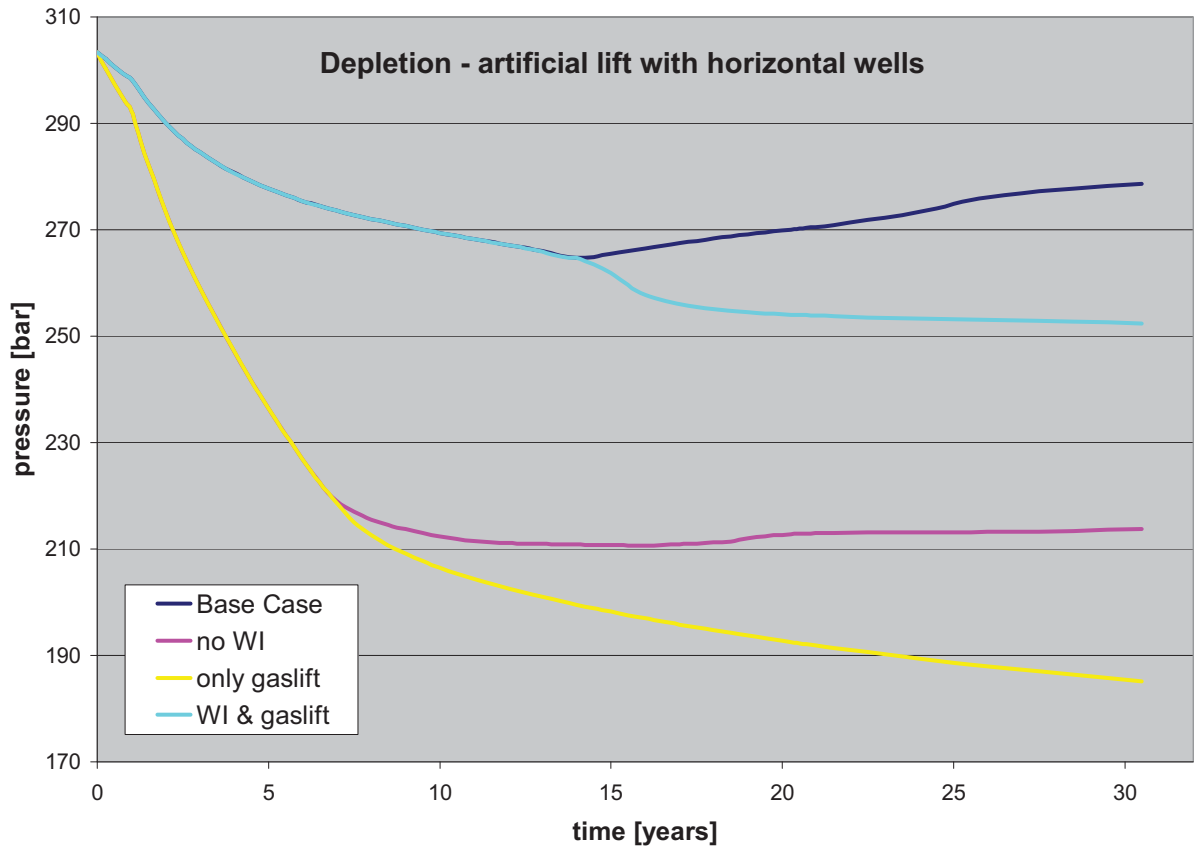


Table 4.11: Result overview Mishrif sensitivity study, artificial lift

OOIP [Mbb]		2253		Np in 2035 (30,5 years) [Mbb]	RF [%]	WC in 2035 (30,5 years) [%]	Avg. reservoir pressure in 2035 (30,5 years) [bar]
Base case				215	9,6%	47,2%	276,0
<b>With vertical wells</b>							
28 vertical production wells, 4 vertical water injection wells, no gas lift	No Wi and No Gaslift	suppress Water Injection		169	7,5%	15,8%	228,1
	Wi and Gaslift	all wells gas lifted		266	11,8%	66,6%	257,6
	Gas lift only	No Water Injection and all wells gas lifted		216	9,6%	46,8%	188,0
<b>With horizontal wells</b>							
22 subhorizontal production wells, 4 subhorizontal water injection wells, no gas lift	No Wi and No Gaslift	suppress Water Injection		190	8,4%	10,5%	213,7
	Wi and Gaslift	all wells gas lifted		306	13,6%	72,2%	252,4
	Gas lift only	No Water Injection and all wells gas lifted		212	9,4%	50,8%	185,2

#### **4.5.4. General conclusions on Mishrif results:**

Regarding reservoir properties, the relative permeability curves and permeability of the drain layers have a big impact in spite of a relatively little change. It would be advisable to take cores to get more reliable data.

The implementation of subhorizontal wells is beneficial for the cumulative oil production, but it significantly increases the water cut. The income due to the increased production has to be balanced against the cost of water treatment. Additionally the principal feasibility of installing water treatment facilities and their cost has to be considered.

It is strongly recommended that artificial lift is retained. Water Injection is essential to give pressure support to the reservoir. Another gain in cumulative production is yielded by combining water injection with gas lift. This however increases the water cut significantly, as in the case of the subhorizontal wells this has to be balanced by the costs of water treatment.

It is not recommendable to employ only gas lift. It will give a production increase compared to natural depletion, but acts detrimental on the pressure regime in the reservoir.

According to economic studies, either water injection or water injection compared with gas lift should be the preferred options.



## 5. RAUDHATAIN / UPPER BURGAN

The Burgan reservoir is one of three reservoirs in the Raudhatain oil field. Raudhatain is located in northern Kuwait and is part of an oil field agglomeration commonly referred to as “Northern Fields”.

The field was discovered in 1954, put on stream in 1959 and has been producing ever since.

The field geometry is a triangular dome-anticline with a four way closure at a depth of approximately 500 ft. The field covers an area of about 20 square miles. The crest is located at about 7400 ft TVDss.

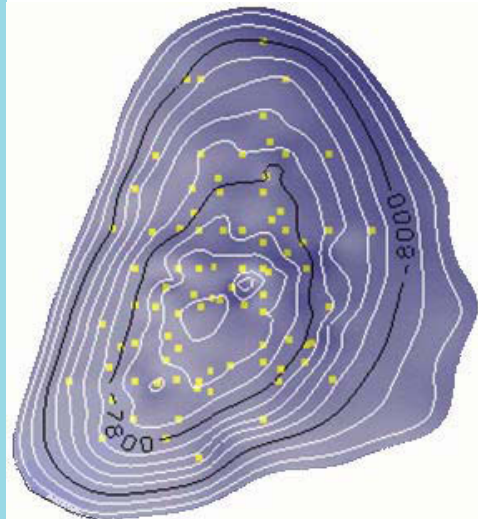
The Raudhatain field comprises three major reservoirs, the carbonate Mauddud formation and the two sandstone formations Burgan and Zubair. This study will be only concerned with the Upper Burgan reservoir.

The Burgan formation is a Cretaceous (Albian) sandstone and shale formation which was deposited in a marine setting. [29]

Fig. 5.1: Raudhatain field location [29]



Fig. 5.2: Top Burgan reservoir [30]



## 5.1. SEDIMENTOLOGY

The Raudhatain field is one member of an agglomeration of several giant fields of predominantly Early Cretaceous (Albian) age which are, to a large extent, clastic oil reservoirs.

The structure of the field is an elongated dome which was formed along with the Kuwaiti Arch during the Late Cretaceous. The flanks of the field have a dip of about 4°.

Numerous northwest and northeast trending normal faults are present in the field; their throws are ranging between 30 and 160 ft. Their origin is believed to lie in salt tectonics, which are supposedly still active today. [31]

The Raudhatain field consists of three main reservoir horizons which can be found in most Kuwait fields. They are shortly presented in the following:

The topmost formation is the Mauddud carbonate reservoir. The top reservoir lies at about 7400 ft and it has an average thickness of 330 ft. It consists of the clean carbonate Upper Mauddud and the carbonate-sandstone mixed Lower Mauddud. The reservoir is faulted and fractured.

Below Mauddud lies the Burgan sandstone reservoir. It is separated into two distinct reservoirs, the Upper and the Lower Burgan, by the tight Middle Burgan. The top reservoir lies at about 7700 ft and it has an average thickness of 575 ft.

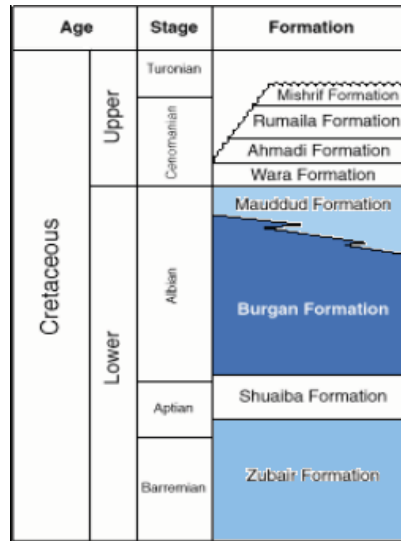
The lowermost reservoir is called Zubair. The top reservoir lies at approximately 9060 TVDs and it is about 1380 ft thick. As Burgan it is a clastic sandstone reservoir. It consists in fact of seven independent reservoirs which all have their own oil-water contacts. [32]

The field zonation is illustrated in Fig. 5.3.

Table 5.1: Raudhatain reservoir properties [29]

	<b>Mauddud</b>	<b>Burgan</b>	<b>Zubair</b>
<b>OOIP</b> [billion STB]	2450	7520	2950
<b>Lithology</b>	Limestone	Sandstone	Sandstone
<b>Thickness</b> [ft]	330	575	1380
<b>Avg. Porosity</b> [%]	17	24 - 28	24
<b>Avg. Permeability</b> [mD]	215	320 - 2560	400 - 4400
<b>Oil Gravity</b> [°API]	28 - 33	31 - 34	31 - 35

Fig. 5.3: Raudhatain reservoir zonation [29]



The deposition of the Burgan formation took place in paralic to offshore environments, initially in response to a relative sea level fall, subsequently responding to a long term/low frequency relative sea level rise. Superimposed short term/high frequency changes of relative sea level have led to a complex depositional evolution. [33]

The base of the Lower Burgan is marked by a long term/low frequency rise in relative sea level. Consequently fluvial processes were dominating during this period. In upward direction however, marine processes gained in influence. In the upper part of the Lower Burgan, the Middle Burgan and the Upper Burgan high frequency relative sea level changes occurred. [33]

The alternation of depositional environments in Upper Burgan is complicated; the following depositional environments have been recognized: marine-influenced channels and estuarine settings, marine mudrocks and shoreface sandstones, tidally influenced deltas.

However, the main depositional feature of Upper Burgan is incision and filling of channels and/or valleys that have been cut into a background of marine sediments. As a consequence most zones are laterally discontinuous.

Upper Burgan is thus a channel-dominated interval, the various genetic channel elements that could be identified and distinguished in the Upper Burgan are shortly presented in the following, with regard to their lithology and their reservoir properties: [33]

**Marine-influenced channels** this are i.e. erosional bases with fining-upward log profile. They are mostly dominated by carbonaceous sandstones. Reservoir quality is usually very good here.

**Laterally accreting muddy channels** this facies is mud – or heterolithic dominated, only on some cores minor sand components were observed. The heterolithic parts are interpreted as estuarine channel fills, while the more muddy part is likely to originate from muddy tidal creeks. It is predominantly a non-pay facies.

Estuarine/marginal-marine mudrocks	this mudrock shows abundant plant remains and other carbonaceous material. Its occurrence is in the most cases associated with channel sandstones of mouthbar facies. Reservoir properties are difficult to determine because they are biased by the associated facies.
Delta top fines	this genetic element contains mostly carbonaceous mudrocks with interbedded coals. Marine influence is not obvious. This is just a minor component of the Burgan formation.
Mouthbar sandbodies	also this facies constitutes only a minor part in Burgan. Its log signature is coarsening upwards, this are commonly associated with minor channels and estuarine mudrocks.
Shoreface sands	this facies is a major genetic element of the Upper Burgan formation. The lithology is predominantly bioturbated sandstone with various burrow types. The log profile is generally coarsening upwards. Because this facies is very mud-rich, the reservoir quality is poor to medium. They are either organized in progradational parasequence sets or in retrogradational packages.
Marine mudrocks	this facies is associated with the shoreface sands and forms the base for the above described coarsening upwards packages. This is a non-pay facies.

## 5.2. RESERVOIR GEOLOGY

The Upper Burgan reservoir was chosen for this study for several reasons. First of all there was interest in studying a sandstone reservoir, which outcasted the Mauddud limestone reservoir. Comparing between the two sandstone reservoirs, Burgan bears more OOIP than Zubair and is therefore more interesting. The Upper Burgan horizon was finally preferred to the Lower Burgan because it is less depleted and shows therefore more potential for future development. [29]

The reservoir quality in Upper Burgan is mainly controlled by the content of ductile matter, i.e. clays. This content is highly variable, between zero and seventy percent but generally higher as in the Lower Burgan, which is a very clean sand.

Petrographical analyses of the cored Upper Burgan intervals have shown the reservoir comprises mineralogically mature, that means quartz-rich, very fine to medium grained sandstones and siltstones. The diagenetic modification of the Burgan reservoir is minor, although it is observed locally. [33]

With the help of cores and wireline logs, Upper Burgan was correlated fieldwide and zoned into different layers. The layering scheme and layer properties are described in the following. As illustrated in Fig. 5.4, the layers are cut in by channel fills, which are laterally discontinuous but comparable. Each layer is therefore a pair of two channel fills. The layers are described from top to bottom. [33]

**Zone UB70/UB65:** in this zone mainly marine-influenced channels are present. High quality channel sands can be found in the UB 70 part, on the contrary in UB 65 there are shoreface sands present which show only a moderate reservoir quality.

**Zone UB60/UB55:** these zones are rather thin because they have been eroded by the overlying channels. Preserved are mainly marine mudstones which are overlying the UB 50 flooding surface. These mudstones are likely to form a significant flow barrier. Some high quality channel sandstones are preserved in the UB 60 zone; apart from that this section is mostly estuarine influenced and has poor reservoir quality.

**Zone UB50/UB45:** this zone comprises interbedded minor marine-influenced channels and estuarine mudrocks. The complex depositional pattern has led to a complex permeability distribution. The sand bodies seem to be interconnected but flow paths are highly tortuous. The UB50 contains the higher quality channel sands; UB 45 accommodates shoreface sands with a medium quality.

**Zone UB40/UB35:** UB40 contains high quality channelized sandstones, whereas in UB35 marine mudrocks and shoreface sandstones dominate. The area in which UB35 prevails acts most likely as an effective flow barrier.

**Zone UB30/UB25:** In these two zones there is less evidence of channeling than in the overlying sections. The marine influence becomes stronger in this zone, as seen in the sediments. The higher quality sandstones are found in UB30, the more marine influenced unit UB25 has poor to at moderate reservoir quality.

**Zone UB20/UB10:** these zones are insignificant as oil producing reservoirs, thus no depositional map has been created. They comprise only marine lithologies and can be considered as tight. They form, together with the Middle Burgan, a major permeability barrier towards the Lower Burgan.

Fig. 5.4: Upper Burgan Zonation [29]

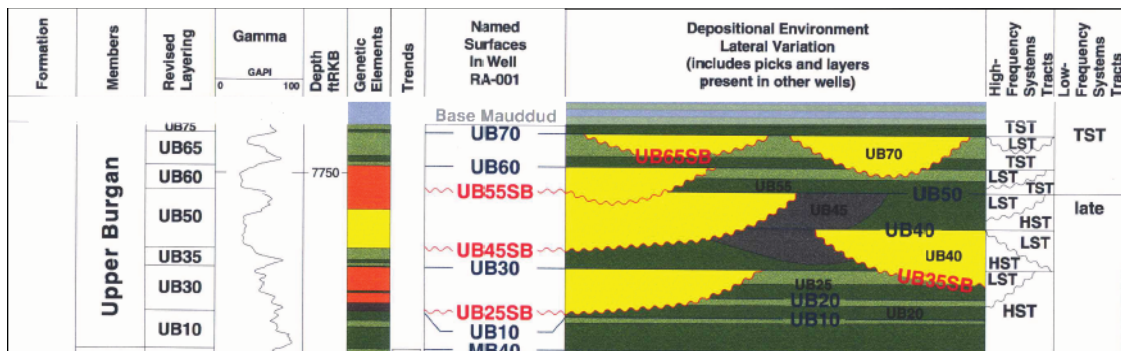


Table 5.2: Upper Burgan average zonal properties [33]

	Porosity (%)	Permeability (mD)		Porosity (%)	Permeability (mD)
UB70	20 - 28	150 - 1700	UB65	12 - 24	< 290
UB60	16 - 33	9 - 4190	UB55	14	4
UB50	14 - 28	200 - 4400	UB45	14 - 22	< 144
UB40	8	117 - 4390	UB35	11	3 - 270
UB30	22	314 - 3819	UB25	17	13 - 91
UB20	< 26	9 - 240	UB10	< 26	5

The top reservoir lies at 7400 ft TVDss, the Upper Burgan oil-water contact lies at -8000 TVDss.

The Upper Burgan was first put on production in May 1959. 44 wells with 60 completions have been drilled since then.

In the year 1990/1991 a blowout with a volume of 20,6 MMSTB occurred.

The reservoir is producing through natural depletion and natural flow through a 3 1/2" tubing or annulus.

The reservoir is abundantly faulted, but the faults have been found to have a minimal effect on the reservoir.

The original oil in place in the Upper Burgan is estimated to be 1,9 Billion STB. By July 2005, 237 MMSTB had been produced, which results in a recovery factor of about 12,5 %. [34]

Table 5.3: Upper Burgan reservoir fluid and oilfield properties [34]

		<b>Upper Burgan</b>
<b>API gravity</b>	[°API]	24 - 34
<b>Viscosity</b>	[cP]	0,8 – 6,1
<b>Initial GOR</b>	[SCF/STB]	83 - 743
<b>FVF</b>	[RB/STB]	?
<b>Reservoir Temperature</b>	°C	81
<b>Original reservoir pressure</b>	[psi]	3775
<b>Pressure gradient</b>	[psi/ft]	?
<b>Formation compressibility</b>	[1/psi]	1E-05
<b>Bubble Point Pressure</b>	[psi]	659 - 2893

## 5.3. UNCERTAINTIES

The following uncertainties were identified from Total in-house literature:

- (1) Aquifer Presence
- (2) Fault Transmissibility
- (3) Layer Transmissibility
- (4) Relative permeabilities
- (5) Permeability Anisotropy
- (6) Impact of horizontal wells

### 5.3.1 Aquifer Presence

The existence of an aquifer has not been mentioned in any report. The one exception is a report referring to the aquifer volume as one history match parameters of the full field model.

Due to the lack of information the base case was modeled without an aquifer. For the sensitivity analysis an aquifer was implemented and connected to all layers. The aquifer parameters are listed in the following table:

Table 5.4: Upper Burgan hypothetical aquifer parameters

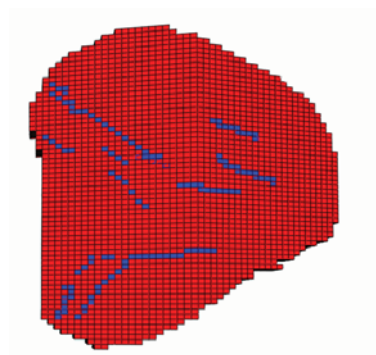
Datum Depth	Permeability	Porosity	Compressibility	Radius	Height	Angle
[ft]	[mD]	[-]	[1/psi]	[ft]	[ft]	[°]
7700	500	0,5	3e-6	10000	1000	180

### 5.3.2 Fault Transmissibility <sup>[35]</sup>

Various faults with small throws from 10-15 ft have been identified. Their influence on flow behavior is supposed to be limited, but this has not been verified.

In the base case the faults were modeled with a transmissibility of 0,1. For the sensitivity analysis they were modeled with a transmissibility of 0 for a high case, and with a transmissibility of 1 for a low case.

Fig. 5.5: Burgan faults



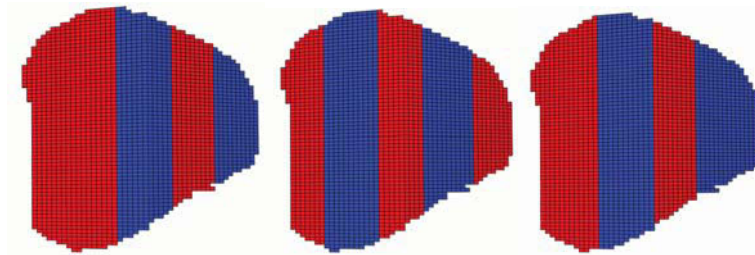
### 5.3.3 Layer Transmissibility <sup>[36]</sup>

Due to the abundant presence of shale layers, respectively layers with poor reservoir quality (cp. chapters Sedimentology and Reservoir Geology) the connectivity of the sand bodies is disrupted. The layers are in good pressure communication, nevertheless, some of the shale layers might act as effective barriers to vertical flow.

In the literature about the full field simulation model, on which this model is based, implemented flow barriers are not mentioned. Thus for the base case no flow barriers were modeled.

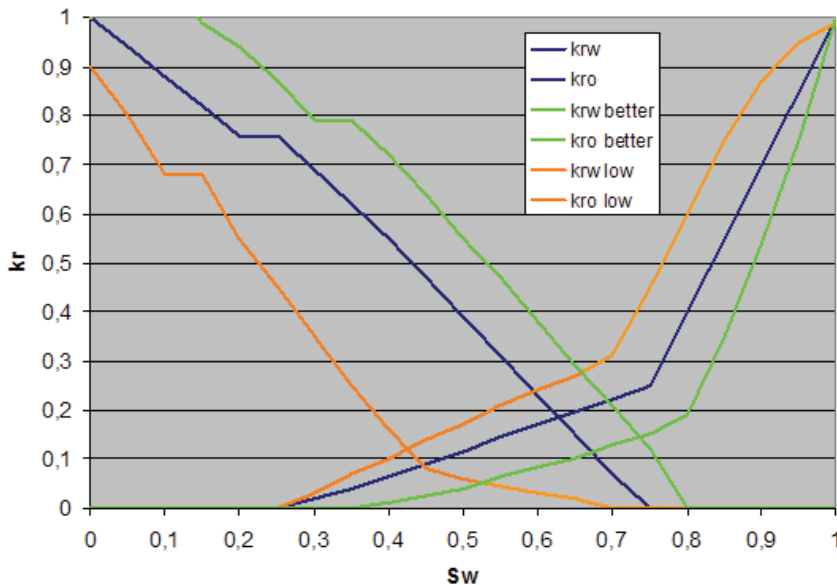
For the sensitivity analysis however, impermeable streaks were implemented according to the information about reservoir quality in the Sedimentology and Reservoir Geology section. Two barrier streaks with zero transmissibility were implemented between the layers 2-3, 4-5 and 5-6. This corresponds to the zones UB60/UB55, UB40/UB35 and UB30/UB25.

Fig. 5.6: Intransmissible barriers, from left to right: layer 2/3, layer 4/5, layer 5/6



### 5.3.4 Relative permeabilities <sup>[36]</sup>

Fig. 5.7: Relative permeability curves





The relative permeability curves are mentioned in the literature as the parameter with which the most uncertainty is associated. The shape of the curves as well as the endpoint saturations have been determined from saturation matching, there exists apparently no experimental data.

The blue curve is the exact same curve that was used for the full field model; it was used for the base case. The green and orange curves represent the favorable, respectively unfavorable cases in the sensitivity analysis.

### **5.3.5 Permeability Anisotropy<sup>[37]</sup>**

The ratio of vertical to horizontal permeability was referred to as a history match parameter in the literature. The original value is very low - 0,001. It was used to match pressure gradients from MDT measurements. The value also takes into account the abundant shale content of the Burgan sands. This value is employed in the basecase.

However, the ratio is likely to be higher in high quality sands. A range of the uncertainty is mentioned in the literature, namely 0,01 as a low case and 0,0001 as a high case. These values for used for the sensitivity analysis.

### **5.3.6 Impact of horizontal wells**

No horizontal wells have been drilled to date for unknown reasons. Nevertheless it is interesting to evaluate the potential for new producers.

The base case contains 42 vertical wells, for the sensitivity analysis four additional horizontal wells start production in January 2006. One well is completed in layer 2, one in layer 4 and two in layer 6. This was chosen according to the observed sweep efficiency after the base case simulation run.

### 5.4. RESERVOIR MODEL

A reservoir model has been built for the Upper Burgan reservoir. It is based on the, for this purpose utilizable, information about the reservoir that has been gathered from various reports. The degree of complexity of the model is a function of the amount and detail of information that could be obtained. The sector model dimensions are detailed in the following table:

Table 5.5: Upper Burgan model dimensions [37]

		<b>Mishrif</b>	
real sector length [ft]		23600 · 23600 · 505	
number of grid blocks		[49] [65] [7]	
length/grid block    [ft/grid block]		X	482
		Y	363
		Z	72

However, some cells were subsequently made inactive to preserve the triangular structure of the field.

Fig. 5.8: Upper Burgan model top view

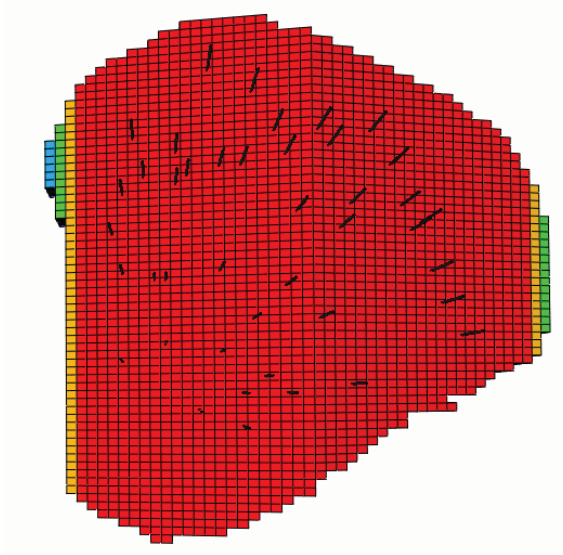


Fig. 5.9: Upper Burgan model side view

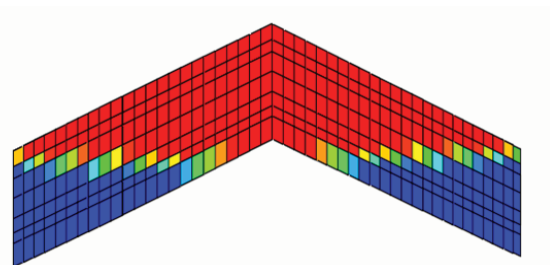


Table 5.6: Upper Burgan wells and completions [35]

	Upper Burgan
<b>number of production wells total</b>	<b>42</b>
number of completions in layers	
<b>1</b>	1
<b>2</b>	8
<b>3</b>	9
<b>4</b>	14
<b>5</b>	5
<b>6</b>	7
<b>7</b>	5
<b>Total number of completions</b>	<b>49</b>

Table 5.7: Upper Burgan reservoir model properties

Layer	h [ft]	avg. $\Phi$ [-]	Avg. K(h) [mD]	$\frac{k_v}{k_h}$ [-]	OOIP [MMBbl]	Formation
1	69	0,187	553,6	0,001	5509	Upper Burgan
2	53	0,118	262,9	0,001	2213	
3	85	0,154	507,1	0,001	3582	
4	89	0,156	476,7	0,001	2743	
5	62	0,162	327,4	0,001	1695	
6	46	0,075	172,2	0,001	514,7	
7	102	0,046	122,6	0,001	582,3	
<b>FIELD AVERAGE</b>	<b>75</b>	<b>14,7</b>	<b>412,2</b>	<b>0,001</b>		

The history match of the model was performed by roughly matching the cumulative oil production, the water cut and the depletion. The wells were opened according to their history schedule and producing at average historic rates as indicated in the literature. Fig. 5.10 gives an illustration of the accuracy of the history match.

The green curves are curves from the (unavailable) history matched full field model, the slightly transparent black curves are the results from the model presented here in this study.

After the successful history match the rates were increased to emphasize the response of the reservoir to production conditions.

The following operational conditions have been implemented in the sector model for the sensitivity analysis:

- A minimum well bottom hole pressure of 100 psi. The wells will shut if the bottom whole pressure falls below this limit. A well tubing head pressure limit could not be set due to the lack of lift tables.
- The wells are put under an individual reservoir fluid volume target rate of 4000 bbl/day.

- The wells start and shut subsequently according to the indicated real production history. In 2005 26 wells are on stream.
- There is a scheduled operation downtime for all wells for two years; this is the time when production was interrupted due to the blowout.
- Duration of the simulation time is 70,5 years (including the two years downtime).

Fig. 5.10: Cumulative oil production match [34]

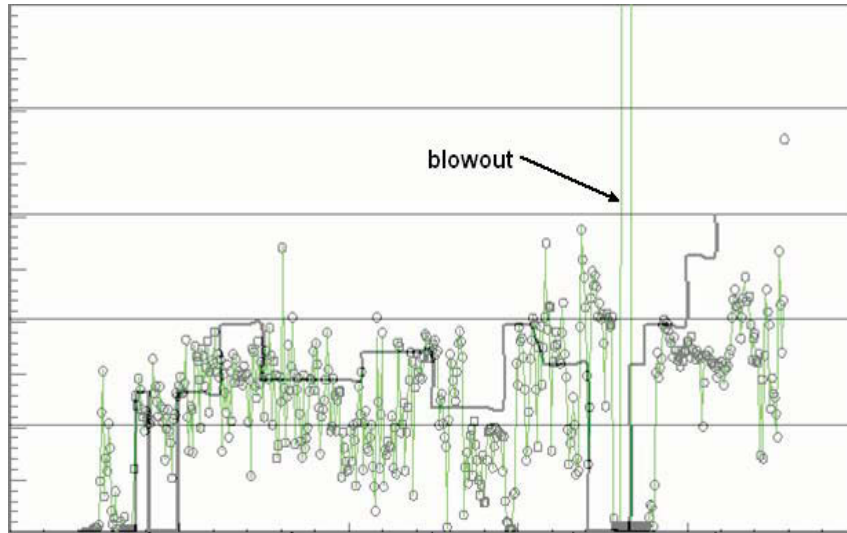


Fig. 5.11: Pressure depletion match [34]

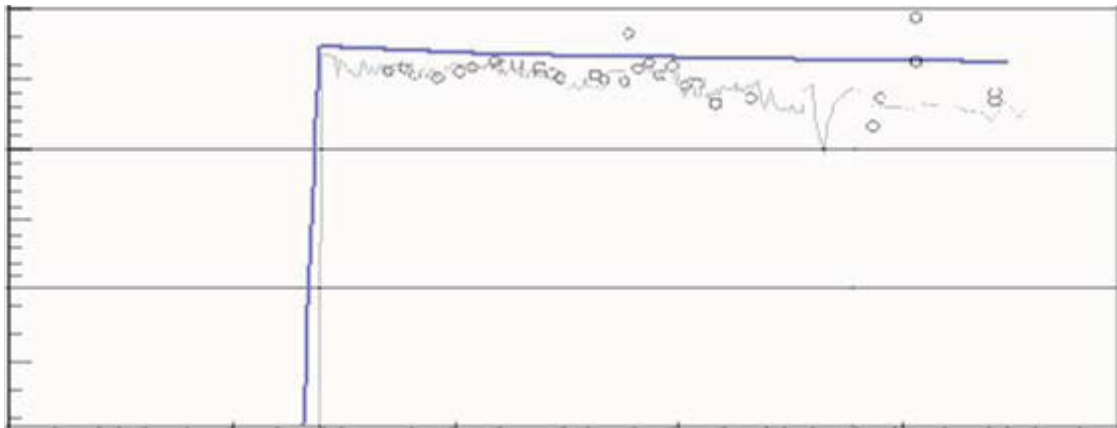
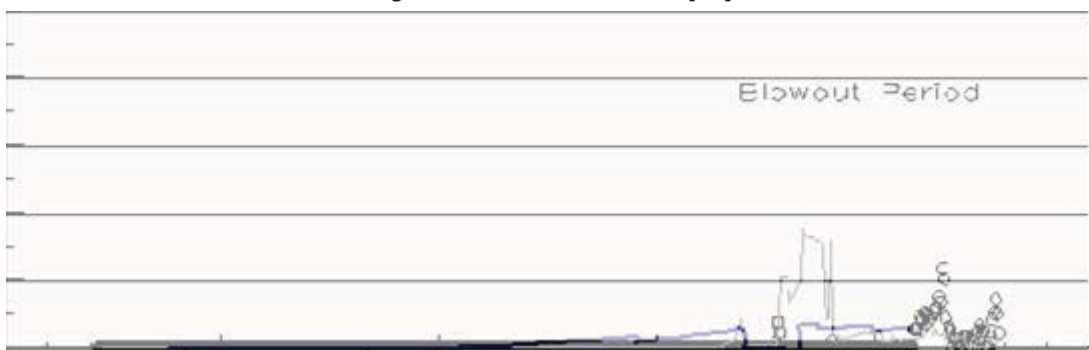


Fig. 5.12: Water cut match [34]

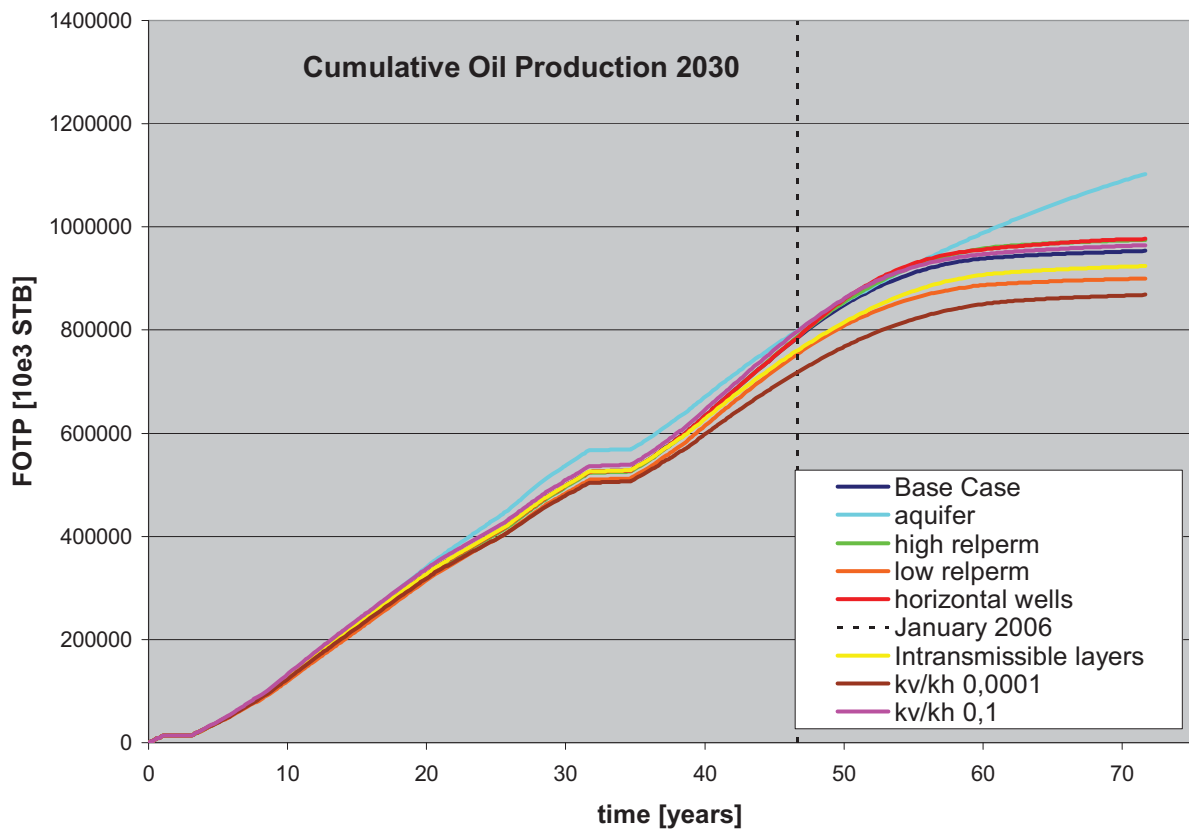


### 5.5. RESULTS AND DISCUSSION

Table 5.8: Sensitivity analysis input data

Uncertainty	Base Case	High Case	Low Case
Horizontal wells	42 vertical wells 0 horizontal wells	42 vertical wells 4 horizontal wells from 2006 on	---
Permeability anisotropy	PermZ = PermX·0,001	PermZ = PermX·0,01	PermZ = PermX·0,0001
Relative permeability curves	curves from analogues and history matching	favourable Corey coefficients and Sor,w	unfavourable Corey coefficients and Sor,w
Aquifer	no aquifer	aquifer present	---
Layer transmissibility	all layers transmissible	some barriers between layers 2-3, 4-5 and 5-6	---

Fig. 5.13: Cumulative oil production, basecase and sensitivities



The presence of an aquifer gives a significant increase in production and yields almost a doubled water cut compared to the base case and to the real outcome. Also, the observed reservoir pressure is much higher than reality. We can thus conclude that if an aquifer is present in reality it has to be rather weak. Nevertheless the possibility that the water is held back by the impermeable shale layers has to be considered.

It is pointed out that pressure decline is important for all other cases and drops below the highest bubble pressure (2893 psi) during year 53. From that time on the GOR rises significantly and limits oil productivity at the wellbore and thus well production. This highlights the urgency of water injection implementation for pressure support.

On the other hand, the aquifer case shows reservoir pressure higher than bubble pressure and thus oil production rate remains relatively high at the end of the production period.

Horizontal wells do not increase the cumulative oil production a lot. This is most likely due to the relatively high compartmentalization of the reservoir and its heterogeneous properties. The likeliness of a horizontal well to encounter a tight shale layer is high. Furthermore horizontal wells are rather suited for formations with high vertical permeability, which is not the case in the Upper Burgan reservoir.

Fig. 5.14: Water cut in the basecase and sensitivities

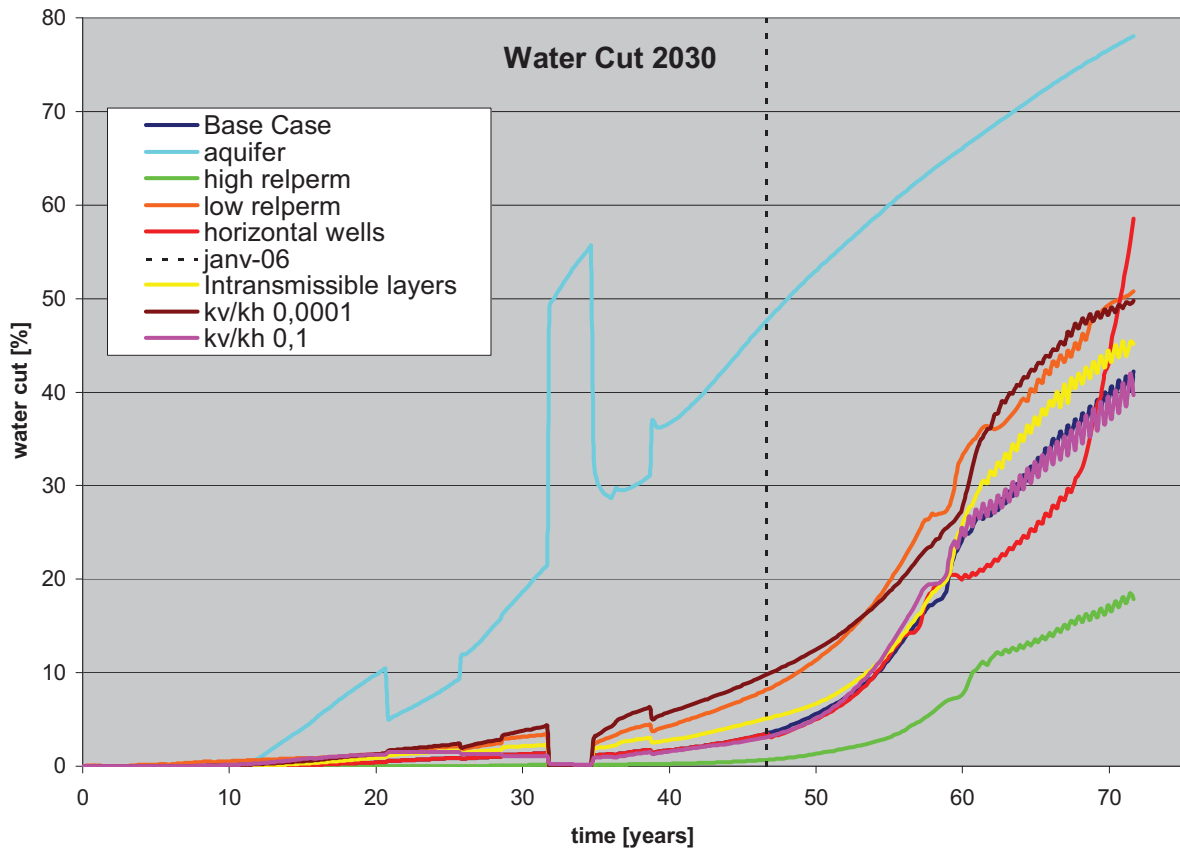
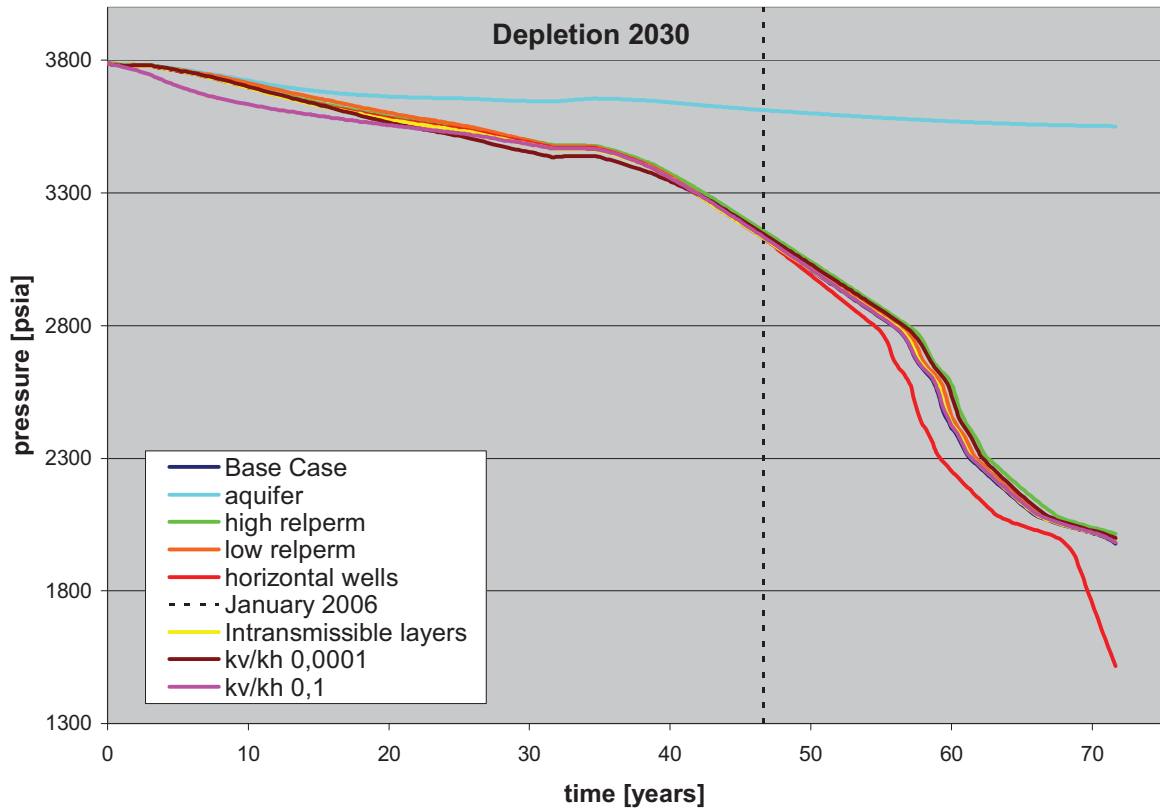


Fig. 5.15: Pressure depletion, basecase and sensitivities



Interestingly, the decrease in vertical permeability anisotropy of a factor of 10 has a rather neglectable beneficial effect, whereas an increase of the same amount is detrimental for production and increases the water cut significantly. It might be the case that water breakthrough happens earlier and therefore impedes oil production.

The same observation can be made on the relative permeability curves, where the favourable curve does not help oil production but decreases the water cut.

This might be due to the relatively low water cut figure for the base case , 4 - 5% at year 50. This leads to a lower gain when relative permeability values are improving but to a higher loss (water cut is 5 - 10% more at year 50 meaning 5 - 10% oil production less) when they are less favorable.

Table 5.9: Result overview of Burgan sensitivity study

OOIP [MBbl]	1900	Np in 2030 (60 years) [MBbl]	RF [%]	WC in 2035 (30 years) [%]	Avg. reservoir pressure in 2030 (70 years) [psi]	
Base case figures	Base case	953	50,2%	42,2%	1978	
	High cases					
	42 oil vertical wells	Horizontal wells 4 new hor.wells from 2006	977	51,4%	58,6%	1515
	kv/kh = 0,001	High kv/kh kv/kh = 0,01	964	50,8%	39,6%	1982
	Curves from analog and history matching	High kr High case curves from changing Corey coefficients and Sorw.	975	51,3%	17,8%	2015
No aquifer	Aquifer Aquifer present	1103	58,0%	78,0%	3551	
All layers transmissible Curves from analog and history matching	Low cases					
	Intransmissible layers	some barriers between layer 2-3, 4-5 and 5-6.	924	48,6%	45,1%	1984
	Low kr	Low case curves from changing Corey coefficients and Sorw.	900	47,4%	50,8%	1997
kv/kh = 0,001	Low kv/kh	kv/kh = 0,0001	868	45,7%	49,7%	2001

**5.5.1 General conclusions on Burgan results:**

Due to its heterogeneity and low vertical permeability the Upper Burgan is not a classical application for horizontal wells. The simulations show that only a neglectable increase in cumulative production is yielded while water cut and depletion increase. It is therefore recommended to rather drill deviated wells in spots with favourable reservoir properties.

Since the presence of an aquifer leads to water cut and depletion level results that do not match with reality, we can assume there is no aquifer present, it is very weak or water influx is blocked by the shale layers. Aquifer activity should be further investigated.

Nevertheless, this negligible aquifer activity in the Upper Burgan reservoir has led to a severe reservoir pressure decline below the bubble point, which has resulted in a dramatic GOR increase and drop in oil production. It is therefore strongly recommended to implement water injection support in this reservoir to maintain reservoir pressure above bubble point in the future.

The decreased transmissibility due to the shale layers and the increase of the permeability anisotropy value do have a negative impact on production. It is advisable to perform further measurements on these parameters to optimize the position of future producers.



## 6. CONCLUSIONS AND RECOMMENDATIONS

The studied reservoirs are quite different in terms of reservoir properties, development options and encountered problems. Therefore, a considerable part of the problems encountered are linked to the particularities of the studied reservoir.

Nevertheless, there are some predominant parameters influencing the production behaviour in all or at least three among the four reservoirs:

Due to reservoir heterogeneity and/or compartmentalization and significant permeability anisotropy, horizontal wells did not benefit as much as expected. Drilling highly deviated wells that penetrate several reservoir layers should be considered as a preferred option.

Reservoir permeability, relative permeability, permeability anisotropy and reservoir vertical transmissibility between layers are crucial parameters. They drive most of the oil production rate and cumulative production.

In order to mitigate development risks, it is strongly advisable to perform appropriate core and log measurements with suitable reservoir coverage to not only reduce the range of uncertainties but also to optimize the position of future producers in locations with favourable reservoir properties.

In case of weak aquifer support, it is recommended to implement pressure support in order to maintain both the reservoir offtake and to avoid that reservoir pressure drops below the bubble point and thus reduces well productivity.

The predominant parameters influencing the production behaviour in Ahwaz are the reservoir rock compressibility and reservoir compartmentalization.

In order to achieve a good history match, the rock compressibility, which was deduced from analogue data of a comparable field, had to be multiplied by three. There exists no physical indication for a value of this order.

Sensitivity runs with the compressibility value from the analogue field indicate that in the long term a significant drop in oil production, rise in water cut and depletion of reservoir pressure can be expected.

It would be advisable to perform core measurements, preferentially under stress conditions. This applies especially in case of a fractured reservoir like Ahwaz.

Ahwaz is a very compartmentalized reservoir, especially in the western and partly in the center sector. Some horizontal and vertical barriers have been identified from pressure measurements; others had to be introduced to accomplish a satisfactory history match. The possibility of a stronger compartmentalization has been repeatedly mentioned in the literature.

The sensitivity runs illustrate a critical decline in oil production if compartmentalization turned out to be more severe than expected. Comprehensive reservoir structural and petrophysical studies can improve well locations and enable the optimal positioning of new producers.

Since Ahwaz is a rather tight and compartmentalized reservoir, horizontal wells have a poor influence on production if they are completed in only one layer, since chances are high to encounter a tight zone. Highly deviated wells that penetrate several layers should be preferred.

In Dorood, the governing factors are the different relative permeability curves and the optimized adding of new production wells.

Due to the unusually strong oil saturation gradient in Dorood and lab measurements which are considered as unreliable, the relative permeability curves are particularly mentioned as one of the greatest uncertainties in Dorood. The curves employed in the full field model were found by history matching.

For the sensitivity run, one more and one less favourable relative permeability curve were used. A significant impact on the cumulative oil production and the water cut could be observed. It is recommendable to carry out further SCAL measurements to get more reliable data. This might require new core taking.

The adding of new wells is of significant importance in the southern and central part of the field where the coverage with existing original oil producers is low and the situation is worsening as wells are shut-in due to operational reasons.

The distribution of high permeable streaks, initially considered a major issue in the literature, is of minor importance in the reservoir simulation, due to the poor permeability difference between these facies and normal matrix. The limited number of grid blocks in the model made the modelling of very thin highly permeable layers difficult. It is recommended to build a sector model especially dedicated to investigate this uncertainty.

Water injection has a moderate impact on oil production as parts of the reservoir are already supported with the Manifa aquifer and reservoir pressure remains high except in the southern part with no aquifer present.

Nevertheless, injection could have significant impact if implemented comprehensively. However, the involved costs, i.e. equipment and higher water treatment costs, will have to be balanced against the gain in production.

The major issues in the Mishrif reservoir are the retention of artificial lift and permeability data.

In spite of an extensive regional aquifer in Mishrif, there exist indications that it is not sufficiently able to provide the necessary pressure support. Artificial lift and/or pressure maintenance methods are therefore envisaged. The possibilities are either water or gas injection or a combination of the two.

The sensitivity study concludes with a strong recommendation that artificial lift should be retained. Water Injection is essential to give pressure support to the reservoir. Another gain in cumulative production can be yielded by combining water injection with gas lift. This however increases the water cut significantly and has to be balanced by the costs of water treatment.

It is not recommendable to employ only gas lift. It will give a production increase compared to natural depletion, but acts detrimental on the pressure regime in the reservoir.

Concerning the reservoir properties, data to characterize the permeability field, the permeability anisotropy and relative permeability, was scarce and partly considered unreliable.

In the sensitivity runs, the relative permeability curves and permeability of the drain layers have a big impact in spite of a relatively little change. It would be advisable to take cores and perform new laboratory SCAL measurements to get more reliable data.

The implementation of subhorizontal wells is beneficial for the cumulative oil production, but it significantly increases the water cut. The income due to the increased production has to be balanced against the cost of water treatment. Additionally the principal feasibility of installing water treatment facilities and their cost has to be considered.

In the Burgan reservoir, the unclear aquifer behaviour is the factor of major concern, apart from that the heterogeneous distribution of the shale layers is worth considering.

The presence or communication of or with an aquifer is not explicitly mentioned in the literature. The modelling of an aquifer leads to a water cut and depletion level that do not match with reality. It can thus be assumed that there is no aquifer present, it is very weak or water influx is blocked by the shale layers. Aquifer activity should be further investigated.

Nevertheless, this negligible aquifer activity has led to a severe reservoir pressure decline below the bubble point, which has resulted in a dramatic GOR increase and drop in oil production. It is therefore strongly recommended to implement water injection to support the reservoir maintaining reservoir pressure above the bubble point in the future.

The decreased transmissibility due to the shale layers has a negative impact on production. It is advisable to perform further log measurements to optimize the position of future producers.

Due to its heterogeneity and low vertical permeability the Upper Burgan is not a classical application for horizontal wells. The simulations show that only a neglectable increase in cumulative production is yielded while water cut and depletion increase. It is therefore recommended to rather drill deviated wells in spots with favourable reservoir properties.

## 7. BIBLIOGRAPHY

- [1] Ahwaz Field - Bangestan reservoir – Brainstorming; Morel D.; 23/09/04; Reference number: TG/COP/IDD
- [2] Reservoir Evaluation Report – Middle East – Ahwaz Field, Zagros Fold Belt, Iran; Digital Analogs, C&CReservoirs
- [3] Ahwaz Bangestan, Synthèse Réservoir – Questions et Incertitudes MDP 2004 – Pilote Injection Gaz Version 0; Glachant B.; 10/2004; Total, Reference number: DGEP/GSR/PN/MO – N° 04/016
- [4] Review of Ahwaz Bangestan Reservoir Studies; Ahmed, H.; June 2003; Reference number: DGEP/GSR/PN/MO-HA
- [5] Comité Gisement du 07/11/2003, Réunion N° 456, Ordre du Jour: Iran – Ahwaz Bangestan
- [6] Ahwaz Field - Bangestan Reservoir, Séminaire PN – 09/12/04; Glachant B.; Total, 2004; Reference number: DGEP/GSR/VDG/MO
- [7] Core Review – Uncertainties, Ahwaz Oil-Field (Iran, Onshore); Total; 05/2004
- [8] Presentation to PEDEC/NISOC, M, Verdier, 05/2004
- [9] Ahwaz Field - Bangestan reservoir – Brainstorming, EOR concerns; Morel D.; 23/09/04; Reference number: TG/COP/IDD
- [10] Comité Gisement Dorood; Paris, March 2006; EPI/GSR
- [11] Commentaire Dorood 2005
- [12] Dorood Field – Geological Model Update; Craig S.; May 2003; Elf Petroleum Iran; Reference Number: D/EP/EPI/DPG/06115
- [13] Iran, Dorood field, Reservoir Geological study, Part 1: Sedimentary models and correlations; Lions, R., Rieupeyroux G.; Pau 2000; Elf EP, Business Area Orient; Reference Number: EP/T/GGC/ORI/R-2000-42/mv
- [14] Comité Gisement Dorood; Paris, January 2004; EPI/GSR
- [15] Dorood; structural Approach: (1) structural style; Charpentier P.; Dubai; March 2002; Total Fina Elf
- [16] Dorood Field - Reservoir Simulation Study 2003; Gholamzadeh S.; Dubai, December 2003; Elf Petroleum Iran; Reference Number: EP/EPI/DPG-08675
- [17] Dorood Field – Sedimentological distribution of high-K streaks in the Yamama formation; Caline B., Maza C., Cantaloube S., Pernin C.; Pau, May 2005; Total Exploration and Production; Reference Number: DGEP/GSR/TG/ISS/CARB/M05-019
- [18] Dorood field Thermodynamic study Update, Elf Exploration Production, Reference Number: EP/T/GGC/ORI R-2000-139

- 
- [19] Dorood Performance Test: Productivity Study; Tison M.; Pau, April 2005; Elf Petroleum Iran; Reference Number: DGEP/TDO/FP/EP/WP/05-0079
- [20] Majnoon Bin Umr - Réunion 04/04/2006; Total; Paris 2006; Reference number: DGEP/GSP/PN
- [21] Majnoon, Mishrif reservoir; Fiche description reservoir
- [22] Majnoon field, Preliminary study, Reservoir; Elf; 1996
- [23] Irak, Réinterprétation du schéma géologique du champ de Majnoon, Formation Mishrif, Conséquences sur les propriétés pétrophysiques; Schepers, K.; TotalFinaElf; Pau, 04/ 2001, Reference number: DGEP/GSR/VDG/GEOL 01.148
- [24] Irak, Majnoon/Bin Umr, Yamama Formation, Geophysical review; Stankoff M.; TotalFinaElf, Paris, 2001, Reference number: DGEP/GSR/VDG
- [25] Mishrif datasheets, Champ de Majnoon (IK), Revue des Incertitudes, Préconisations sur acquisitions de données et études à entreprendre, Elf EP, 1996
- [26] Majnoon field, Mishrif formation; TotalFinaElf
- [27] Majnoon Field Development, Initial Overall Program, Elf Petroleum Iraq, 1997
- [28] Majnoon field, New reservoir simulations of the Mishrif formation, Horizontal wells; Knoff, Th.; Elf EP; Pau, 2000; Reference number: EP/T/GCC-ORI/R2000-84
- [29] Kuwait-Northern Area Project, Burgan Reservoir, Raudhatain & Sabiriyah Fields; Chevron
- [30] Upper Burgan Reservoir Geostatistical Modeling; Chevron
- [31] Kuwait – North Fields Synthesis; Lefebvre, Ch.; TotalFinaElf; 06/2002; Reference number: 00AB711-0924
- [32] Subsurface Review, Kuwait Project – Northern Fields; Chevron; Kuwait; 11/2005
- [33] Geological study of the Burgan Formation reservoir, Raudhatain and Sabiriyah fields, North Kuwait; Bradley, Ashton & Associates Ltd., 1997; Reference number: 00AB699-0692
- [34] Upper Burgan Formation - Raudhatain Field; Comité Gisement; Total; 10/2003; Reference number: VDG/RES PhS
- [35] Kuwait Northern Fields Supplemental Reservoir Simulation Evaluations, October 2003, Chevron Texaco Consortium
- [36] Raudhatain Field, Upper Burgan Reservoir, Technical Review, June 30 - July 1, 2001, Reservoir Simulation
- [37] North Kuwait – Incertitudes Chevron Texaco, PhS; Raudhatain Field, Upper Burgan Reservoir, Technical Review, June30 - July 1, 2001, Reservoir Simulation